Surface Finish Analysis of Composite Automotive Panels

Shilian Hu

A Thesis

in

The Department

Mechanical and Industrial Engineering

Presented in Partial Fulfillment of the Requirements

For the Degree of Doctor of Philosophy at

Concordia University

Montreal, Quebec, Canada

January 2007

Your file Votre référence
ISBN: 978-0-494-30142-5
Our file Notre référence
ISBN: 978-0-494-30142-5

Abstract

Surface Finish Analysis of Composite Automotive Panels

Shilian Hu, Ph.D.

Concordia University, 2006

Composite plates and panels are increasingly used in automotive body parts. These composite structures possess excellent strength and stiffness properties. For these applications, the surface finish of exterior surface of the composite panel is of critical importance to obtain customer acceptance. Automakers pursue to attain surface finish of class A for composite panels, in which they believe class A's surface finish should be very smooth and beautiful. Due to the lack of a good objective method to describe Class A surface finish, the surface finish of Class A is often determined by visual observation.

On the other hand, for low cost operation, Resin Transfer Molding (RTM) is used to manufacture composite panels. Process parameters of RTM affect the surface quality of molded panel. There is a strong desire on the part of the automakers to obtain objective means for evaluation of surface finish. This objective means may allow automated correlation between process parameters and surface finish. This facilitates process optimization. Composite plates made by the RTM process using different process parameters (i.e amount of Low Profile Additive(LPA), process temperature and time) may have variations in the surface finish.

Current objective surface measurement techniques can not differentiate the qualities of these surfaces, thus can not be used easily to optimize the process parameters.

Work done in this thesis has resulted in the development of a new technique that is capable of objectively differentiating the quality of the surface of one composite plate to another.

Acknowledgements

I would like to thank all those faculty members who have contributed to my study and research. In particular, I wish to thank sincerely the my supervisors, Dr. Suong V. Hoa, Dr. Rajamohan Ganesan, Auto 21 project, Ford Co and McGill University for their support and guidance during my study. I am also grateful to my supervisors for their careful reading and corrections of this thesis.

I thank the support of University of Calgary for computer facilities.

Finally, I am also grateful to my wife, Yanling Huang, and my daughter, Ruoxi Hu for their encouragement, support and help. I also thank my parents, brothers and sister as well as my parents in law for their encouragement and support.

Table of Contents

List of Figures

List of Tables

Chapter 1

Introduction

1.1 Introduction

Composites are highly desirable in automotive applications due to their high strength to weight ratio, design flexibility and corrosion resistance [1-4]. There has been increasing interest to use composites to make automotive components, particularly automotive panels [5-7]. For these applications, the finish of the exterior surface of the composite panels is of critical importance to obtain customer acceptance. Automobile makers pursue to attain surface finish of class A for composite panels, in which they believe surface finish of class A should be very smooth and beautiful. Due to the lack of objective parameters to describe Class A, the surface finish of Class A is often determined by visual observation [8-10].

On the other hand, for low cost operation, Resin Transfer Molding (RTM) is believed to be a good method for the manufacturing of these composites panels [11-14]. Processing parameters of RTM, such as, pressure, time, temperature along with resin formulation and fiber perform patterns, are important parameters that may have influence on the surface quality of the molded panels [15]. While it is important to control these parameters during the manufacturing process, it is equally important to have a good, reliable and objective means for the evaluation of the surface finish of the components.

Current technique using subjective evaluation does produce results that meet with customer satisfaction [16]. However, subjective evaluation does not provide specific information as to what particular characteristics of the surface that gives rise to a class A finish. As such, for the development of manufacturing process, subjective evaluation using visual observation is not adequate. This is because subjective evaluation has the disadvantage of being "subjective". In order to avoid the skewing of the results by a limited number of individuals, a statistically large number of evaluations are required. This is time consuming, costly and it can not lead itself to automation.

It is well known that the techniques of surface measurement and evaluation of metal parts have been developed for about 80 years [17]. Parameters of evaluation are required to evaluate surface quality of composite material [18]. However, there are differences between composite materials and metallic materials. The surface finish of metal depends on cutting tools and cutting parameters. Once cutting tool and cutting parameters are fixed, roughness, amplitudes and frequencies of all surfaces can be determined. Surfaces of Composite materials are more complex. The surface quality is related to many factors, such as, shrinkage of materials, temperature, pressure and surface of mold. Therefore, current evaluation methods that are used to evaluate surface of metal can not be used to evaluate the surface quality of composite panel very well.

1.2 Measurement and evaluation of surface finish

In this section a brief history of measurement and evaluation of surface quality is presented, followed by the principles of measurement and measurement systems currently available.

1.2.1 History of measurement and evaluation of surface roughness

Methods for measuring surface roughness of metal parts have been developed for a long time in industry. G. Schmalz developed the first stylus instrument and presented the evaluation parameter and the concept on measurement of a basic line in 1929 [19, 20]. Such foundation work provided big progress on the research of surface roughness.

The first instrument for measuring surface roughness in the market was made by E. J. Abbott in 1936 [21]. The instrument can produce output from the mechanical probe to an electrical signal so that substantial magnifications could be achieved. Talysurf that used a stylus to measure surface roughness was made in Britain in 1940 [22]. Since then, many countries have developed many types of instruments: the microscopes for measuring surface roughness were made in Germany and Russia in 1951 and 1958 [23]; Talysurf-5 that uses a computer to process data and profile was invented by Taylor-Hobson in 1975. Such device had reached resolution of 1nm. In recent years, SEM, Laser and AFM technologies have also been used for measuring surface roughness [24, 25].

Methods for measuring surface quality generally can be divided into two categories: contact measurement and non-contact measurement. For contact measurement, a stylus is used to touch the surface to be measured. Signals can be transferred from mechanical to electrical while the stylus is moved. In this way, the surface profiles can be attained. Many measurement instruments of surface finish belong to this type including AFM (Atomic Force Microscope).

For non-contact measurements, optical microscope, electronic microscope or optical sensors are used to measure and collect surface parameters [25]. Now a few optical systems can use Gloss, Orange Peel and DORI of the surface to evaluate the surface quality [26, 27]. These types of systems are mainly used to evaluate the surface of painted parts.

The measurement methods of surface quality can be described in Fig. 1.1.

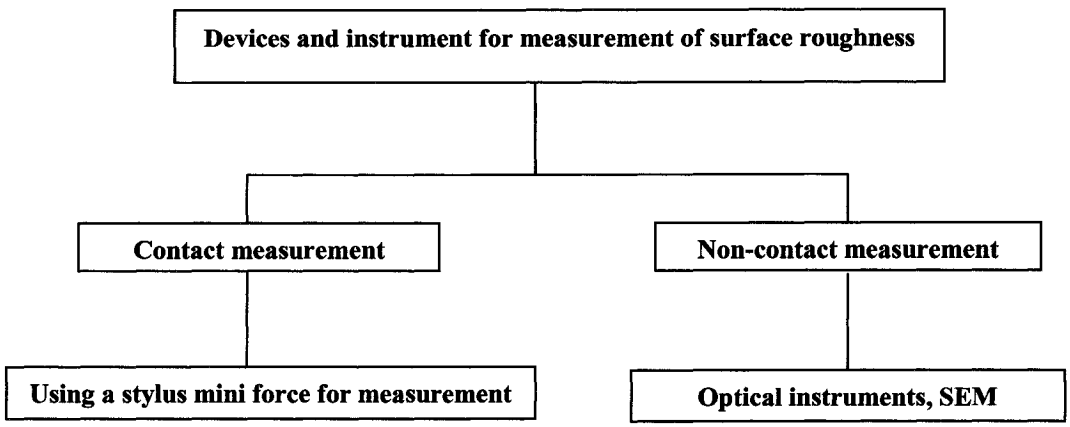

Fig.1. 1: Methods of measurement of surface quality

At present, many parameters and technical standards (for instance, ISO1997, ANSI 1995 and so on) to evaluate surface roughness are used [25]; computers are used to plot 3-D graphics.

It has been pointed out that there exist relationships between surface properties, using properties (such as friction property) of mechanical parts and evaluation parameters [28]. The parameters can be also used as quality control parameters in the production line [29].

1.2.2 The principles of measurement of surface quality

In this section the principles of contact measurement and non contact measurement are described.

Stylus Instruments [30-36]

Stylus instruments are based on the principle of running a probe across a surface in order to detect variations in height as a function of distance. A transducer converts vertical displacement into an electrical signal. This signal can then be processed by the instrument electronics to calculate a suitable roughness parameter and surface profile. A schematic representation of this instrument is depicted in Figure 1.2.

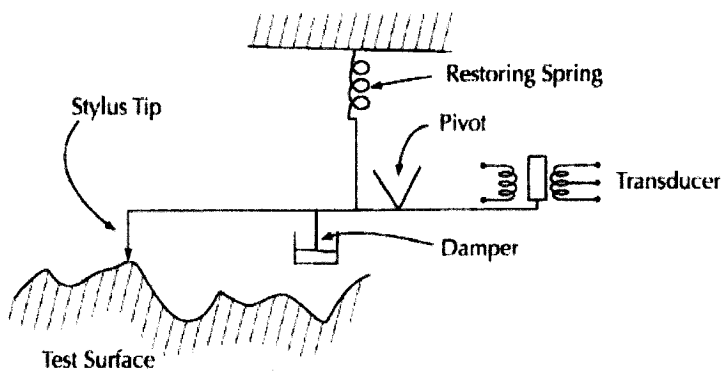

Fig.1.2: Stylus measurement system

This kind of instrument has high resolution, for instance, Mitutoyo SJ402's resolution is 1.25nm/800μm.

Some error can be introduced in roughness measurements when a stylus instrument is used because of several factors. Some of these factors are the size of the stylus, stylus load, stylus speed, and lateral deflection by asperities.

Optical Instruments [26, 27, 30-36]

A beam of electromagnetic radiation can be reflected off a surface in three different ways: specularly, diffusely, or both. This is illustrated in Figure 1.3.

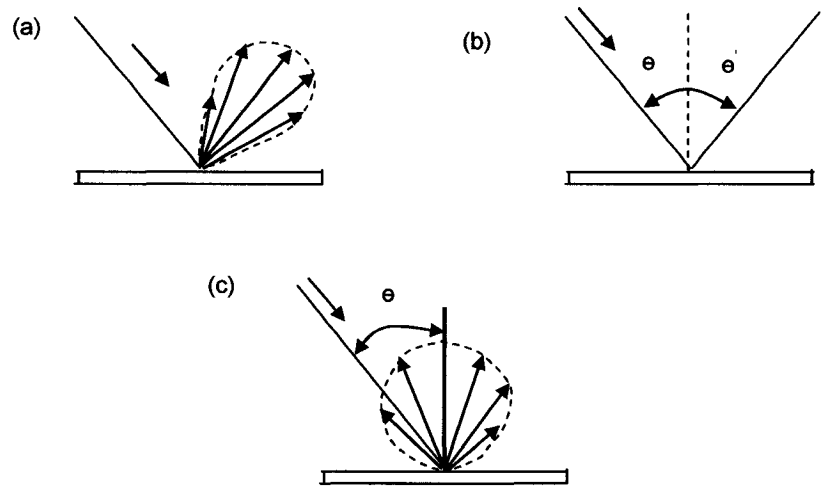

(a) Combined Specular and Diffuse; (b) Specular Only; (c) Diffuse Only

Fig.1.3: Modes of reflection

Depending on the surface roughness, radiation of a certain wavelength may be reflected specularly, while radiation of another wavelength may be reflected diffusely. Thus, the amount of specular and diffuse reflections can be used to determine surface roughness.

One instrument that employs specular reflection to characterize roughness is the light section microscope. An image of a slit is projected onto the surface and the objective lens captures the image at the specular reflection angle. If the surface is smooth, the image obtained will be straight; however, if the surface is rough, an undulating pattern will be observed. This instrument is suitable to measure peak-to-valley roughness with a vertical resolution of about 0.5 μm.

The interaction of polarized light with a surface can also be employed to evaluate surface roughness. Such is the case of the long-pathlength optical profiler, which focuses a laser

beam onto a surface by means of an arrangement of mirrors. Before reaching the specimen, the laser goes through a Wollaston prism that polarizes the beam into two orthogonal components. The beams are then focused onto the surface where they reflect back to the prism. Finally, the reflected beams are directed to a beamsplitter, which sends each beam to a different detector. The phase difference of the polarized beams, which is related to the height difference at the surface, results in a voltage difference that can be measured. This instrument was reported to have a vertical range and resolution of 2 μm and 0.025 nm, respectively.

The instruments that measure the intensity of specular reflection are known as glossmeters. The ability of these instruments to measure roughness is based on the inverse correlation between the intensity of specular reflection and roughness. One major advantage of this technique is that it allows for quick inspection of similar surfaces. It has been found, however, that roughness measurements using this technique do not correlate very well with stylus measurements. As a result, the instrument readings must be normalized for each type of material that is examined.

There are three routes of development for the measurement of geometric attributes. These are the analysis of reflected image, the measurement of intensity of reflected light beams and measurement of reflecting surface profile. The three parameters are Gloss, Distinctness of Reflected Image (DORI) and Orange Peel.

Gloss (Shininess/ reflectivity)

Gloss is found by measuring the average difference between the brightness of the reflection of the light and the brightness of the surrounding area. It is therefore contrast gloss.

When observing reflective surfaces, it is found that a sudden increase in brightness occurs when the angle of observation is equal to the angle of incidence, called specular reflection. Gloss is defined as the ratio of the intensity of reflected light to the intensity of the incident light in the plane of specular reflection. Any diminution of gloss at an air/ surface interface arises primarily from imperfections in, and roughness of the surface. This causes light to be reflected at angles slightly offset from the specular (shown in Fig.1.4). Fig. 1.4 (a) displays the light intensity distribution detected by the camera if reflected off an "ideal" surface with no scattering of light. Fig. 1.4(b) depicts the light intensity distribution detected by the camera when reflected off of a real surface. The reduction in peak intensity is a measure of diminution of gloss. Some colors are more reflective than others, so when comparing gloss readings, the surfaces should be the same color.

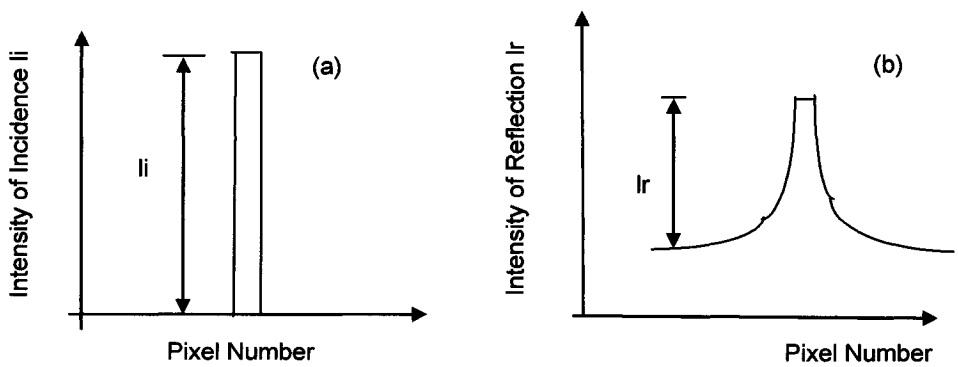

Fig.1.4: Definition of gloss

Distinctiveness of Reflected Image (DORI) (Sharpness of reflection)

DORI is calculated by finding the rate at which the image changes from dark to bright at the edge of the reflection of the light.

It has been defined as the rate of change in intensity of the reflected light as a function of small changes in specular reflection. Therefore DORI is related to the gradient of the

light intensity distribution curves produced by the reflections (shown in Figure 1.5). Distinctness of Image (DOI) is related to the gradient of light intensity distribution curves detected by the camera in Oblique Angel Optical Diffusion methods. The lower the gradient, the greater the light scatters due to surface distortions. The DORI value describes structures ranging from from around 0.5-0.25mm

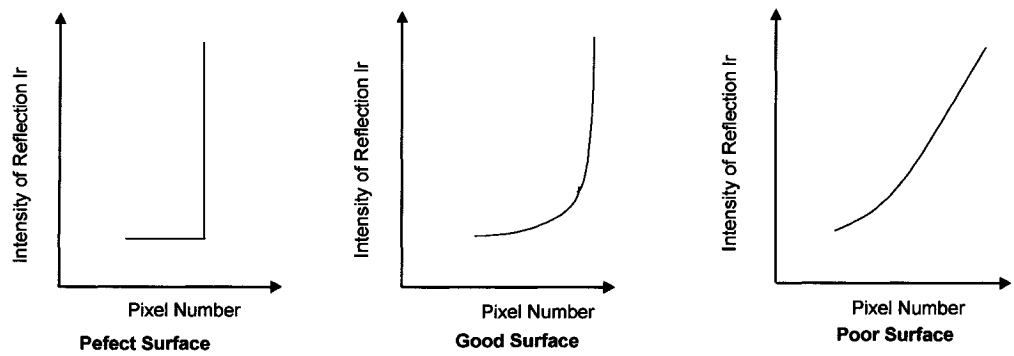

Fig.1.5: Definition of distinctiveness of image

.Orange Peel (Surface Texture/ Roughness)

The Orange Peel value measures the severity of the visible surface dimples by analyzing the degree of distortion of the reflected image of the light. Orange peel describes the degree of deformation of the light reflection by existing surface structures ranging from around 5-1.25 mm.

From the engineering point of view, the two methods (stylus and optical) are complementary. Table 1.1 summarizes the situation regarding the optical and stylus methods, in which sign √ represents advantage of the method. It is clear that on the balance, the stylus methods are best for engineering surfaces, but they do contact the surface.

Table 1.1: Summary of optical and stylus methods

Stylus	Optical
Possible damage	No damage √
Measures geometry √	Measures optical path
Tip dimension and angle independent √	Tip and angle dependent
Stylus can break	Probe cannot be broken √
Insensitive to tilt of workpiece √	Limited tilt only allowed
Relatively slow speed	Can be very fast scan √
Removes unwanted debris and coolant √	Measures everything good and bad
Can be used to measure physical parameters and geometry √	Only optical path
Roughness calibration accepted at all scales √	Difficult to calibrate by standards
Temporal and spatial influence/dynamic effect	Spatial influence/geometric effect

1.2.3 Surface measurement systems currently available

Typical measurement systems used by automobile companies are QMS system and ONDULO quality control system [26, 27, 37]. These systems use optical principles to measure the surface of plates. These systems are used to measure surface quality of painted parts.

QMS is an oblique angle optical diffusion device. Figure 1.6 shows schematic of QMS oblique angle optical diffusion device.

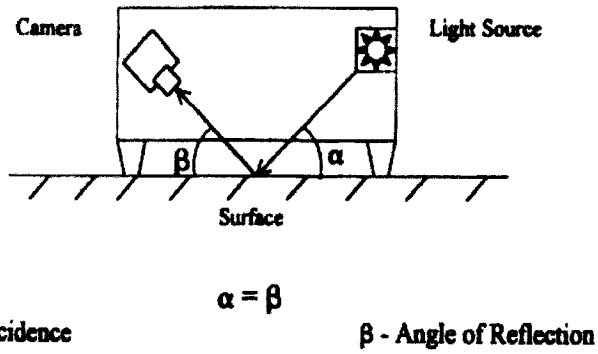

Fig.1.6: Schematic of QMS oblique angle optical diffusion device

The device operates by way of a video camera aimed at the desired surface, at steep angle, in a direction close to the normal. A fluorescent lamp is positioned so that the camera receives the light reflection from the surface. The camera therefore sees a bright bar surrounded by darker area. An image processor digitizes the image and three painted appearance parameters are calculated: Gloss, Distinctiveness of Reflected image (DORI) and Orange Peel.

Surface roughness accounts for the much larger visible deviations on a surface that causes it to distort the smoothness of the reflected image. On painted metallic surfaces this texture would be caused by orange peel (rippling of paint occurring in drying process).

Analysis has been undertaken by QMS to relate the three parameter readings with stylus traces. The work showed that there were three distinct spatial frequency ranges, each of which corresponds to one of the three surface parameters.

Each of these parameters is affected in different ways for a given change in process conditions. The availability of all three process parameters makes it easier to diagnose the process problems. However when the measurements are used to make a decision on

whether a specific panel or car body is acceptable, one composite figure is more useful. Research has shown that a person's assessment of a finished part is most dependent on the severity of the Orange Peel on metallic parts (for composite parts this would be interpreted as distortion of-image through pin-holes, fiber-strike through or the underlying pattern of the surface veil). DORI is the next most important and Gloss has a lesser effect. It was found that an Overall paint quality value can be calculated from the three parameters as follows:

Overall = 50% Orange Peel + 35% DORI + 15% Gloss

These weightings give an Overall parameter, on a scale of 0.0 to 99.9.

The equipment is portable and simple to use. Readings can be taken in a matter of seconds, stored on a floppy disc and imported to an Excel spreadsheet. Two different QMS devices exist, one for high gloss applications and one for low gloss applications. Each device also has three further settings, according to the paint surface of the part: Top Coat, Primer and Electrocoat. Hence the QMS is designed to measure surface finish of paint appearance rather than part finish. However, the system was found to be acceptable to measure surface finish of unpainted moulded plaques.

The ONDULO Quality Control System [37], manufactured by TechLab (France) or CamSys (US) is used by most major car manufacturers. These include Ford-US, Toyota, Nissan, Fiat, GM and Peugeot. It allows surface defects to be optically visualized and characterized. Examples of applications include automotive composite and stamped parts. The system observes the image of a regular geometrical pattern (grid) reflected by the sample, and is then able to analyze deformation due to the defects.

A defect of appearance, or aspect, is defined by a fast variation of the slope across a short distance. A geometrical pattern (grid) is projected onto a screen (not on the part, as in classical structured light systems), and is observed by the reflection off the part with a camera. Light rays are reflected off the surface of the part and a local slope variation can be modified in the direction of the light rays.

Finally, a representative image of the slopes is obtained. The measurement of these local slopes determines the local curvatures and therefore characterizes the defects. 3D visual software is used to display the defects. The resolution of the system is about a few micrometers. Fig.1.7 is a photo of ONDULO system. Fig. 1.8 and Fig. 1.9 are examples of defect detection using ONDULO.

Fig.1.7: ONDULO system

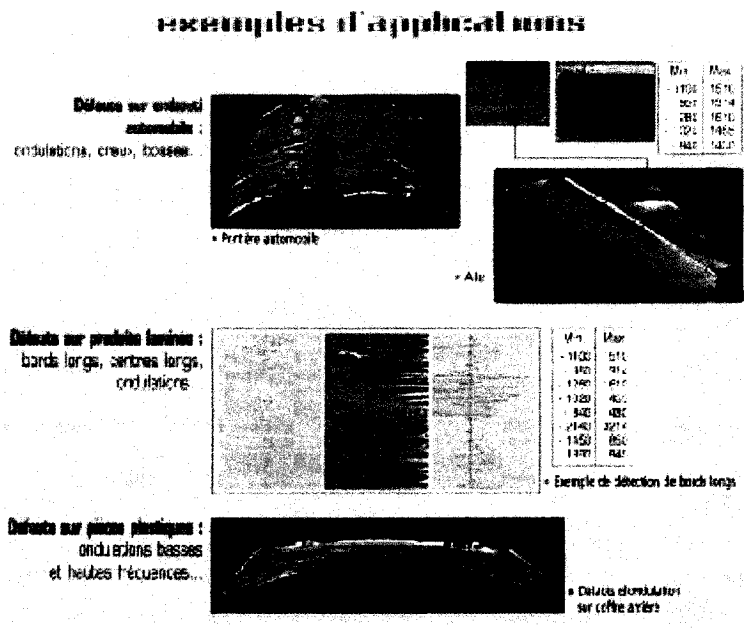

Fig. 1.8: Examples of defect detection using ONDULO

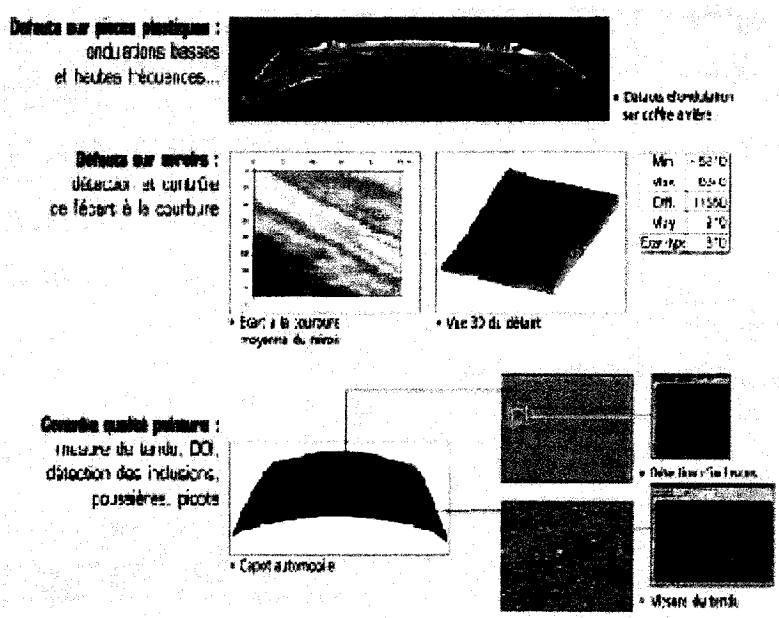

Fig. 1.9: Example of defect detection with ONDULO and control quality

The base price of ONDULO system hardware only is about $65,000(in 2002).

It was also found that the process of varnishing has a great effect on the surface deflections. Several devices are available to measure surface waviness. Daimler Benz (now DaimlerChrysler) has developed the DB Surface Analyzer [38]. It mechanically scans the surface to ascertain its profile. The standard deviation of the measurement points, with respect to the profile centerline, represents the degree of surface waviness. The Laser Optic Refected Image Analyzer ILORlAl uses an optical scanning method. 21 laser lines are projected onto a 100 square inch area of the sample. The distortion of the recorded reflected image gives an indication of the waviness. Long-range waviness leads to a curvature of the laser line, short-range waviness causes a widening of the laser line. The Wavescan-plus, offered by Byk-Garb [38], is a device that meets a growing market. It is also based on an optical scanning method. Laser beam scans a surface line (100 mm length) at a 60° angle to the surface normal. A detector records the profile of brilliancy after reflection. The standard deviation of the mean brilliancy provides quantitative values for the waviness.

By using a profilometer, composite material surface roughness can be directly measured. Typical of such instrument is Proscan 2000 which uses laser technology and it is a type of non-contact measurement instrument [39]. Fig.1.10 illustrates a Proscan 2000 instrument. Fig.1.11 is a surface measurement example using Proscan 2000.

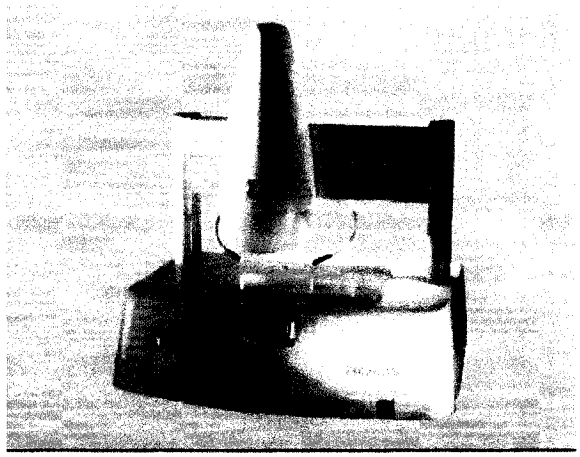

Fig. 1.10: Proscan2000 true laser surface roughness measurement

This system is capable to produce surface 2 D isometric and 2 D cross section views. Its resolution is 3 nanometers and the spot of light is 2 micrometers. 150mm×100mm is the maximum area that the instrument is able to measure. Listing price is about $90,000 (2002 year).

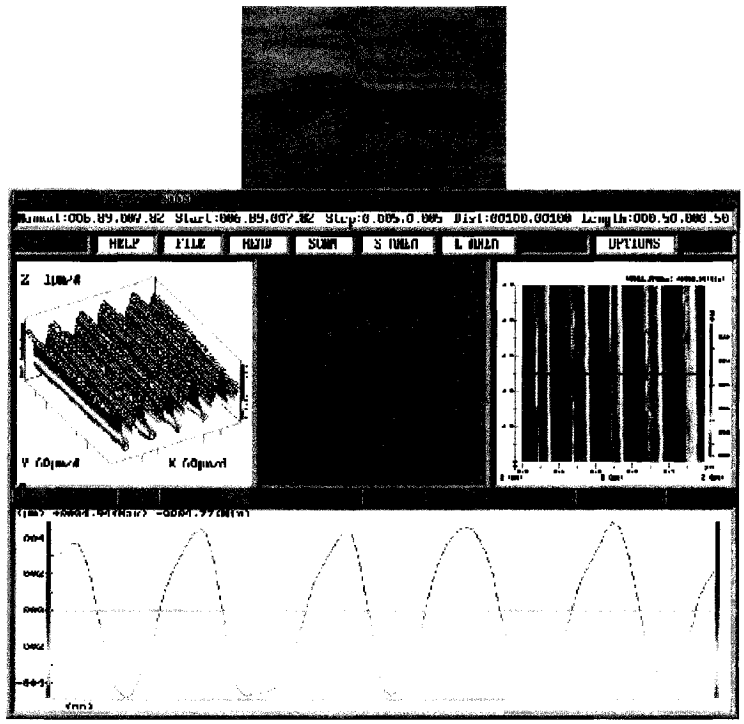

Fig. 1.11: An example of surface measurement

There is also a similiar equipment in the market, such as Nanosurf by UBM Corporation [40, 41], which allows Non-contact profilometry. It is illustrated in Fig. 1.12 and Fig. 1.13.

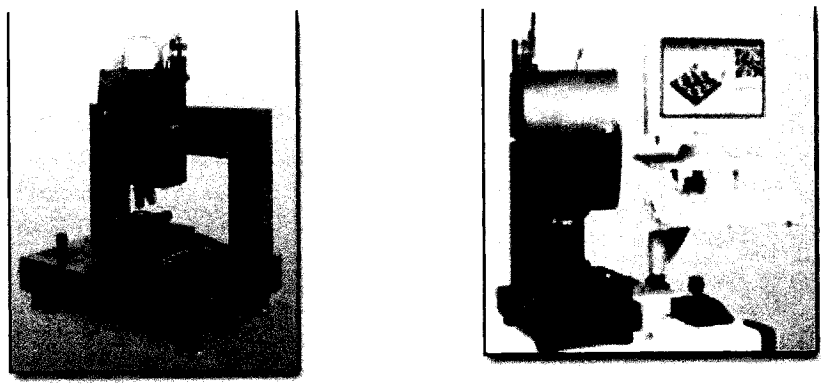

Bridge Configuration *Column Configuration*

Fig. 1.12: Nanosurf by UBM Corporation

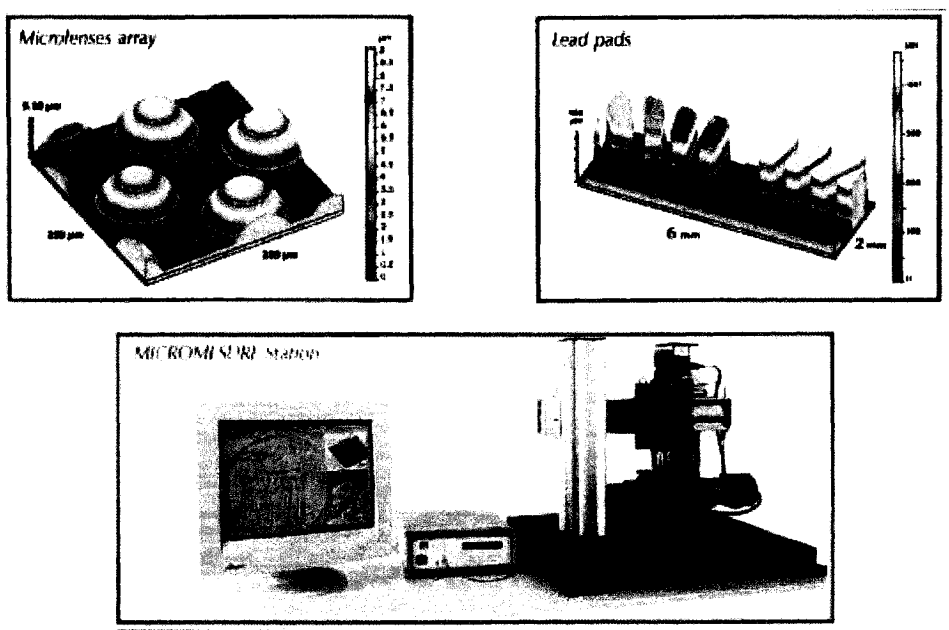

Features or the MicroMeasure Profilometry Systems

Fig. 1.13: Micro Photonics's profilometry system

Contact measurement type instruments have good accuracy and high resolution since they have been developed for many years. Their measurement length can be several inches and 2-D or 3-D analysis can be performed using a computer. Their prices are much lower than non-contact measurement systems. The listing prices are from $2,000-$19,000 (2002 year). Many companies make this kind of equipment. Fig.1.14 and Fig.1.15 are two typical such instrument systems, they are products of Mahrfederal and Mitutoyo [42, 43].

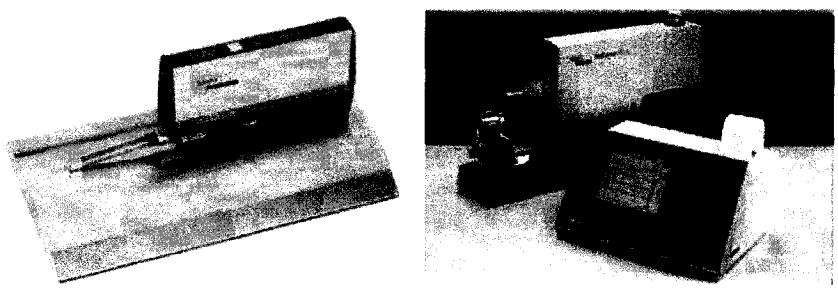

Fig. 1.14: Mahr Federal's Surf instruments and system

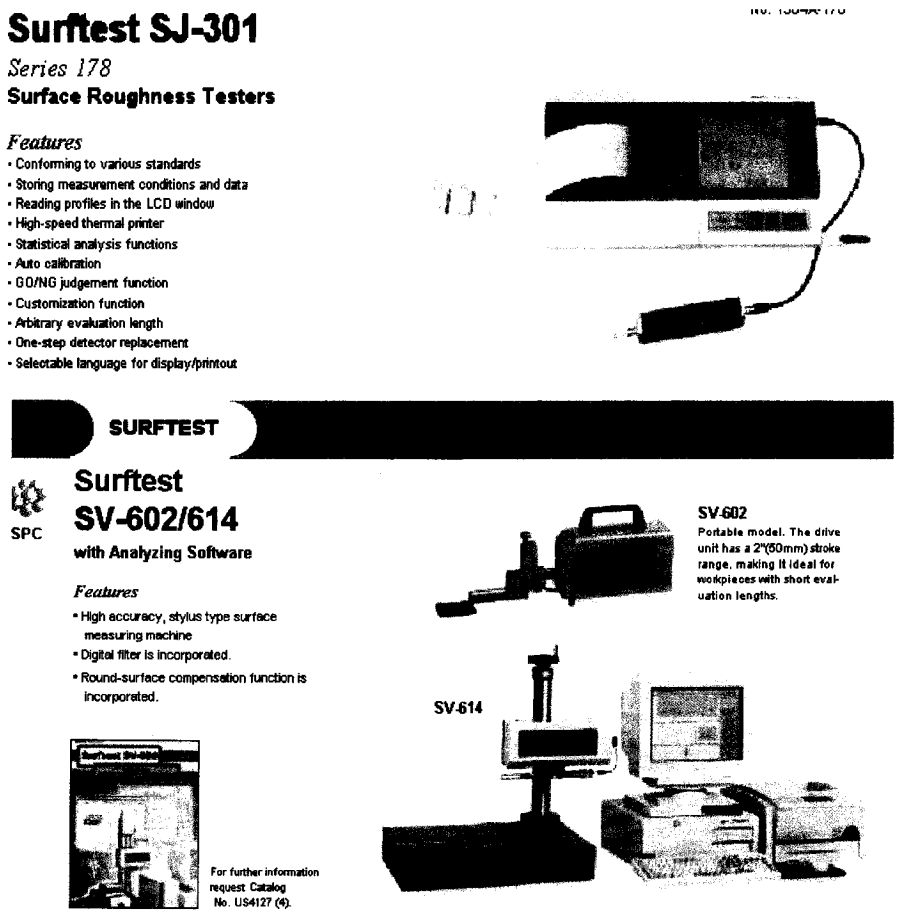

Fig. 1.15: Mitutoyo's Surf instruments and system

Table1.2 lists some commercial surface measurement systems and their estimated prices.

Table1.2: Commercially available surface measurement systems

Name of Product	Features	Measurement Type	Estimated Price (USD) (2002 year)
QMS	Painted part, Gloss, DOR, Orange peel	Non-contact	
ONDULO	Measurement of large area, resolution about 1.5μm	Non-contact	$65,000
Wavescan DOI	Similar to QMS	Non-contact	$15,000
Proscan2000	Measurement 150×100mm resolution 2 nm	Non-contact	$90,000
Nanosurf	Measurement 100×100mm, resolution 5nm	Non-contact	$90,000
Series 4655 OEM USB roughness sensor	Measurement 0.78-10mm^2, average Ra	Non-contact	$1,000-2,000
Lasercheck	Measurement 5×1mm area, average Ra value	Non-contact	$9,500
MicroMeasure Profilometry Systems	Measurement 100×100mm, Max resolution 1nm	Contact	$70,000
Mahr Federal's Surf Instruments and System	Measurement length 0.15-120mm resolution 12nm	Contact	$2,000-19,000
Mitutoyo's Surf Instruments and System	Measurement length 0.08-200 mm max resolution 8μm - 0.0002μm	Contact	$2,000-19,000
Fowler Pocket Surf	Resolution 0.1μm measurement length 4mm	Contact	$2,000
Links-Hommel T2000series	Measurement length 0.025-40mm max resolution 0.001μm	Contact	$2000-19000
TR100, 200,240	-	Contact	$1000-2500

It can be seen from Table 1.2 that non-contact measurement systems are more expensive than contact measurement systems. Optical non-contact measurement systems are fast and suitable to a variable size field. However, a disadvantage of the method is that scattered intensity depends on the wavelength of the light, colors and the pigmentation of the surface [44]. Measurement accuracy used to evaluate painted surface still has problems. Many instruments can supply data of surface, each piece of data or parameter only reflects a characteristic of the surface from a view. Due to the complexity of the surface of composite materials, the surface can be evaluated only by one or a few statistic average parameters. There may be no relationship between some parameters of physical significance, for instance, waviness and roughness. Therefore, it is difficult to discriminate between the materials of different colors and close surface qualities by using one or a few statistic parameters. All types of surface information attained from different measurements should be obtained. However, a good theoretical analysis method and model should be developed, in this way, the information can be well used. Therefore, a good process and analysis model still needs to be set up and developed in order to discriminate surface quality level between composite plates.

Current techniques can provide signatures of surfaces but can not differentiate one surface from another when they have approximate quality. Also they can not determine whether a surface is of class A quality. The objective of work for this thesis is to develop a method that can objectively differentiate surfaces of approximate quality. This allows a means to optimize the manufacture process. Also the technique can allow the determination to see how close to class A the surface is.

1.3 Manufacturing composite panels by Resin Transfer Molding (RTM) [4-7, 45-47]

Resin transfer molding, or RTM, has been gaining popularity in the aerospace, automotive, and military industries. RTM was originally introduced in the mid 1940's but did not gain commercial success until the 1960's and 1970's. During the 1970's, RTM was used to produce commodities that benefited from RTM's ability to make complex shapes more efficiently.

Figure 1.16 shows the schematic diagram of Resin Transfer Molding (RTM) process

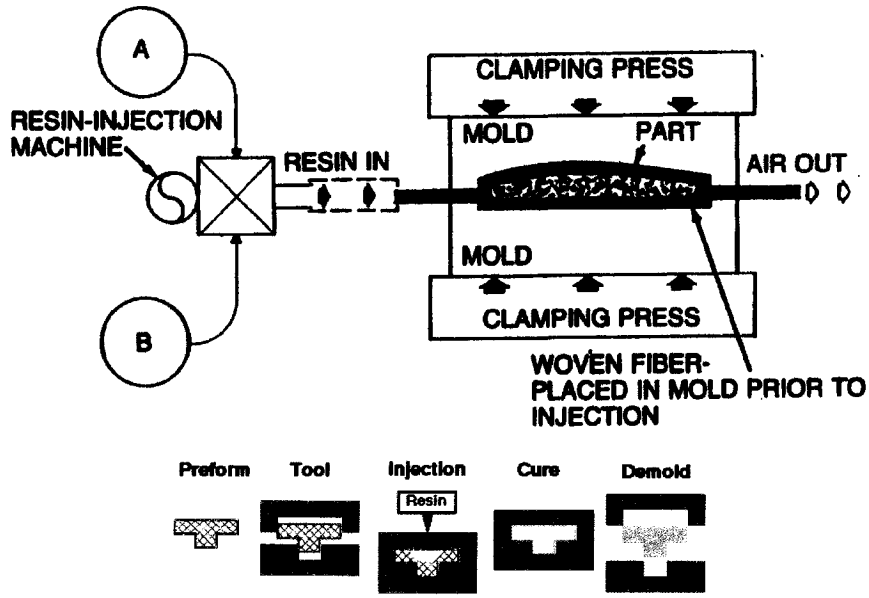

Fig.1.16: Schematic diagram of Resin Transfer Molding (RTM) process

The resin transfer molding process is as follows:

1. A two-part, matched-metal mold is used as the tool
2. A preform of fibers is placed into the mold

The preform is a fiber reinforcement that is pre-shaped and oriented into a skeleton of the actual part.

3. The mold is closed

4. The pre-mixed resin/hardener (a low viscosity fluid) is pumped under low pressure through injection ports into the mold.

Once the mold is closed, a low-viscosity fluid is injected into the tool. This fluid is known as the matrix material. It must be low viscosity in order to flow through the fibers of the preform. The displaced air escapes from vent ports placed at strategic points. During the injection stage, the resin "wets out" the fibers. This means that each fiber is wetted with resin or other matrix materials.

5. The mold, fibers and resin are heated.

The resin cure begins during filling and continues after the filling process. Heat applied to the mold activates polymerization mechanisms that solidify the resin.

6. The part is demolded.

Once the part develops sufficient green strength, it is demolded. Green strength refers to the strength of a part before it has completely cured. When a part comes out of the mold it is still warm, and therefore still reacting.

The structure of the preform must be designed based on the thermomechanical loading the part is expected to undergo, and the influence of the microstructure on the permeability. This influence of the perform material and structure affects the following:

- Time to fill the mold - The tighter the fibers are packed, and the more complex the perform structure is, the longer it will take to wet out the fibers.

- Resin selection – A resin must be selected that has properties such that the resin and fibers have a 'good' bond.
- Viscosity – The viscosity of the resin must be such that the resin can flow through the preform in a reasonable amount of time, and wet out the fibers thoroughly.
- Processing temperature – The processing temperature is a direct result of the matrix material chosen.
- Selection of tooling material – A mold material must be chosen such that the resin does not bond to the mold. Non-stick coatings or layers of plastic (like those used in vacuum bagging) are often used to aid in the demolding process.
- Demold time – Depending on the resin used, the time to achieve green strength, and the time to remove a sometimes complex mold is affected.

A primary benefit of RTM is the separation of the molding process from the design of the fiber architecture. Having the fiber preform stage separate from the injection and cure stages enables the designer to create tailored preforms to fit precisely into the mold. Fiber volume is easy to control in RTM since both the resin and the fibers can be monitored separately. The matrix volume can be monitored by the dispenser, while the fiber volume can be obtained by weighing the preform.

Main advantages of RTM are Good surface quality, Tooling flexibility, Large and, complex shapes, Ribs and cores and inserts, Parts integration, Range of available resin systems, Range of reinforcements and Controllable fiber volume fraction.

Therefore, RTM technique has been widely used to manufacture composite parts in the automobile industry. RTM is capable of satisfying the low-cost, good properties and high-volume of the automotive industry.

For the composite automobile components, surface finish is of critical importance for RTM process to make automobile panels, the following factors have effect on the quality of the surface of the final composite parts.

- Surface of the mold.

This is true for the molding of all parts and not necessarily for composites only. The better is the quality of the surface of the mold, there is more chance of better quality of the surface of the parts.

- Shrinkage of the resin

Normally resins such as polyester shrink about 8% as it changes from the liquid state to the solid state. If the resin shrinks away from the surface of the mold, then the final composite plate may not assume the surface quality of the mold. If the temperature history of the resin or the surface is not uniform there may be ununiform shrinkage and this may cause waviness. One way to combat the shrinkage of the resin is to add fibers. Adding fibers may reduce the shrinkage of the resin but too many fibers may cause print-through and this can also create poor surface finish. One other way to reduce shrinkage is add Low Profile Additive (LPA) into the resin. Low Profile Additives are usually thermoplastics such as polyvinyl acetate.

1.4 The problem posed by Ford Motor Company

As part of a larger project on surface finish of polymer composites made by the RTM process of the Canadian Network of Centers of Excellence (NCE) AUTO 21, Ford Motor

Company supplied three plates to Concordia Center for Composites. One plate is a painted steel panel. The other two plates are composites made using glass/polyester and RTM technique. For plate 2a, no Low Profile Additive (LPA) was used while for plate 2b Low Profile Additive was used. The painted steel plate is black and the two composite plats are white. Low magnification surface photographs for painted steel plate, composite plates 2a and 2b from Ford are shown in Fig. 1.17.

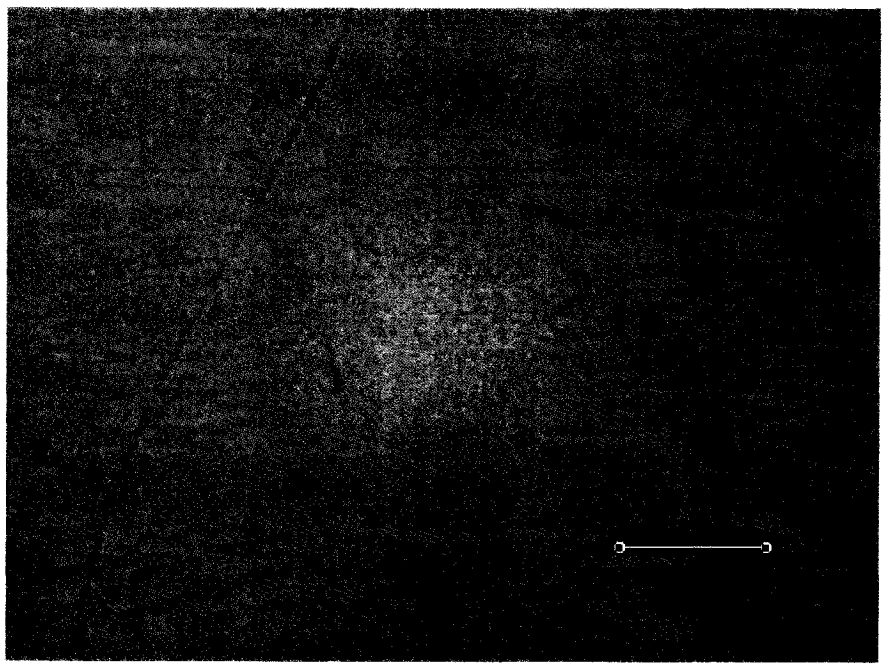

Painted steel plate

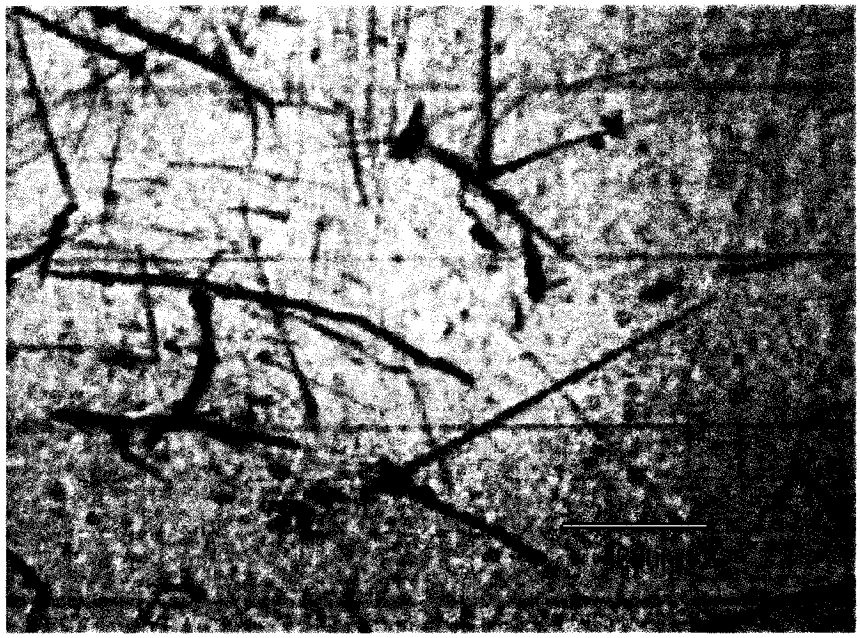

2a

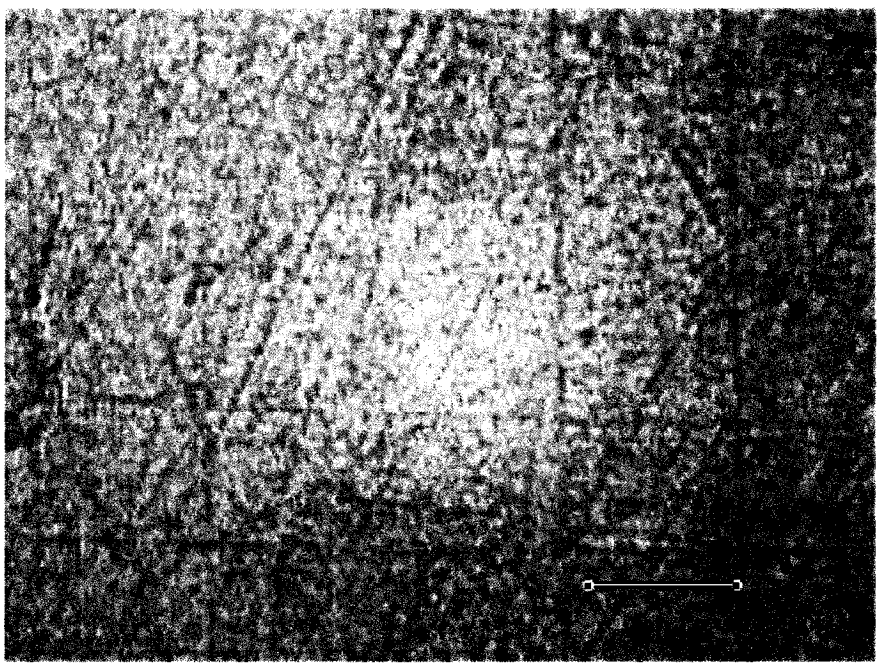

2b

Fig.1.17: Surface photographs for painted steel plate, composite plates 2a and 2b from Ford Motor Company

By visual observation out of the three plates it is easy to find that the painted steel plate has the best surface finish in the three plates. Also plate 2b has better surface finish than plate 2a. However, by normal surface measurement parameters it is very difficult to discriminate the surface finish of composite plates 2a and 2b.

Profilometry was used to examine the surface quality of the three plates. Ra values are shown in Table1.3 [48].

Table1.3: Ra values of samples from Ford Motor Company

Sample	2a	2b	Steel
Ra(μm)	0.2196	0.1954	0.07824

It can be seen from Table 1.3 that the painted steel plate has the lowest Ra. However, it is hard to discriminate surface quality of composite plates 2a and 2b because Ra values are very close. Ra values are most widely used to evaluate surface finish of metals in practice. Ford Motor Company also tried out different methods of surface measurements, which could not reach in a quantitative means to distinguish the surface 2a and 2b For this situation, how to distinguish the surface quality between the two composite plates? Ford Motor Company through Auto21 posed the challenge to search for a new evaluation method of surface finish of automobile composite panel to differentiate the surface quality of these plates.

It should be mentioned that class A surface finish in the automobile industry is important. While one understands that a class A surface finish should be smooth, beautiful and pleasing to the eyes, there is no systematic and quantitative definition of a class A surface finish. The determination of whether a surface is of class A quantity depends on the subjective judgment of a panel of visual observation. The challenge posed by Ford Motor

Company can be derived from the fact that there is no objective description or objective method of determination on the quality of a surface.

1.5 Objective of the thesis

The objective of this thesis is:

To search for a method to objectively discriminate the quality of the surfaces of automobile composite panels made by the RTM process. This method can also objectively determine the quality of a surface with reference to a surface that is known to be of class A quality (as agreed by a panel of observers). This allows the need to use the observation only once (the first one for the reference surface). This new comparing analysis model of multiple attributes provides a more scientific way to determine surface quality.

Chapter 2

Literature survey on surface finish and signature analysis

In this chapter the situation of surface finish analysis is briefly reviewed. The concept of surface finish parameters is introduced. The surface profile recorded is a type of random signal. Therefore, concepts and methods in signal processing should be introduced to study the surface profiles. The concepts of stochastic treatment of signal, trace mix, Fourier analysis, filtering analysis, correlation analysis, and similarity analysis are discussed.

2.1 State of the art of surface finish analysis

The measurement and evaluation of surface finish can be dated back to 1929 [19, 20]. Research of surface finish mainly contains the four aspects: measurement techniques, evaluation methods, the relationships between process parameter and surface finish and relationships between performances and surface finish of materials [25, 30].

In Chapter 1 measurement techniques have been introduced. Here the other three aspects will be introduced.

For metallic material, quantitative evaluation methods of surface finish, the relationships between its performances (called function) and surface finish and also relationships of process parameters and surface finish have been well established.

For example, process and surface finish have corresponding relationships. Table 2.1 shows typical surface roughness values for commonly used machining processes [30].

Table 2.1 Typical surface roughness values for commonly used machining processes [30]

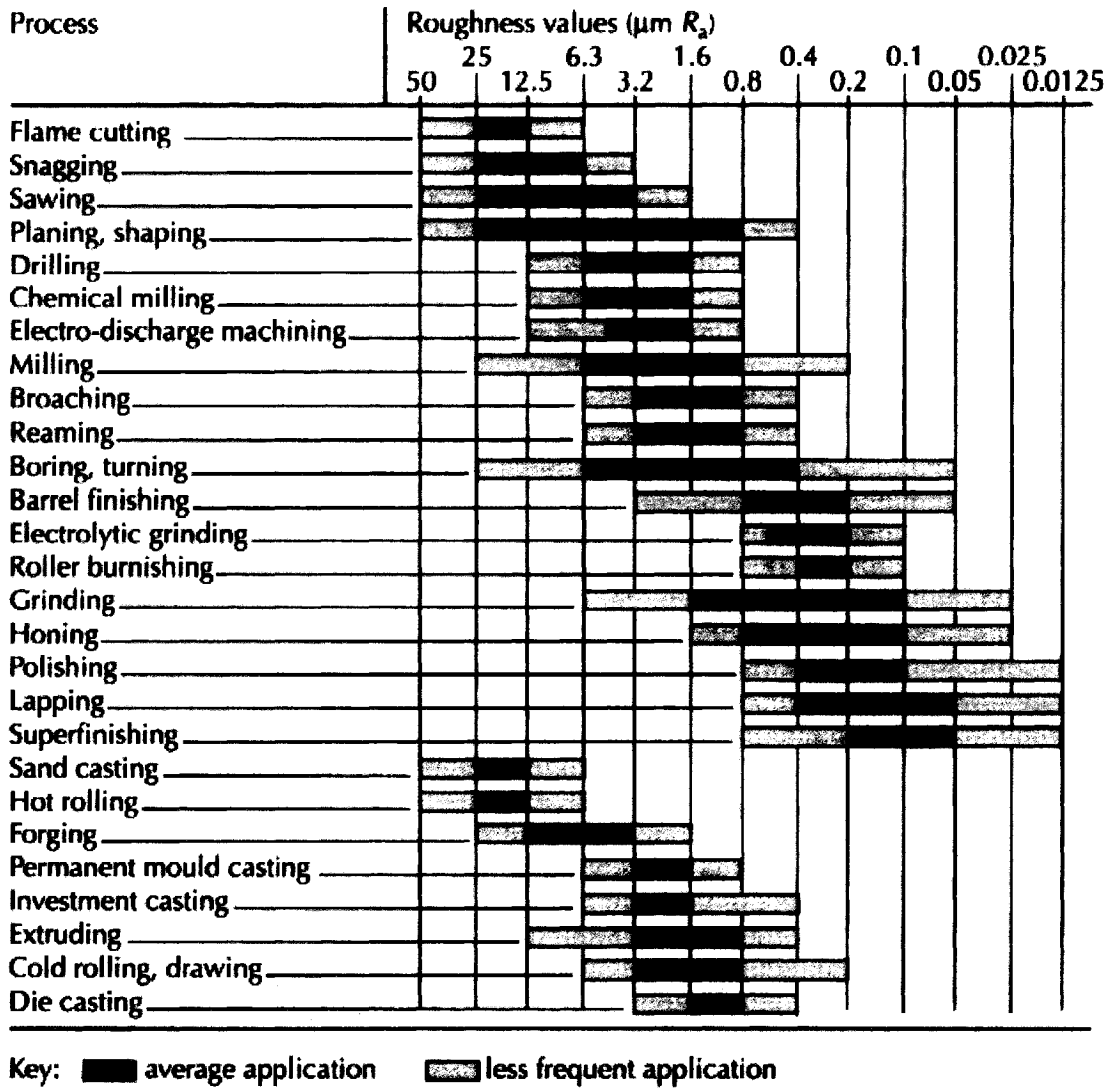

Table 2.1 shows once a machining process is used, the corresponding surface finish can be obtained.

There is a great variety of evaluation parameters, many of which have been defined for industrial use or appear in national standards. These evaluation parameters include amplitude parameters, spacing parameters, hybrid parameters, random analysis.

Amplitude parameters are most common statistical descriptors of surface height. They are also widely used in industry. However, the magnitudes of the values are not directly related to performances, appearance quality and characters of material. Space parameters and hybrid parameters can be used to describe the relationships in some extent. For instance, the shapes of surface profiles will affect on lubricated slide, these parameters help to quantify the differences between these surfaces [49].

Surface profile can be considered as a random signal. Random analysis and frequency spectrum analysis are also used to research surface profiles. For example, frequency spectrum and period analysis for signatures are helpful to find the relationships between vibrations of cutting tool or machine and surface finish [49]. This allows surface quality to be improved.

In recent years, fractal analysis is used to analyze surface friction properties and to simulate surface roughness [50-55]. Monte Carlo simulation is also used to study surface roughness [56, 57]. The analysis is very important for studying anti-friction parts and simulation friction surface is also of importance for studying of robotic hand.

The relationships between manufacture, measurement and function are shown in the Fig. 2.1 [30].

(1) Past and present situation

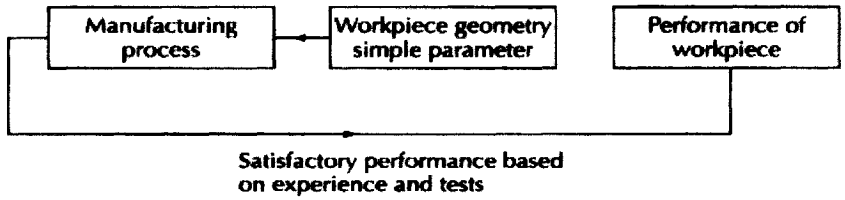

(2) Future situation – manufacturing control

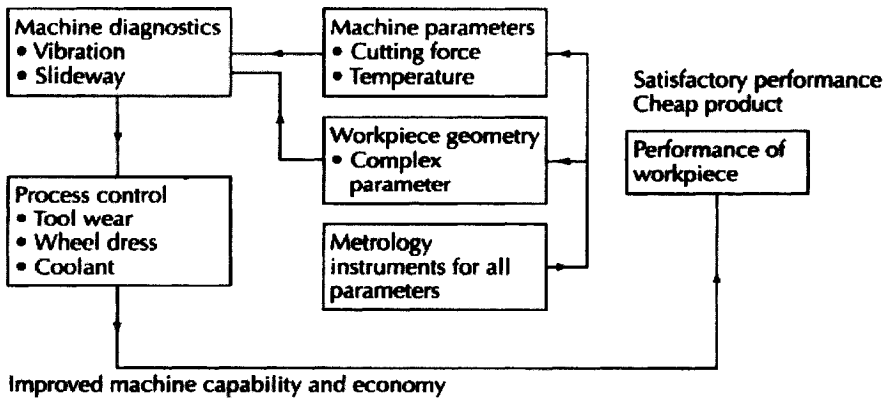

(3) Function optimization

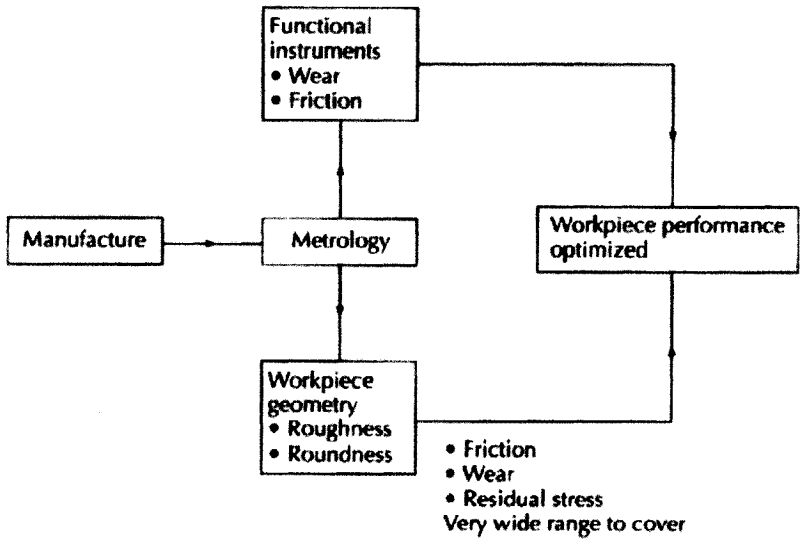

Fig.2.1: The relationships between manufacture, measurement and function

In Fig.2.1 (1) the conventional situation is shown. This is basically a trial and error approach usually augmented by experience. Fig.2.1 (2) demonstrates use of metrology to encompass the machine as well as the process. Fig.2.1 (3) brings in the function.

Ultimately, the emphasis will be shifted from Fig.2.1 (1) to Fig. 2.1(3) because it is the function that is important rather than the manufacture. Taguchi's method is used to optimize process parameters to obtain good surface quality [57]. For metallic and composite materials, most research work will be focused on the field of optimizing the relationships between manufacture, measurement and function in the future [57, 58].

Recent years Resin Transfer Molding process has been used to make automotive panels. The exterior parts are required to have Class A surface finish. However, Class A surface finish does not have a clear definition. Now Class A surface finish is only defined as: "a substrate made of composite material represents a Class A surface, if its optical appearance is identical to adjacent steel panel."[38]. Due to lack of quantitative definition of Class A surface finish, the evaluation of surface quality of automotive panel still depends on visual observation [38].

Typical measurement systems used in automotive industry are QMS, BYK wave scan, DB Surface Anlyzer, Diffracto-D-Sight and ONDULO quality control system [26, 27, 37]. Evaluation parameters, such as, Gloss, DOI, Orange Peel and waviness as well as visualization software are used to evaluate surface quality for painted parts [27, 37, 38,]. Due to the limitations of light wavelength, color and pigmentation of the surface, Class A surface finish can not be described by parameters and techniques yet [44].

Surface quality of exterior composite parts is related to resin, reinforcement and mold. The weight content the reinforcement may influence the roughness of surface. The stronger the reactivity of the resin is, the more important the shrinkage is. The shrinkage may cause waviness of the surface and produce mold cavity between the surface of mold and the surface of composite plate, which would affect the surface quality. It is no doubt

that the surface finishing of the composite panels depends on the surface finish of the mold. Based on RTM process, it is clear that the process parameters (for instance, pressure, time, temperature along with resin formulation and fiber preform patterns) will affect on the surface quality level of composite panels.

To achieve Class A surface finish, many process parameters are researched. The work include resin formulation, part and tool design, control parameter and in-molding coating.

The research of resin formulation mainly finds the optimum composition to reduce the shrinkage in order to obtain good surface finish. These researches are involved in resin, styrene, catalyst, accelerator, de-molding agency, filler and low profile additive. In recent years, a number of resin manufacturers have introduced resin with low profile additives for reduced shrinkage and enhanced product surface finish. Many papers studied effects of LPA [61-67]. Reducing the shrinkage will be helpful to improve surface finish.

Surface finish of mold is essential to obtain high surface quality. To make surface of the plate of RTM touch the surface of mold in the processing, tool and mold need to have optimization design [68, 69]. Therefore, good surface finish of mold and tool design is important to obtain Class A surface finish for composite panel.

Control parameters (such as, temperature, pressure, injecting rate) will affect surface quality of composite panels. Optimization the control parameters can achieve good surface quality [10, 63]. For instance, a very accurate mold temperature control is essential to achieve the phase separation. Uniform extent of temperature distribution will also affect on the surface quality.

Research shows that using in-mold coating and gel coat technique can achieve high quality's surface [46, 71]. In most of cases these techniques added further time and cost to manufacturing.

An investigation was conducted into the effects of variation on the degree of surface in RTM products using Statistical Experimental Design (SED) techniques [15]. Based on gloss and Ra value SED was used to determine the importance of various factors and their interactions in the influencing certain aspects. The research shows that gloss increased with lower filler content, fiber volume fraction and mold temperature, and with higher injection pressure. Whereas roughness was reduced with higher filler content and injection pressure, and lower fiber volume fraction (least important) and mold temperature.

Therefore, for composite panel, an important problem is how to describe Class A surface finish quantitatively in order to distinguish the surface quality of composite panels [72].

At present evaluation parameter used still is Ra values [8, 9, 38]. Debolt [72] tried to use waviness's amplitudes to calculate Ra values in order to describe Class A surface finish. Due to the limitation of Ra, it is difficult to find a standard method and procedure for Class A finish.

In summary, accurate control is vital in achieving consistent component specification such as an acceptable degree of surface finish in final products. This, however, has been hampered by the lack of a clear definition of the so called class A surface finish, the absence of "knowledge based" engineering model of process and taking into account the contribution of processing and material variables on the final appearance of the product. Therefore objective analysis of surface quality is helpful to set up the relationships

between surface quality and process parameters for composite panels. In this way, process parameter will be correlated to surface quality. Surface quality levels will be improved greatly.

2.2 Introduction of basic surface finish parameters [30, 73-75]

1. Amplitude parameters

A typical surface profile signal is shown in Fig. 2.2

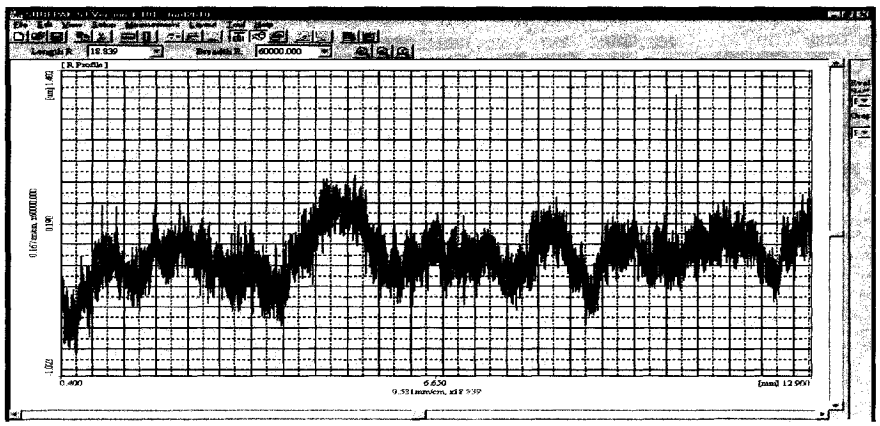

Fig. 2.2: A typical surface profile signal

Fig.2.3 shows an expanded portion of the signal. Parameter Ra of the surface roughness is the arithmetical mean of the absolute values of the profile deviations (Y_i) from the mean line. It can be defined as:

$$R_a = \frac{1}{n}\sum_{i}^{n}|Y_i| \qquad (2.1)$$

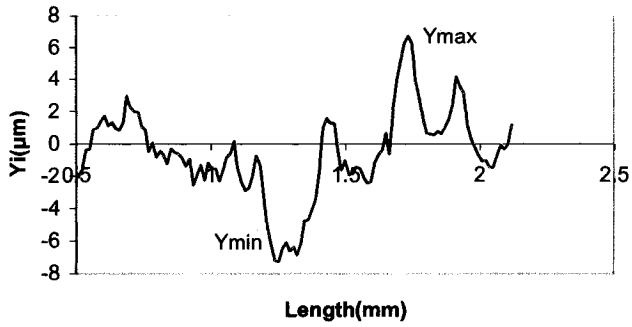

Fig.2.3 Amplitude versus length of the signal

Rq is the square root of the arithmetical mean of the squares of the profile deviations (Yi) from the mean line.

$$Rq = \left[\frac{1}{n}\sum_{i}^{n} Y_i^2\right]^{1/2} \tag{2.2}$$

And Ry is the sum of height Y_{max} of the highest point from mean line and of depth Y_{min} of the lowest point from the mean line.

$$Ry = Y\max - Y\min \tag{2.3}$$

Fig. 2.4 shows relationship of roughness and waviness. Roughness refers to fluctuations with high frequency and waviness refers to fluctuations with low frequency. By filtering out the high frequency components waviness curves can be attained. In the same way as roughness parameters, waviness parameters can also be defined, such as Wa, Wq, Wy.

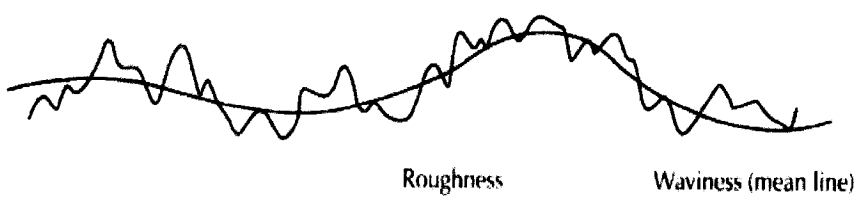

Fig. 2.4: Roughness and waviness

2. Spacing parameters

From Fig. 2.5, RS_m is defined as mean spacing between profile peaks along the mean line.

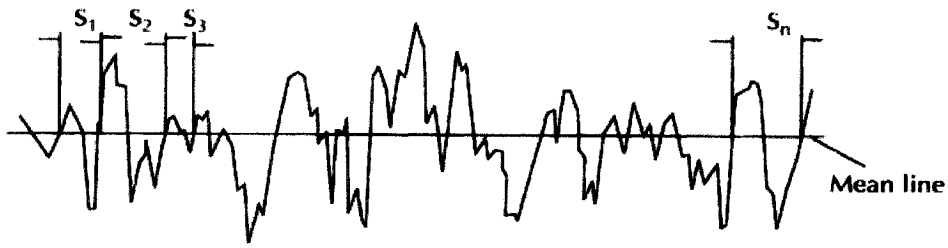

Fig. 2.5: Mean spacing

If n is number of peak spacing, then:

$$RS_m = \frac{1}{n}\sum_{i=1}^{i=n} S_i = \frac{S_1 + S_2 + S_3 ... + S_{n1}}{n} \qquad (2.4)$$

WS_m is the corresponding parameter from the waviness profile.

3. Hybrid parameters

$R_{\Delta q}$ is the RMS slope of the profile within sample length (l_r) (shown in Fig.2.6 and equations (2.5) and (2.6)). This parameter is very useful for assessing reflectivity, friction, adhesion, vibration etc and is a measurement of the angular slope of the profile. Generally, the lower is the angle, the better is the reflection and the higher is the angle, the greater is the friction.

$$R_{\Delta q} = \sqrt{\frac{1}{l_r}\int_0^{l_r} |\theta(x)|^2 dx} \qquad (2.5)$$

$$\theta = \frac{dY_i}{dx} \qquad (2.6)$$

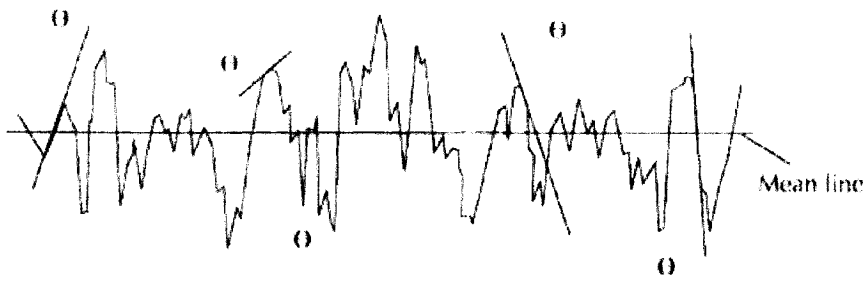

Fig.2.6: Slopes of profile ($R_{\Delta q}$)

$R_{\lambda q}$ is a root mean square wavelength of the profile.

$$R_{\lambda q} = \frac{2\pi}{R_{\Delta q}} R_q \tag{2.7}$$

Also

$$R_{sk} = \frac{1}{R^3{}_q}\left[\frac{1}{l_r}\int_0^{l_r} Y_i^3 dx\right] \tag{2.8}$$

$$R_{ku} = \frac{1}{R^4{}_q}\left[\frac{1}{l_r}\int_0^{l_r} Y_i^4 dx\right] \tag{2.9}$$

R_{sk} is the measure of the symmetry the profile about the mean line and R_{ku} is a measure of sharpness of the surface profile.

So far many parameters have been described. In practice the integrated and average parameters are the most widely used in engineering because they are measurable and stable. In practice Ra value is the most widely used to describe surface roughness. At present time many papers and research work use Ra as a parameter of surface finish for composite plate [15, 18].

2.3 Stochastic treatment of signals [76-79]

Surface profile can be considered as a random signal. Many concepts and methods in signal processing can be used to study surface quality. In this section basic concepts of random signals and background knowledge are introduced.

2.3.1 Random process

In many cases the signals of interest are very complex due to the randomness of the environment around them, which leaves them noisy and often corrupted. This often causes the information contained in the signal to be hidden and distorted. Surface profile is a kind of random signal. For this reason, it is important to understand the characteristics of random signals and to find a way to use them to understand the surface profile.

Most signals and systems deal strictly with deterministic phenomena. Each value of these signals is fixed and can be determined by a mathematical expression, rule, or table. Because of this, future values of any deterministic signal can be calculated from past values. For this reason, these signals are relatively easy to analyze as they do not change, and the accurate assumptions about their past and future behavior can be made. Unlike deterministic signals, random signals cannot be characterized by a simple, well-defined mathematical equation and their future values cannot be predicted. Rather, probability and statistical methods are used to analyze their behavior. Also, because of their randomness, values from a collection of signals are usually studied instead of analyzing one individual signal.

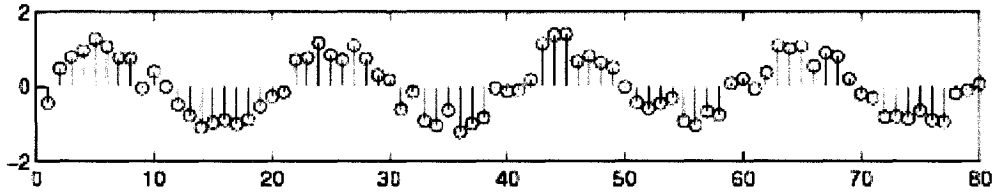

Fig. 2.7: Random signals of sine wave and added random noise

Fig. 2.7 shows a random signal produced by a sine wave plus a random component. As mentioned above, a collection of these signals instead of just one instance of the signal should be studied. This collection of signals is called a random process.

Random process is a family or ensemble of signals that correspond to every possible outcome of a certain signal measurement. Each signal in this collection is referred to as a realization or sample function of the process.

As an example of a random process, let us look at the Random Sinusoidal Process below. $f[n] = A\sin(\omega n+\varphi)$ is used to represent the sinusoid with a given amplitude and phase. Note that the phase and amplitude of each sinusoid are based on a random number and is different from each other, thus making this a random process (shown in Fig.2.8).

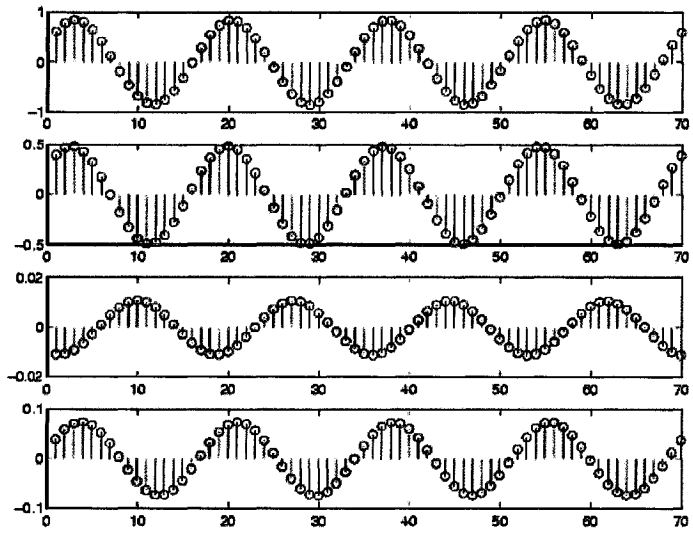

Fig.2.8: A random sinusoidal process

A random process is usually denoted by $X(t)$ or $X[n]$, with $x(t)$ or $x[n]$ used to represent an individual signal or waveform of the process.

For a discrete random process, sometimes it is just called a random sequence, t represents time and it has a finite number of values. If t can take on any value of time then the process becomes a continuous random process.

2.3.2 Probability functions of random process

The distribution P_X of a random variable X is simply a probability measure which assigns probabilities to events on the real domain. The distribution P_X is used to answer the following question:

What is the probability that X lies in some subset F of the real domain?

In practice, one summarizes P_X by its Probability Mass Function - pmf (for discrete variables only), Probability Density Function - pdf (for continuous variables), or Cumulative Distribution Function - cdf (for either discrete or continuous variables).

1. Probability Mass Function (pmf)

Suppose the discrete random variable X can take a set of M real values $\{x_1, \ldots, x_M\}$, then the pmf $p_X(x_i)$ is defined as:

$$p_X(x_i) = Pr[X = x_i] = P_X(\{x_i\}) \qquad (2.10)$$

where $\sum_{i=1}^{M} p_X(x_i) = 1$

2. Cumulative Distribution Function (cdf)

The cdf can describe discrete, continuous or mixed distributions of variable X and is defined as:

$$F_X(x) = Pr[X \leq x] = P_X\{(x_i)\} \qquad (2.11)$$

For discrete X:

$$F_X(x) = \sum_i \{p_X(x_i) \mid x_i < x\} \qquad (2.12)$$

F_X has the following properties

(1) $0 \leq F_X(x) \leq 1$

(2) $F_X(-\infty) = 0, F_X(\infty) = 1$

(3) $F_X(x)$ is non-decreasing as x increases

(4) $Pr[x_1 < X \leq x_2] = F_X(x_2) - F_X(x_1)$

(5) $Pr[X > x] = 1 - F_X(x)$

When there is no ambiguity one will often drop the subscript X and refer to the cdf as $F(x)$.

3. Probability Density Function (pdf)

The pdf for a given variable X is defined as the derivative of the cdf:

$$f_X = \frac{d}{dx} F_X(x) \qquad (2.13)$$

The cdf is the integral of the pdf and should always go from zero to unity for a valid probability distribution.

pdf has the following properties:

(1) $f_X(x) \geq 0$

(2) $\int_{-\infty}^{\infty} f_X(x)dx = 1$

(3) $F_X(x) = \int_{-\infty}^{x} f_X(\alpha)d\alpha$

(4) $\Pr(x_1 < X \leq x_2) = \int_{x_1}^{x_2} f_X(\alpha)d\alpha$

When there is no confusion that can arise, the subscript X is often dropped from formula and pdf is simply written as $f(x)$.

2.3.3 Stationary and nonstationary random processes

All random processes are composed of random variables, each at its own unique value at each point in time. Because of this, random processes have all the properties of random variables, such as mean, correlation, variances, etc. When dealing with groups of signals or sequences it will be important to show whether or not these statistical properties hold true for the entire random process. To do this, the concept of stationary processes has been developed.

A random process is called stationary process if all of its statistical properties are independent with time. A random process is called nonstationary if its property or properties vary with time.

- First-Order Stationary Process

A random process is classified as first-order stationary if its first-order probability density function remains equal regardless of any shift in time to its time origin.

Let x_{t_1} represent a given value of the random variable at time t_1, then a first-order stationary process satisfies the following equation:

$$f_x(x_{t_1}) = f_x(x_{t_1+\tau}) \tag{2.14}$$

The most important result of this statement, and the identifying characteristic of any first-order stationary process, is the fact that the mean is a constant, independent of any time shift. Below we show the results for a random process, X, which is a discrete-time signal, $x[n]$.

$$\overline{X} = m_x[n] = E[x(n)] = \text{ contant with time } t \tag{2.15}$$

- Second-Order and Strict-Sense Stationary Process

A random process is classified as second-order stationary if its second-order probability density function does not vary over any time shift applied to both values.

In other words, for values x_{t_1} and x_{t_2}.

$$f_x(x_{t_1}, x_{t_2}) = f_x(x_{t_1+\tau}, x_{t_2+\tau}) \tag{2.16}$$

for an arbitrary time shift τ.

This equation can also be described as

$$Pr\,[X(t_1) \le x_1, X(t_2) \le x_2] = Pr\,[X(t_1 + \tau) \le x_1, X(t_2 + \tau) \le x_2] \tag{2.17}$$

The random processes that satisfy (2.17) are often referred to as strict sense stationary (SSS). Autocorrelation function is often used to reveal one of most important properties of a second-order stationary process: If a second-order stationary process depends only on the time difference, then all of these types of processes have the following property:

$$R_{XX}(t, t+\tau) = E[X(t, +\tau)] = R_{XX}(\tau) \tag{2.18}$$

- Wide-Sense Stationary Process

The strict requirement of a SSS process is often more than necessary in order to adequately approximate the calculations on random processes.

Wide-sense stationary (WSS) definition is introduced to relaxed requirements yet still able to provide with adequate results.

A random process is called wide-sense stationary (WSS) process if it satisfies

1. $\overline{X} = E\,[x\,[n]]$ = constant

2. $E\,[X(t + \tau)] = Rxx\,(\tau)$

Note that a second-order (or SSS) stationary process will always be WSS; however, the reverse will not always hold true.

2.3.4 Basic properties and operations of a random process

1. Expected values of probability functions

The expected value of a function $f(\cdot)$ of a random variable X is defined as

$$E[f(X)] = \int_{-\infty}^{\infty} f(x) p_X(x) dx \qquad (2.19)$$

Some special cases for a random process's expected value:

(1) $f(X) = X$. The expected value or mean of a random variable is the center-of-mass of the probability density function. Expected value is denoted as m_X or just m when the meaning is clear. An important property of the expected value of a random variable is linearity: $E[aX] = aE[X]$, where a is a scalar.

(2) $f(X) = X^2$. $E[X^2]$ is known as the mean squared value of X and represents the "power" in the random variable.

(3) $f(X) = (X - m_X)^2$. The so-called second central difference of a random variable is its variance, usually denoted by σ_X^2. This expression for the variance simplifies to

$$\sigma_X^2 = E[X^2] - (E[X])^2 \qquad (2.20)$$

(4) $f(X) = X^n$. $E[X^n]$ is the nth moment of the random variable and $E[(X - m_X)^n]$ the n^{th} central moment. The nth moment can also be expressed as $m_i = E[X^i]$.

2. Correlation and covariance

Correlation and covariance are techniques for measuring the similarity of one signal to another. For a random process $X(t, \alpha)$ they are defined as follows.

(1) Auto-correlation function:

$$r_{XX}(t_1,t_2) = E[X(t_1,\alpha)X(t_2,\alpha)] = \iint x_1 x_2 f(x_1,x_2)dx_1 dx_2 \qquad (2.21)$$

where the expectation is calculated for all $\alpha \in A$ (i.e. the whole ensemble), and $f(x_1, x_2)$ is the joint pdf, x_1 and x_2 are samples taken at times t_1 and t_2 from the same random event α of the random process X.

(2) Auto-covariance function:

$$C_{XX}(t_1,t_2) = E[(X(t_1,\alpha) - \overline{X(t_1)})(X(t_2,\alpha) - \overline{X(t_2)})]$$

$$= \iint_{x_1 x_2} (x_1 - \overline{X(t_1)})(x_2 - \overline{X(t_2)}) f(x_1,x_2)dx_1 dx_2 \qquad (2.22)$$

$$= r_{xx}(t_1,t_2) - \overline{X(t_1)}\,\overline{X(t_2)}$$

where the same conditions apply as for auto-correlation and the means $\overline{X(t_1)}$ and $\overline{X(t_2)}$) are taken over all $\alpha \in A$. Covariances are similar to correlations except that the effects of the means are removed.

(3) Cross-correlation function:

Let $X(t, \alpha)$ and $Y(t, \alpha)$ be two different processes from the same random event α, the cross-correlation is defined as

$$r_{XY}(t_1,t_2) = E[X(t_1,\alpha)Y(t_2,\alpha)] = \iint x_1 y_2 f(x_1,y_2)dx\ dy \qquad (2.23)$$

where $f(x_1, y_2)$ is the joint pdf and x_1 and y_2 are samples of X and Y taken at time t_1 and t_2 from the same random event α. Again the expectation is computed for all $\alpha \in A$

(4) Cross-covariance function:

If $X(t, \alpha)$ and $Y(t, \alpha)$ are two processes similar to where is described in (3) then the Cross-covariance funcion for X(t, α) and Y (t, α) is defined as

$$C_{XY}(t_1,t_2) = E[(X(t_{1,},\alpha) - \overline{X(t_1)})(Y(t_2,\alpha) - \overline{Y(t_2)})]$$

$$= \iint_{x_1 y_2} (x_1 - \overline{X(t_1)})(y_2 - \overline{Y(t_2)}) f(x_1, y_2) dx_1 dy_2 \qquad (2.24)$$

$$= r_{xy}(t_1,t_2) - \overline{X(t_1)}\,\overline{Y(t_2)}$$

2.4 Fourier and filtering analyses [80-83]

2.4.1 Basic concept of Fourier transforms

Fourier, an eighteenth-nineteenth-century mathematician, originally established that any sequence of data could be regarded as the sum of a series of sinusoidal functions (sine and cosine waves) with specified amplitude, frequency and phase. Fourier analysis calculates the amplitude and phase for each frequency of wave, and the data can then be represented in this new form - the data are said to be transformed into the frequency domain.

The spectrum of the signals can be achieved by Fourier transform for any signals. Fourier analysis includes the Fourier transform of continuous time signals and discrete Fourier transform. Calculation formulae of frequency and spectrum can be referred to in appendix.

2.4.2 Basic concept of filtering [81]

In signal processing, the function of a filter is to remove unwanted parts of the signal, such as random noise, or to extract useful parts of the signal, such as the components lying within a certain frequency range.

The following block diagram (Fig.2.9) illustrates the basic idea.

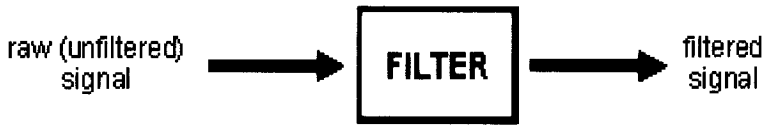

Fig.2.9: Filtering of signals

There are two main types of filter, analog and digital. They are different in their physical makeup and in how they work.

An analog filter uses analog electronic circuits made up from components such as resistors, capacitors and op amps to produce the required filtering effect. Such filter circuits are widely used in such applications as noise reduction, video signal enhancement, graphic equalisers in hi-fi systems, and many other areas.

There are well-established standard techniques for designing an analog filter circuit for a given requirement. At all stages, the signal being filtered is an electrical voltage or current which is the direct analogue of the physical quantity (e.g. a sound or video signal or transducer output) involved.

A digital filter uses a digital processor to perform numerical calculations on sampled values of the signal. The processor may be a general-purpose computer such as a PC, or a specialised DSP (Digital Signal Processor) chip.

The analog input signal must first be sampled and digitised using an ADC (Analog to Digital Converter). The resulting binary numbers, representing successive sampled values of the input signal, are transferred to the processor, which carries out numerical calculations on them. These calculations typically involve multiplying the input values by constants and adding the products together. If necessary, the results of these calculations,

which now represent sampled values of the filtered signal, are output through a DAC (Digital to Analog Converter) to convert the signal back to analog form.

Note that in a digital filter, the signal is represented by a sequence of numbers, rather than a voltage or current.

The following diagram (Fig.2.10) shows the basic setup of such a system.

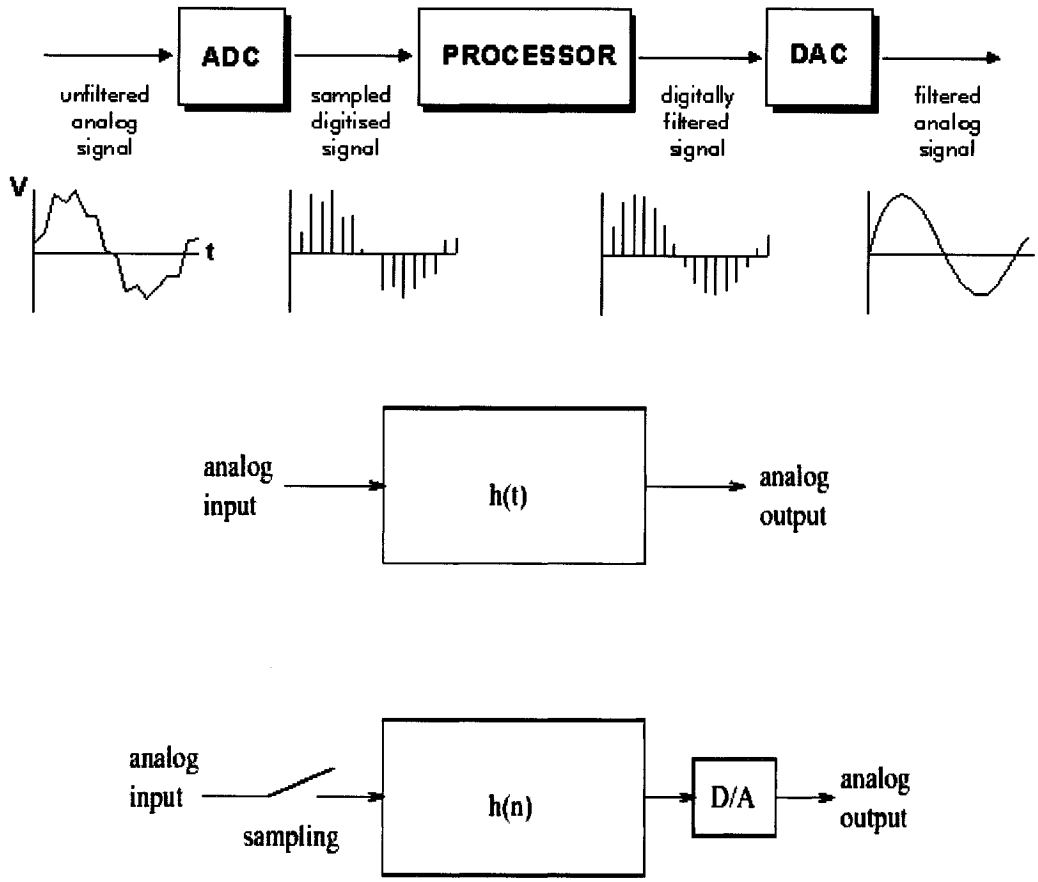

Fig. 2.10: Digital filter and analog filter

Analogue filter takes an analog input signal and output analog signal. Digital filters, with the sampling device and digital-to-analog converter, can do the same job as analog filters. Analog filters are specified by its impulse response $h(t)$ and the output signal $y(t)$ for input signal $x(t)$ is given by the convolution integral.

$$y(t) = \int x(t-u)h(u)dt \qquad (2.25)$$

Similarly, digital filters are specified by its impulse $h(n)$ and the output sequence $y(n)$ for the input sequence (samples of input analog signal) $x(n)$ by the discrete convolution

$$y(n) = \sum_{k=0}^{N} h(k)x(n-k) \qquad (2.26)$$

The filter design problem is to design the impulse response *h(n)* so that the digital filter, together with the sample and D/A converter, performs the same processing as the analog filters. There are many possible ways to pick h(n) to implement filtering.

Fig. 2.11 shows the four basic frequency responses. The purpose of these filters is to allow some frequencies to pass unaltered, while completely blocking other frequencies. The passband refers to those frequencies that are passed, while the stopband contains those frequencies that are blocked. The transition band is in between. A fast roll-off means that the transition band is very narrow. The division between the passband and transition band is called the cutoff frequency. In analog filter design, the cutoff frequency is usually defined to be where the amplitude is reduced to 0.707 (i.e., -3dB). Digital filters are less standardized, and it is common to see 99%, 90%, 70.7%, and 50% amplitude levels defined to be the cutoff frequency.

The four fundamental filters are:

Lowpass -- blocks high frequencies, allowing low frequencies through

Highpass -- blocks low frequencies, allowing high frequencies through

Bandpass -- blocks all frequencies except those within a certain range

Bandstop -- blocks only the frequencies within a certain range, allowing all others to pass through

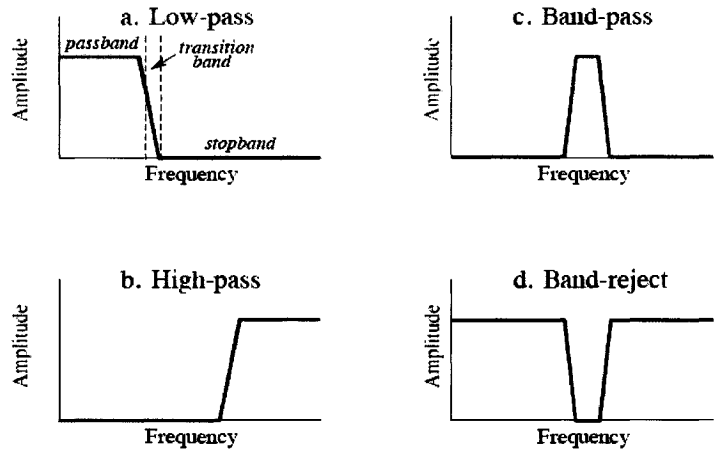

Fig. 2.11: Ideal frequency domain representations of the four fundamental filters

2.5 Basic concept of similarity analysis [88-90]

In our daily life, pattern recognition is characteristic to all living organisms. However, different creatures recognize differently. If a human would recognize another human by sight, by voice or by handwriting, a dog may recognize a human or other animal by smell thirty yards away which most humans are incapable of doing. A blind person would recognize various items just by touching them. But recognition is not restricted to objects that can be identified using biological senses. In a conversation we can suddenly identify an old argument that we heard years ago. All of these examples are classified as recognition. It is well known that the recognition actually is done by comparison with their similarity. What is similarity and how to evaluate similarity between objects? These questions will be discussed below.

Most analyses undertaken are based on the assessment of an object in relation to some externally defined scale, such as, a measurement scale on a roughness sensor. This allows observations to be theories or laws which are defined in terms of measurements, for

example, surface roughness curve. However, such measurement can only provide some signals for the surface. The crucial aspect of an observation may not be that a measurement of plate A is x and of plate B is y, but that the difference between them is x-y. The basis of analysis will be measures of similarity or difference between objects. This approach is very important because in engineering many problems are, and should be, done on the basis of comparison between objects. It is also an important means and pattern in pattern recognition.

There are two main categories of similarity measures.

1. Distance coefficients.
2. Correlation coefficients.

Cross correlation analysis can describe similarity between objects. Cross correlation coefficient is a kind of processing of normalization for covariance. When C_{xy} is defined by equation (2.24) and σ_x, σ_y are defined by equation (2.20), cross correlation coefficient γ_{xy} for two random variables X and Y can be expressed as

$$\gamma_{xy} = \frac{C_{xy}}{\sigma_x \sigma_y} \tag{2.27}$$

If $|\gamma_{xy}| = 1$, random variables X and Y are in total correlation; if $\gamma_{xy} = 0$, random variables X and Y are of no correlation. Therefore, cross correlation coefficient is an indicator of similarity. It can show the extent of correlation for the two random variables.

Distance coefficient is an important method of describing similarity between objects. It is easy to see how distance between two points can be used to measure similarity. Zero distance between two points clearly means that there are no numerical differences between two objects; they are completely similar. Greater distances correspond to lesser

similarity, so distance measures are often called dissimilarity, rather than similarity coefficients.

The most intuitive distance measure is the direct straight line distance- Euclidean distance. In two dimensions (i.e. with two variables x_1 and x_2) the distance d_{AB} between two points A and B is obviously the length of the hypotenuse of a triangle, where the sides are $(x_{1A}-x_{1B})$ and $(x_{2A}-x_{2B})$:

$$d_{AB} = \sqrt{(x_{1A} - x_{1B})^2 + (x_{2A} - x_{2B})^2} \tag{2.28}$$

In the multivariate general case (with m variables) this becomes as follows.

Euclidean distance coefficient:

$$d_{AB} = \sqrt{\frac{1}{m}\sum_{i=1}^{m} (x_{iA} - x_{iB})^2} \tag{2.29}$$

Manhattan distance is the simple sum of absolute differences.

Manhattan distance coefficient:

$$d_{AB} = \frac{1}{m}\sum_{i=1}^{m} |x_{iA} - x_{iB}| \tag{2.30}$$

2.6 The basic concept of trace mix[84, 91]

Trace mix is a method used to reduce the variation from trace to trace. The input data can be processed with trace mix. For each trace in the mix, the value at a given sample location is multiplied by a weighting factor. All the weighted values are then added, and this sum is assigned as the sample value for the central trace. The "rolling" filter then moves forward one trace, and the process is repeated. At the edges of the data, when the specified number of traces for mixing is not available, the filter uses the available traces to "roll-on" and "roll-off."

This weighted trace mix is designed to reduce the variation from trace to trace, thus producing a smoother looking section and enhancing the continuity of material. It is smooth treatment for measurement data. On average, smoothed profile of the surface of the material reflects the surface characters of this material. Fig. 2.12 shows an example of trace mix. The sum of the weighting factors is always 1. So if one chooses equal weighting for a trace mix of three traces, the samples from each trace will be multiplied by 0.333.

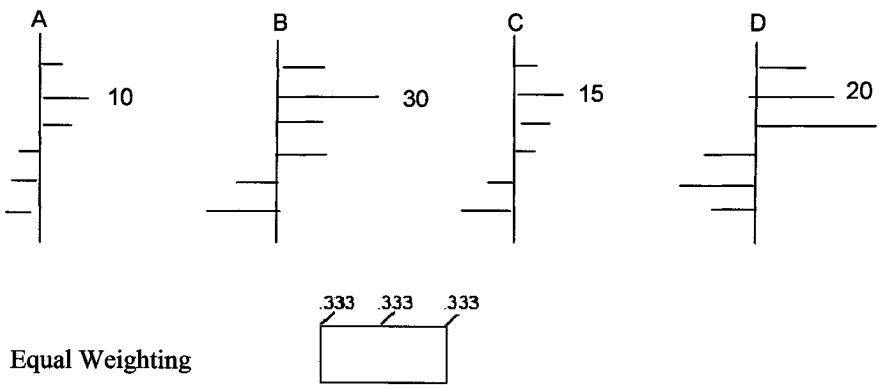

Fig. 2.12: An example of a trace mix of 3

$$B^* = A*0.333+B*0.33+C*0.333$$

$$=10*0.333+30*0.333+15*0.333$$

$$=18.31 \qquad (2.31)$$

The "rolling" the filter moves forward one trace to C.

$$C^* = B*0.333+C*0.333+D*0.333$$

$$=30*0.333+15*0.333+20*0.333$$

$$= 21.67 \qquad (2.32)$$

The "rolling" the filter move forward one trace to D.

$$D^*= C*0.333+ D*0.333+0* 0.333$$

$= 15*0.333+20*0.333+0*0.33$

$= 11.67$ (2.33)

The weighting factor can be different, for example 1/4, 1/2, 1/3 and so on.

2.7 Use of techniques of signature treatment for surface signature analysis

It has been known that parameters used to evaluate surface finish are all expressed as some type of statistical average. Methods of statistical average are used to describe surface quality; so far this is the most popular method of evaluation of material surface finish. However, the method of evaluation often does not consider many characteristics of material surface very well. The surface of composite material is more complex. The gloss of a surface would affect perception of people. Humans often judge the appearance of the material surface by visual observation. Actually, there are many technical standards and several parameters to describe surface properties. Though many statistical average parameters are used to describe surface profile, none of them can indicate which one would affect human perception for the surface. That is the reason why human still assess surface of composite panel by physical perception.

For example, different surface waveforms can have the same surface roughness Ra. It is clear that different surface profiles would have different frictional properties. Such as, for the surface of an anti-friction part, the shape of its surface profiles should be considered because parts having the same Ra values may not have same the frictional property. Geometric shapes of surface profiles would affect on the frictional properties of the part.

This simple example shows that conventional statistic average method would exclude many surface characteristics. The parameter defined by the method can be used to describe the problem only from one view. Human judgments depend on a lot of quantity information from all views.

These analyses show research work should surpass conventional evaluation method and develop new ideas or model. The key for success is to extract all information that can reflect the various aspects of the surface properties and use it during the evaluation process.

In the last decades, human society has entered into information epoch. New knowledge and technology of information processing provide us with powerful tools for research on surface finish evaluation. It is possible that newly developed theory and software system of artificial intelligence and pattern recognition are replacing human eyes to discriminate surface quality levels.

Based on this discussion, new approaches are proposed to find a way to distinguish composite surface of approximate quality.

A few new approaches have been attempted to search for a good technique to distinguish the quality of the surface of composite panels made by RTM process with variables in process parameters. The technique should also be able to indicate whether a surface is of class A quality and if not, then how far is it from class A quality. The approaches consist of following.

1. Probability distribution profiles of Ra:

Ra is the absolute average of amplitudes of one scanned profile. When many profiles over a surface are obtained, there are variations in Ra. The distribution profile of these Ra

values may provide an indicator of the quality of the surface. For example, if a surface is perfectly smooth such that all the profiles have the almost same Ra values, then the probability profile should be a vertical line as shown in Fig. 2.13. If Gaussian distribution function is used to fit the data, then some of the characteristics of distribution curves may be used to study the surfaces. For instance, the better is the quality of the surface, the narrower is the width of the distribution profile (shown in Fig. 2.14).

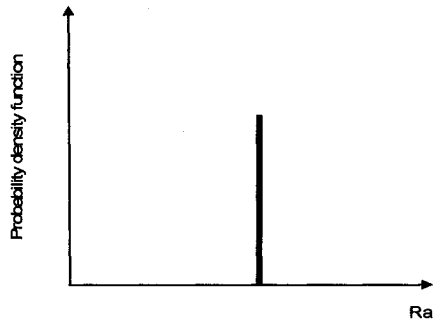

Fig.2.13: The probability distribution of Ra in a surface of equal Ra

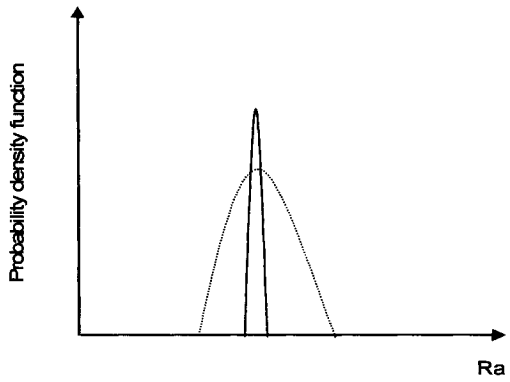

Fig. 2.14: The schematic diagram of the probability density distribution of Ra

2. Frequency and spectrum analysis:

Apart from amplitude analysis on Ra, the profiles of a surface may consider roughness and waviness, which represent waveforms of different frequencies. By converting the

signatures from the time domain to frequencies domain, frequency characteristics of signal can be revealed and this may be used to study the quality of surfaces.

3. Filtering analysis:

Continuing from the discussion in item (2) above, there are ranges of frequencies in the spectrum of frequencies of the surface signatures that may reveal special characteristics of the surface. Filtering analysis may be used to bring out these frequency ranges for surface study.

4. Similarity or dissimilarity analysis:

As mentioned above, the ability to characterize a surface may be done by absolute quantities such as Ra, distribution of Ra, frequency analysis or filtering analysis. However, there are situations where comparison of surface under study with a reference surface may reveal characteristics that are not possible using absolute quantities. Similarity or dissimilarity analysis of the surfaces under study with a reference surface was also investigated for the study of the composite surface.

The above four approaches have been investigated. The details and results from these techniques will be presented in chapters 4 and 5.

Chapter 3

Experimental measurement and current approaches to treat the data

In this chapter work on the measurement of surface profiles form plates supplied from Ford Motor Company is described. The building of a new measurement system is discussed. The surfaces of three plates from Ford Motor Company (painted steel plate, RTM plates without low profile additive plate 2a, RTM plate with low profile additive plate 2b) were measured using the profilometer. The data and results measured are presented and discussed.

3.1 Building a measurement system for surface profiles

3.1.1 Primary design of measurement instrument

The purpose of building the instrument was to obtain surface information as much as possible. First task was to select available sensors to construct an inexpensive instrument that can be used to measure the surface profile. There are a few difficulties for choosing available commercial sensors with which the accuracy and resolution are high enough. Many contact sensors and laser sensors have been evaluated [92]. However, their accuracy and resolution do not seem to be high enough if they are directly used. The accuracy and resolution of typical contact sensors and laser sensors depend on the

accuracy of several micrometers. Fig 3.1 shows examples of contact and non-contact sensors.

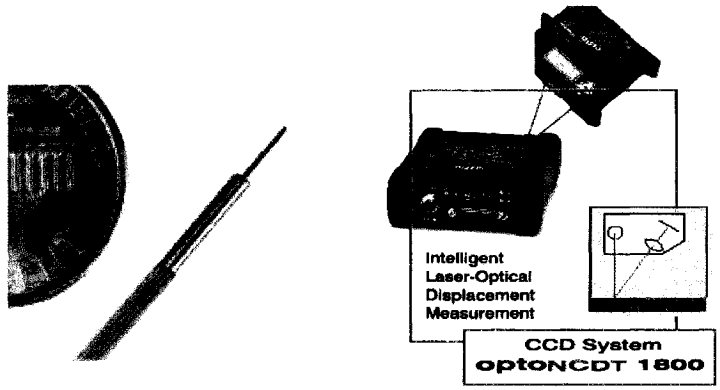

Fig. 3.1: Microminiature DVRT® and laser sensors

At first, Mitutoyo Surf 301 was used to measure the surface of composite panel [43]. This is a device of contact measurement. It was found that the contact measurement can be used for composite panel since the surface of composite panel is sufficiently hard. Table 3.1 shows the initial experimental data for composite panel surface roughness.

Table 3.1: The initial experimental data for surface roughness of a composite panel

Parameters / Position	R_a (μm)	R_y (μm)	R_z (μm)	R_q (μm)
Area 1	0.5	3.78	2.14	0.62
Area 2	0.43	3.5	1.96	0.56
Area 3	0.29	2.42	2.58	0.38
Area 4	0.25	3.83	3.05	0.41
Average Value	***0.37***	***3.38***	***2.43***	***0.49***

Series 4655 OEM USB roughness sensor [93], which is an optical sensor, was also used to measure the surface of another composite panel. The average R_a is 0.5 micrometer. These experiments and data show:

- Contact measurement can be used to measure the surface roughness of composite panel, and non-contact system is more expensive than contact system.
- The main difficulty for building an inexpensive and higher accuracy measurement system was to develop new higher accuracy sensors.
- The data measured from composite panel indicate that the surface roughness for composite panel is relatively higher than that of metal surface..

These observations and primary research results were used to build the measurement instrument.

3.1.2 The Design of an instrument for surface profiles measurement

Based on results of a few experiments, the design of a measurement system was done and is shown in Fig. 3.2. The method of contact measurement is used in the design plan because the sensor is inexpensive and has enough resolution and accuracy. X-Y table can be used to fix the sample. The sensors in X-Y direction can be used to control the position to be measured. The position of X-Y table needs to be accurate, so the X-Y table of a microscope was used in the design. In this way, surface profile of different positions can be achieved.

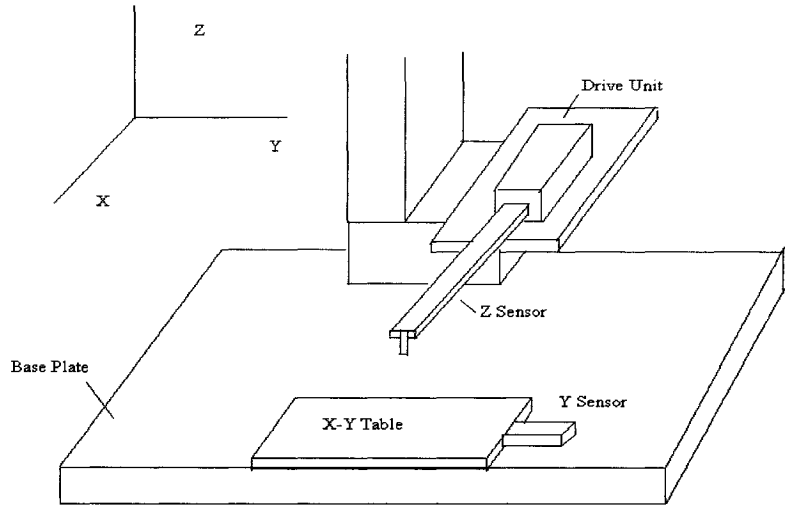

Fig. 3.2: Schematic of the profilometer

3.1.2.1 Structures of the instrument

The main parts of the instrument are as follows:

- A SJ402 sensor is used in Z-direction and drive unit is able to scan 50mm in X-direction. Accuracy of measurement is 1.25nm/800um.
- Micrometer heads are used as Y-sensor and X-Y table moves in Y-direction. The Max displacement is 50mm. Resolution of control is 0.001mm.
- Z-sensor can be adjusted; Z stand can move in Z- direction and can also move on the base plate.

3.1.2.2 Measurement and data acquisition system

The relationships among all parts are shown in Fig. 3.3.

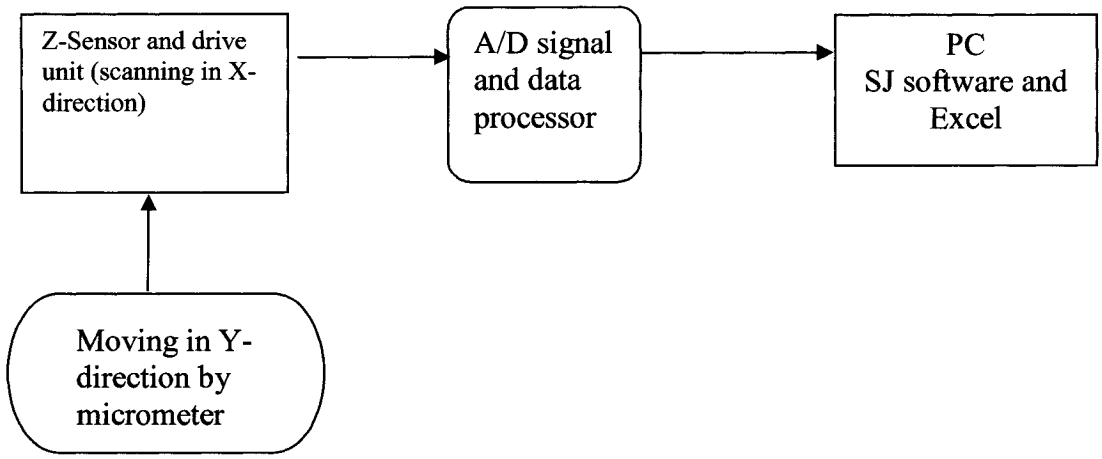

Fig. 3.3: Relationships among all parts in the measurement system

- Computer can control scanning length in X-direction. The maximum scanning length is 50 mm.
- More than 30 evaluation parameters and raw data as well as graphs can be attained by data processing of SJ software and exported to Excel.
- A few surface profiles' evaluation parameters can be obtained by combination of moving X-Y table in Y-direction with Z-sensor's scanning in X-direction.

3.1.2.3 Schematic principle of a surface profiling instrument [94]

- **Coordinate system**

It is convenient to use a standard right-handed coordinate system when referencing profile or surface topography measurements. If X and Y are the coordinates in the plane of the surface and Z is displacement from the surface, then the coordinate

system is demonstrated as below. X as the direction of travel of the transducer across the surface is chosen (shown in Fig. 3.4).

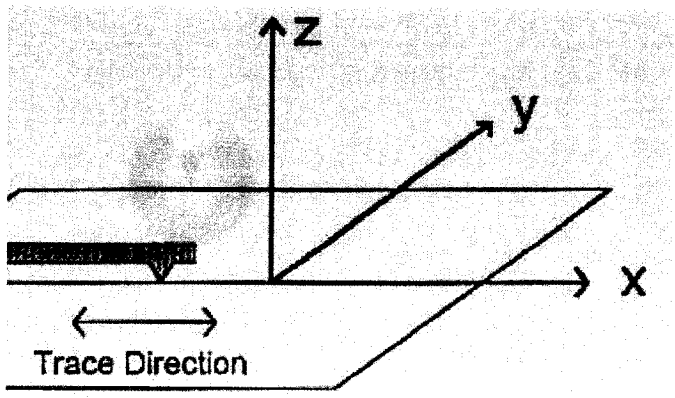

Fig. 3.4: The coordinate system for profiling a surface

This coordinate system differs from the 2-D coordinate system that is often used in simple profiling, namely x horizontal and y vertical. By making z the vertical displacement one can use the same coordinate system whether we are discussing 2-D profiles or 3-D surfaces.

- **The instrument measuring loop**

The measuring loop of an instrument comprises of all the components of the instrument and fixture that contribute to converting the real surface profile into an electrical (analog or digital) representation of the profile (see Fig. 3.5).

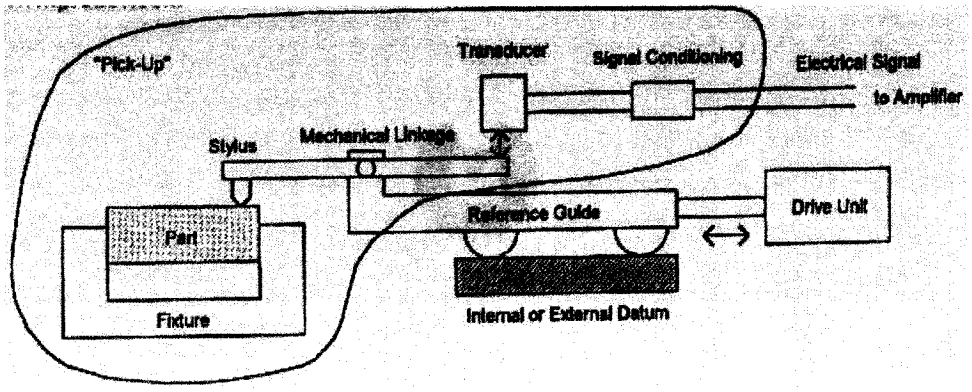

Fig. 3.5: The measuring loop of a profiling instrument

- **Internal (Skid) reference datum**

Several methods can be used to establish an instrument reference line from which profile height can be measured. The simplest approach is to use a skid riding on the surface itself as a reference. Usually the arm to which the skid is tied pivots a long distance away from the measurement. The skid assembly and transducer are designed to measure the difference in height between the skid height and the stylus tip height. The skid rides over imperfections in the surface and acts as a mechanical filter of the surface: it smoothes out longer wavelength undulations on the surface. Therefore, this approach is suitable for roughness profile measurement only (see Fig. 3.6).

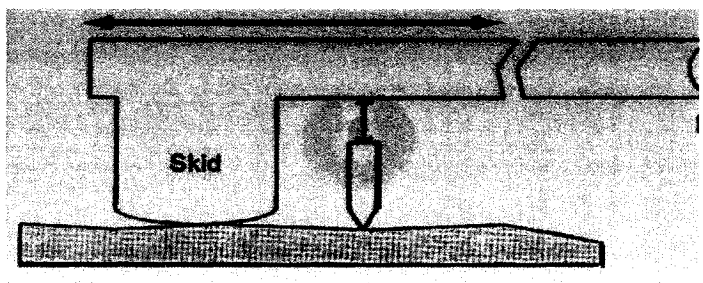

Fig. 3.6: The structure of skid- attached nosepiece external reference datum

More advanced profiling instruments measure a surface relative to an external datum as shown below (see Fig.3.7).

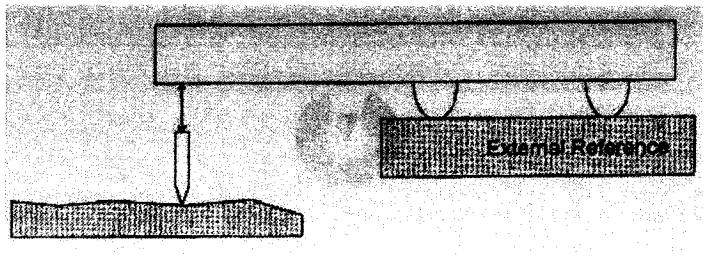

Fig. 3.7: The structure of skidless nosepiece

- **Surface measurement transducers**

Linear variable differential transformers (LVDT*s) are widely used as high quality displacement transducers in surface finish measurement (see Fig.3.8).

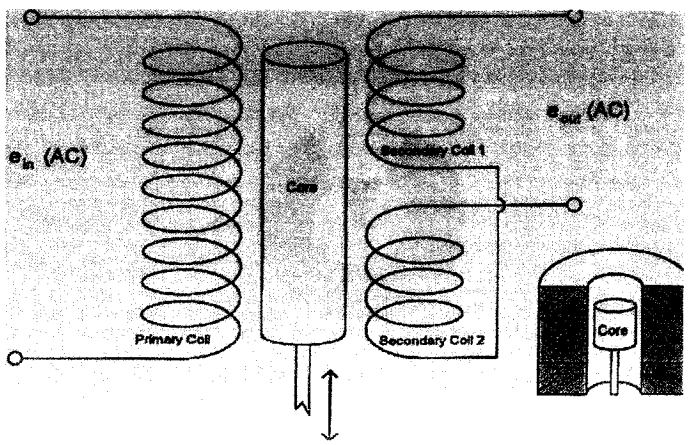

Fig. 3.8: A linear variable differential transformer (LVDT) consists of two transformers

LVDT's function is to compare the output of two parallel transformers with a common core. As the core moves up or down, one or the other transformer becomes more efficient because of better magnetic coupling between the primary and secondary coils. In

the simplest wiring scheme, the two transformers are wired in series. Then the voltage out is proportional to the displacement and the direction of displacement from the zero point is indicated by the phase of the output relative to the input. The output has the opposite phase in one case because the transformers are wired in opposite directions. More complicated detection electronics look at both transformers independently.

LVDT is linear and repeatable. It has a definite zero point and has good response as far as the highest frequency (shortest profile wavelength) it can resolve. It has the disadvantage of being somewhat larger than other surface finish transducers.

LVDT are commonly used in profiling and contouring instruments.

- **Signal processing**

Once a profile has been converted to an electrical signal it enters the amplifier of the instrument where it is not simply amplified, but converted to a digital representation and analyzed for all the desired surface parameters. Higher capability instruments can display parameter results and plot profiles. Fig. 3.9 shows schematic diagram for signal processing.

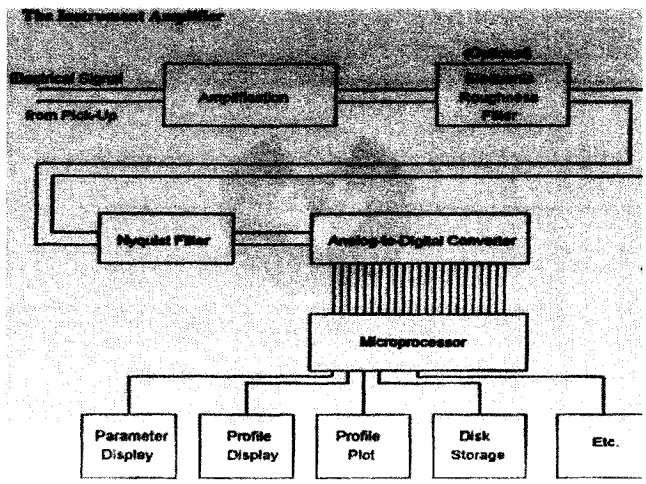

Fig. 3.9: Schematic diagram for signal processing

3.1.2.4 Design and installation of the measurement system

1. Main structural parts:

- X-Y stage (Moving displacement 50mm)
- Micrometer head (measuring X-Y displacements)
- Transfer stand and small plate (fixing sensor, moving in Z direction)
- Base plate (fixing X-Y stage and transfer stand)
- SJ402 sensor (scanning length 50mm for surface measuring)
- A/D signal and data processor
- PC and printer
- SJ software and other Software for processing data

The system for measurement of surface profile is shown in Fig. 3.10.

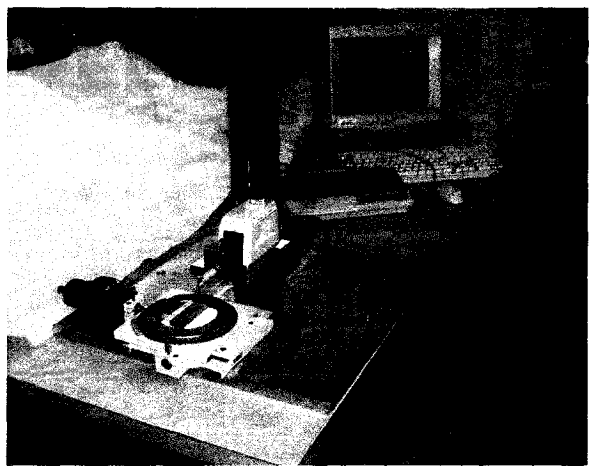

Fig. 3.10: The system for measurement of surface profile

X-Y stage is shown in Fig. 3.11. It can move in 50x50mm.

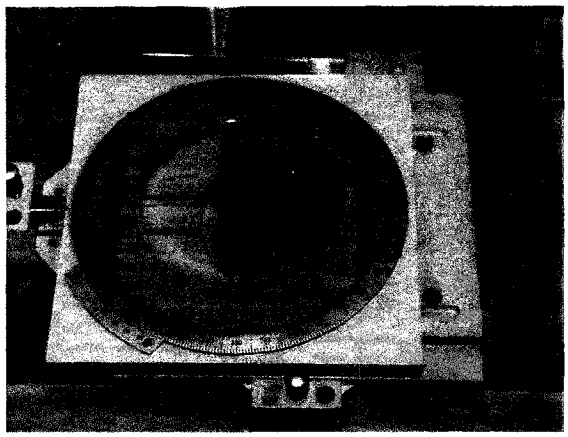

Fig. 3.11: X-Y stage (moving 50x50mm)

Micrometer Head (Controlling displacement in Y- Direction) is shown in Fig. 3.12.

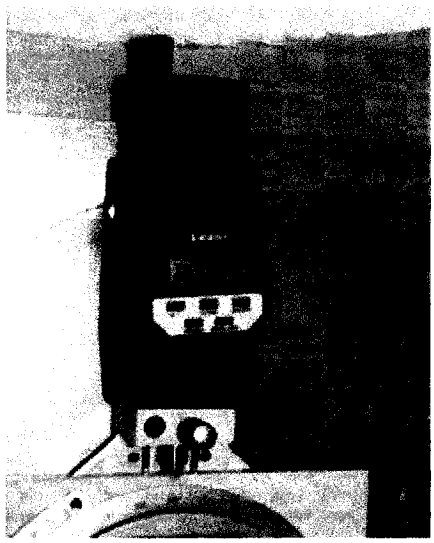

Fig.3.12: Micrometer head (controlling displacement in Y- direction)

Transfer stand is shown in Fig. 3.13. A sensor can be fixed on it and can also be moved in Z direction.

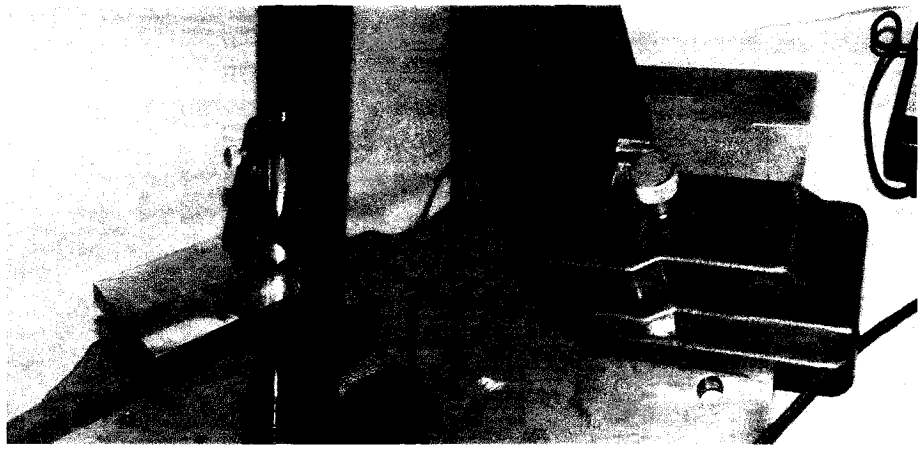

Fig. 3.13: Transfer stand

SJ 402 Sensor (It is fixed on the small plate in Transfer stand and can scan 50mm) is shown in Fig. 3.14.

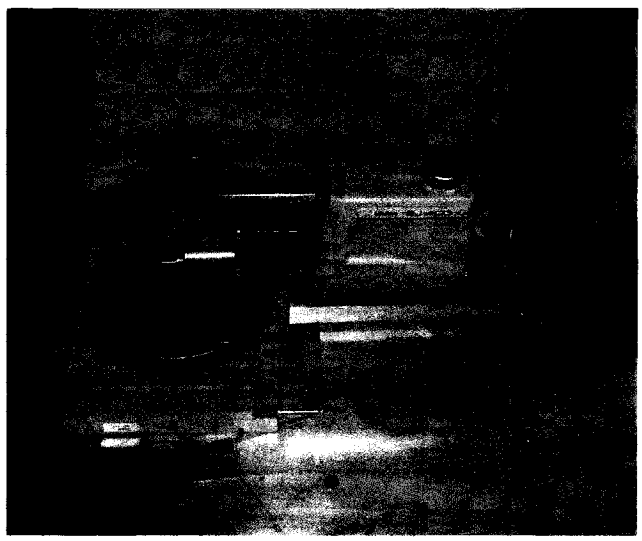

Fig.3.14: SJ 402 sensor

(It is fixed on the small plate in transfer stand and can scan 50mm)

A green button can be used to adjust the level of sensor as shown in Fig. 3.15.

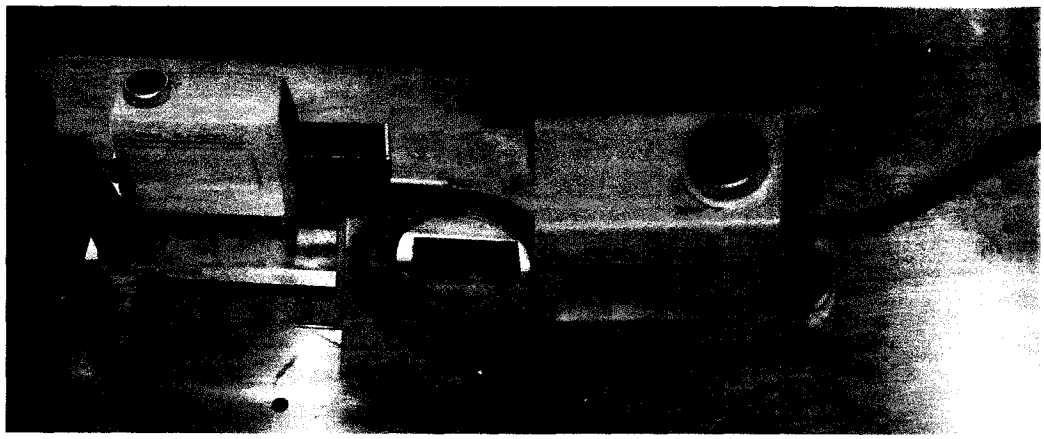

Fig. 3.15: Adjustment level of sensor by a green button

A/D signal and data processor is shown in Fig. 3.16.

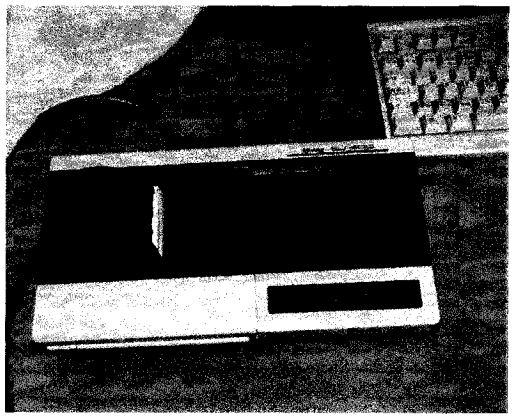

Fig. 3.16: A/D signal and data processor

A PC connecting data processor can do remote controlling measuring process as shown in Fig. 3.17. The PC can acquire raw data, more than 30 parameters and analysis graphs for surface roughness.

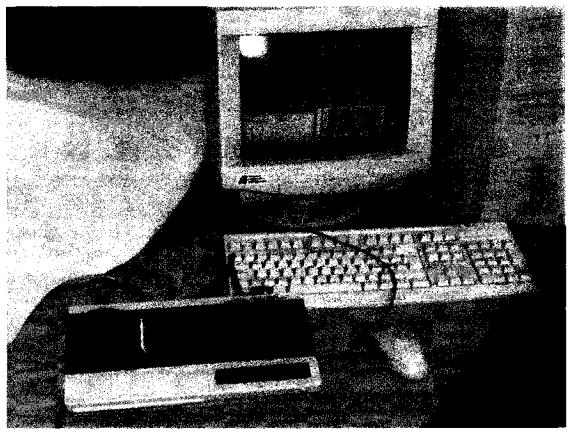

Fig. 3.17: A PC connecting data processor can do remote controlling measuring process

2. An example of a scanned profile

The surface profile of a composite panel, R341-CUF-20, was measured by using the system. Results are shown in Fig. 3.18.

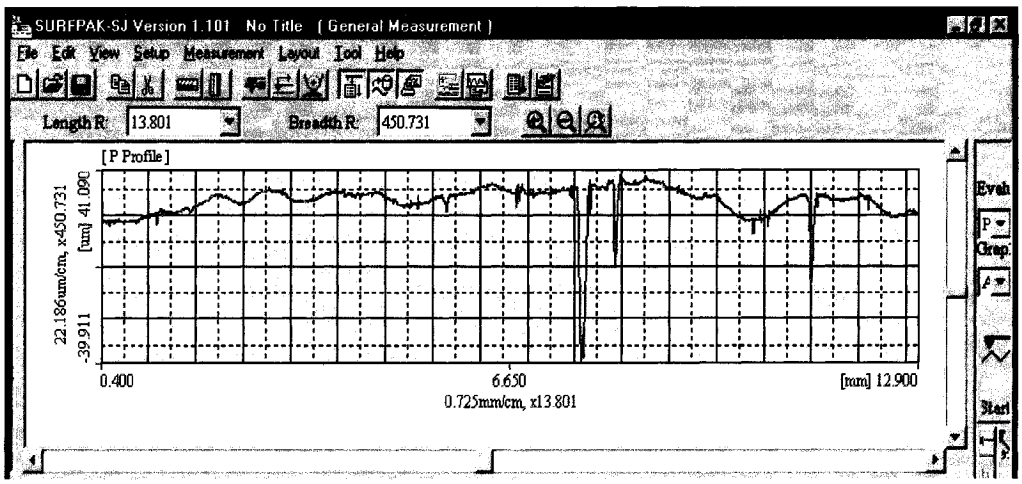

Fig. 3.18: A curve of surface profile from a composite panel, R341-CUF-20

In the measurement, the measurement length is about 13.33mm. Ra = 2.998 μm. Five world main standards for surface evaluation can be used and about 30 evaluation parameters for surface analysis can be calculated.

3.2. Measurements and discussions of surface profiles from plates supplied from Ford Motor Company

Ford Motor Company supplied 3 plates, steel, 2a and 2b. The steel plate has painted surface, 2b is a composite plate made by RTM with Low Profile Additive (LPA), 2a is a composite plate made by RTM without LPA.

On each plate, 25 lines were scanned using the profilometer. The length of each line is 13.3 mm. The distance from each line to the other is 0.5 mm.

The software used for the measurement system is Surfpark [72]. The software has 4 standards. They are Oldmix, JIS1994, ISO 1997 and ANSI1995 [50]. Each standard has definitions for the surface parameters such as Ra, Ry, Rq and so on. For the purpose of this thesis, any of the four standards can be used. Oldmix standard is used. The cut-off wavelength is 2.5 mm. Typical surface roughness curves are shown in Fig. 3.19.

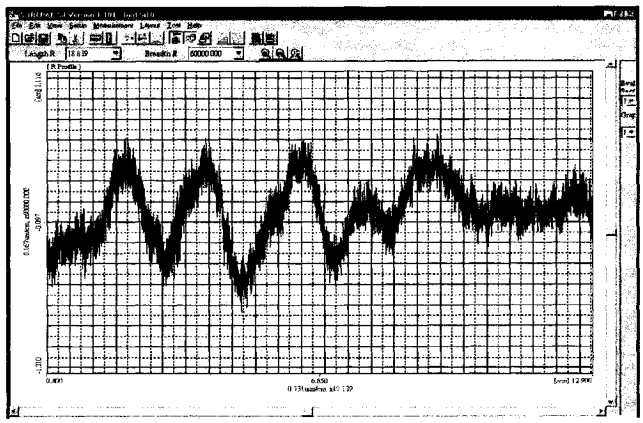

2a

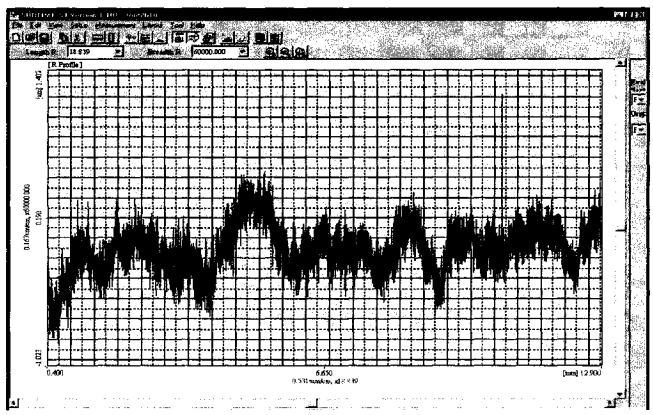

2b

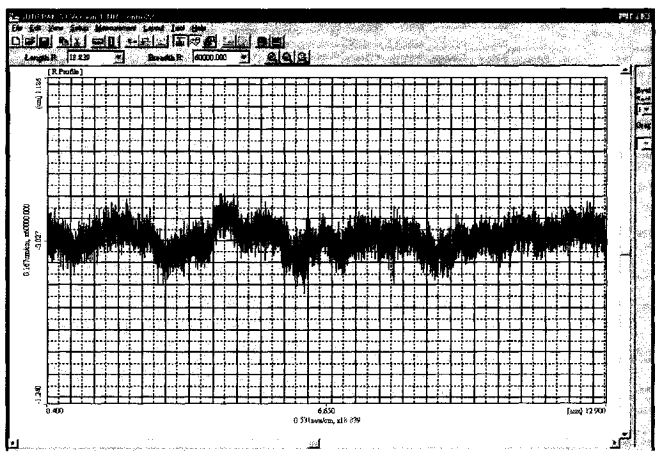

Painted steel plate

Fig. 3.19: Typical roughness curves of composite plate 2a, plate 2b and painted steel plate

1. Ra values

The roughness parameters Ra for the three samples are calculated and are shown in Table 3.2 and Fig. 3.20. Each trace can be also transferred to digital data to output in Excel format and then transferred to binary data in order to input it to analysis software system.

Table 3.2: Ra of painted steel plate, and composite plates 2a and 2b

Measurement	2a Ra (μm)	2b Ra (μm)	Steel Ra (μm)
1	0.213	0.202	0.077
2	0.2	0.2	0.092
3	0.184	0.22	0.084
4	0.236	0.176	0.073
5	0.267	0.177	0.074
6	0.211	0.178	0.075
7	0.231	0.207	0.068
8	0.221	0.202	0.073
9	0.177	0.195	0.077
10	0.201	0.165	0.07
11	0.246	0.171	0.077
12	0.227	0.162	0.068
13	0.225	0.137	0.087
14	0.187	0.193	0.079
15	0.175	0.194	0.077
16	0.191	0.254	0.091
17	0.26	0.227	0.078
18	0.247	0.203	0.068
19	0.247	0.187	0.077
20	0.218	0.164	0.082
21	0.218	0.184	0.083
22	0.217	0.233	0.088
23	0.235	0.229	0.082
24	0.236	0.204	0.076
25	0.22	0.221	0.08

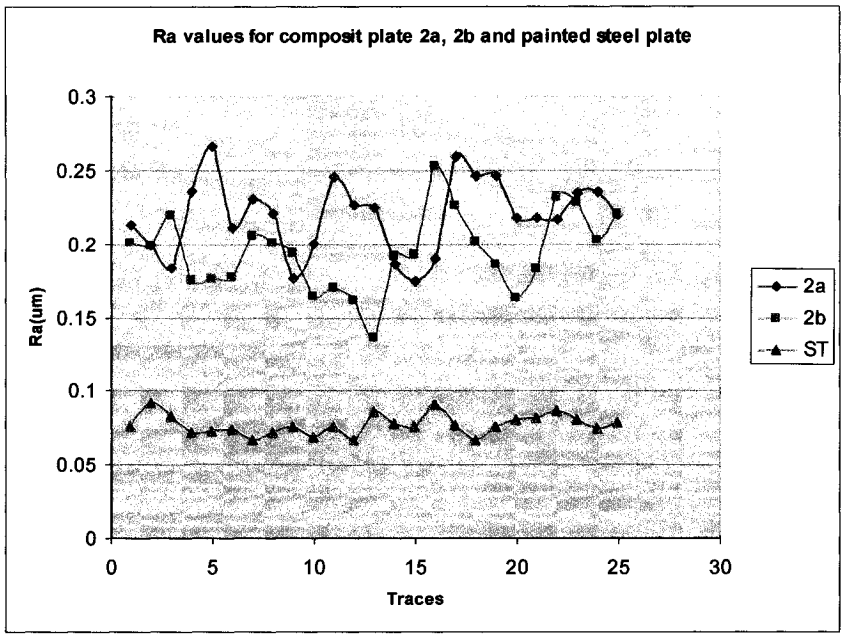

Fig. 3.20: Ra values for composite plate 2a, 2b and painted steel plate

The Ra values shown in Table 3.2 are obtained from a whole scan length of 13.3 mm. From these signals, data for shorter scan lengths were extracted out for treatment. Data segments for scan lengths of 0.5 mm, 1 mm, 2 mm, 4 mm and 8 mm were treated. Different Ra values were obtained for each scan length. The results are shown in Fig. 3.21. The error bar represents one standard deviation. It can be seen that for composite plates, the scanned length has to be at least 4 mm to obtain Ra values that are scan length independent.

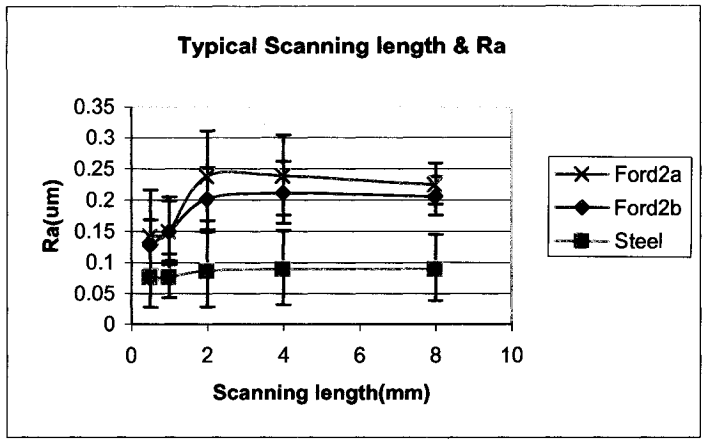

Fig. 3.21: Curves of Ra for different scanning lengths

2. Spectrum analysis of signals from three surfaces

The traces measured in time domain were converted to frequency domain using Fourier transform available in Surpark software in the measuring system. Spectrum of one trace can be achieved by the software. Typical power spectrum graphs of the three plates are shown in Fig.3.22.

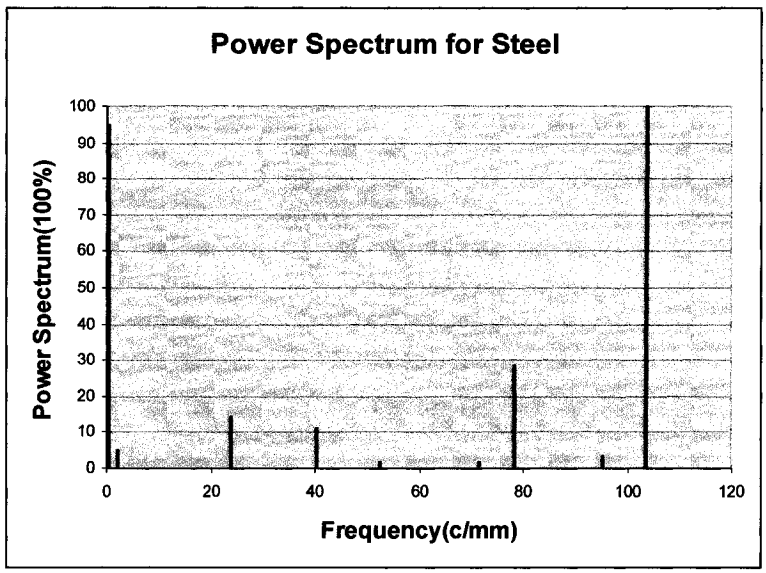

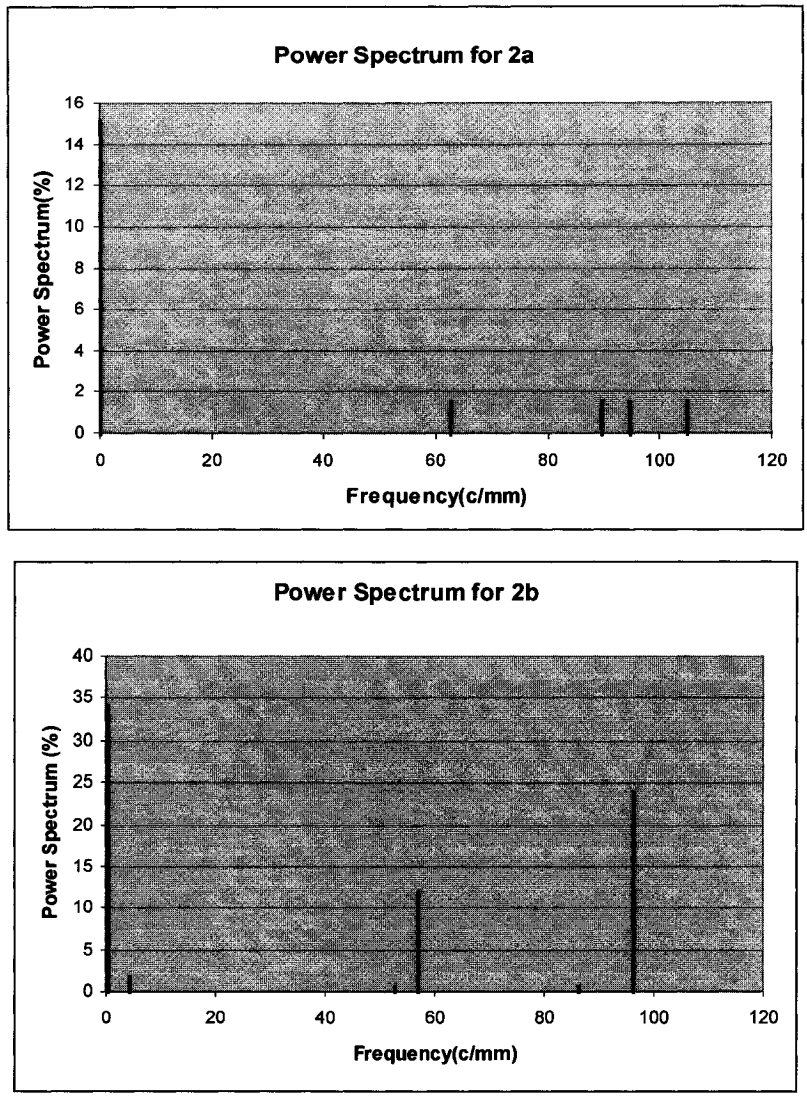

Fig. 3.22: Typical power spectrum graphs for the three plates

It can be seen that the steel plate has a few dominant frequencies, plate 2a does not exhibit dominant frequency and plate 2b exhibit different dominant frequencies.

3. Optical observation and microstructures of the plates

The surfaces of the three plates were observed using an optical microscope. These are shown in Fig. 3.23. It is obvious that painted steel plate has the best surface quality in the three plates by visual observation. Visual observation also shows that plate 2b has better surface finish than plate 2a. However, Ra results as shown in Fig. 3.20 and 3.21 are not as

definitive. This shows that the objective indicator was not as good as subjective visual observation.

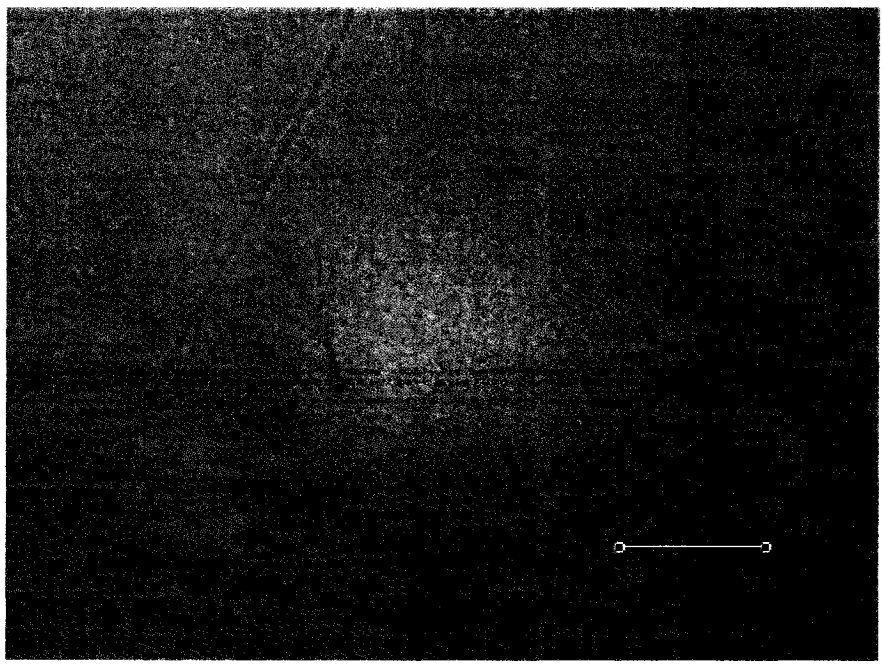

Painted steel plate

2a

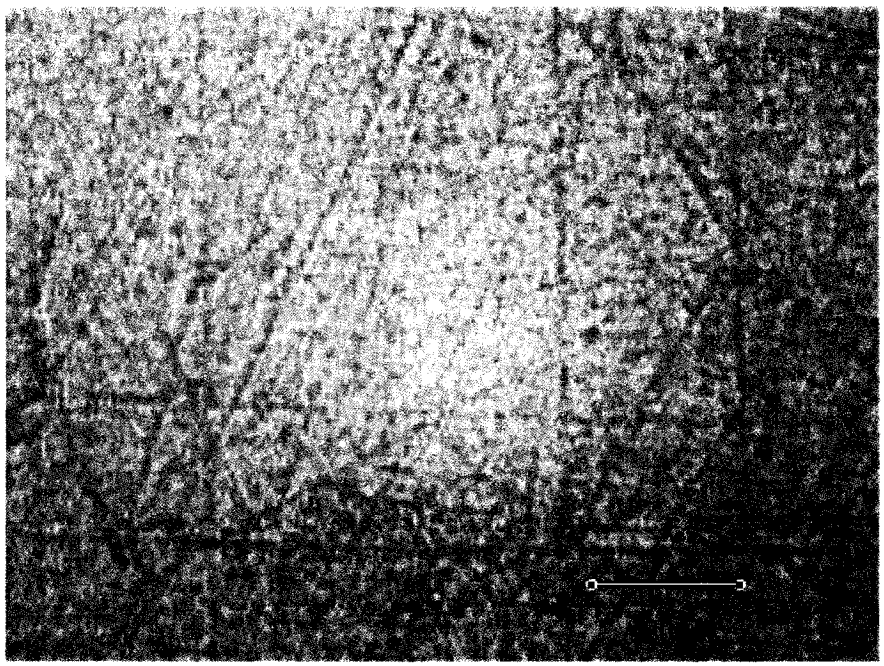

2b

Fig. 3.23: Surface appearance of three plates

Optical observation was also made on cross sections of the plates. Microstructure of cross section of composite plates 2a and 2b are shown in Fig. 3.24.

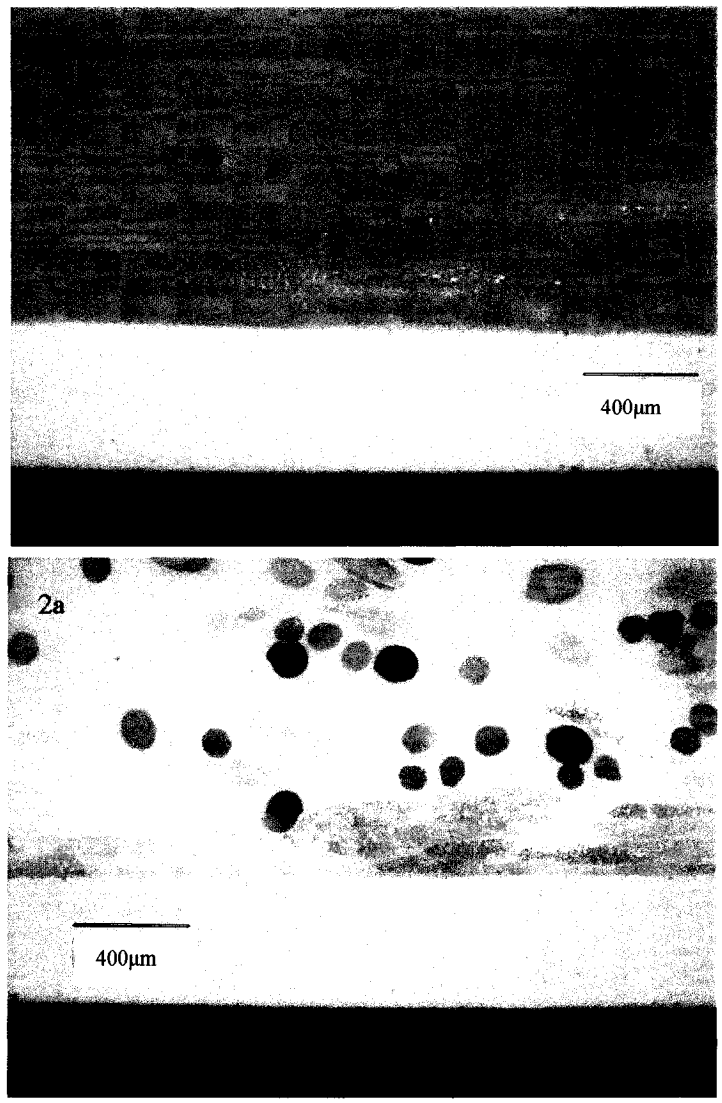

Fig. 3.24: Microstructure of composite plates 2a and 2b

The microstructures show that there is layer of pure resin (lower part of figure) in the composite plate. The resin layer helps to avoid the print-through of the fibers which may affect the appearance and surface finish. This indicates that the difference in surface finish between plates 2a and 2b is not due to effect of fibers but more due to the interaction between the resin and the mold surface.

3. Discussion and conclusion

It can be seen that the R_a value for the painted steel plate varies between 0.073 and 0.092 μm (variance 0.006μm), values for the composite plate 2a vary between 0.177 and 0.267 μm (variance 0.02μm) while values for the 2b composite plate vary from 0.14 to 0.254 μm (variance 0.026μm). It is clear from the R_a values that the painted steel plate has better surface finish, and this corresponds well with the visual observations and photographs in Fig. 3.23. However, it is not as obviously evident that the R_a values for plate 2b are better than those for plate 2a, taking the fluctuation of the values into consideration. This does not correspond well with the micrographs in Fig. 3.23 where that the surface of plate 2b appears to be better than that of plate 2a.

The above results indicate that the use of Ra is not sufficient for the distinction of the quality of surface finish for composite surfaces that are of approximate quality.

It should seem from Fig. 3.22 that steel plate has characteristic frequencies. Composite plates 2a and 2b seem to be different from painted steel plate in characteristic frequencies. The characteristic frequencies of composite plate 2b are also different from composite plate 2a. However, it is difficult to judge the quality of the surface only by the frequency spectrum of one trace.

It can be seen from Fig. 3.24 that composite plates have a layer of resin, thickness of which is round 0.4mm. Therefore, shrinkage of the resin may effect on the surface quality. The research shows that the resin layer smoothes the surface and reduces the amplitude of waves without being able fully to eliminate the specific waviness [38].

The lack of the ability to distinguish quantitatively the plates calls for the need to develop new methods to treat the data. Some other quantitative method is essential to bring out the difference.

Chapter 4

New approaches

Based on discussions in preview chapters, it is clear that conventional treatment methods are not sufficient for the distinction of the quality of surface finish for surfaces of composite panels that are of **approximate** quality. Some other quantitative method is essential to bring out the difference. Therefore, new procedures and models need be proposed to discriminate surface quality of composite panels in this section.

In chapter 2, rationale for the different new approaches was presented. These new approaches are presented in this chapter. First, the probability distribution functions of Ra of surface profiles are examined. After that frequency spectrum of the traces on the surface are investigated. Subsequently filtering analysis is used to see whether distinct characteristics of the signals can be revealed. Finally similarity or dissimilarity analysis of the signals will be carried out.

4.1 Maximum Entropy Method for Ra analysis

The signatures of surface of the plates can be considered as random variables. One possible way to study their signatures would be to plot their probability distribution functions. The most common distribution is normal distribution. The normal distributions for the Ra of the three plates are shown in Fig. 4.1.

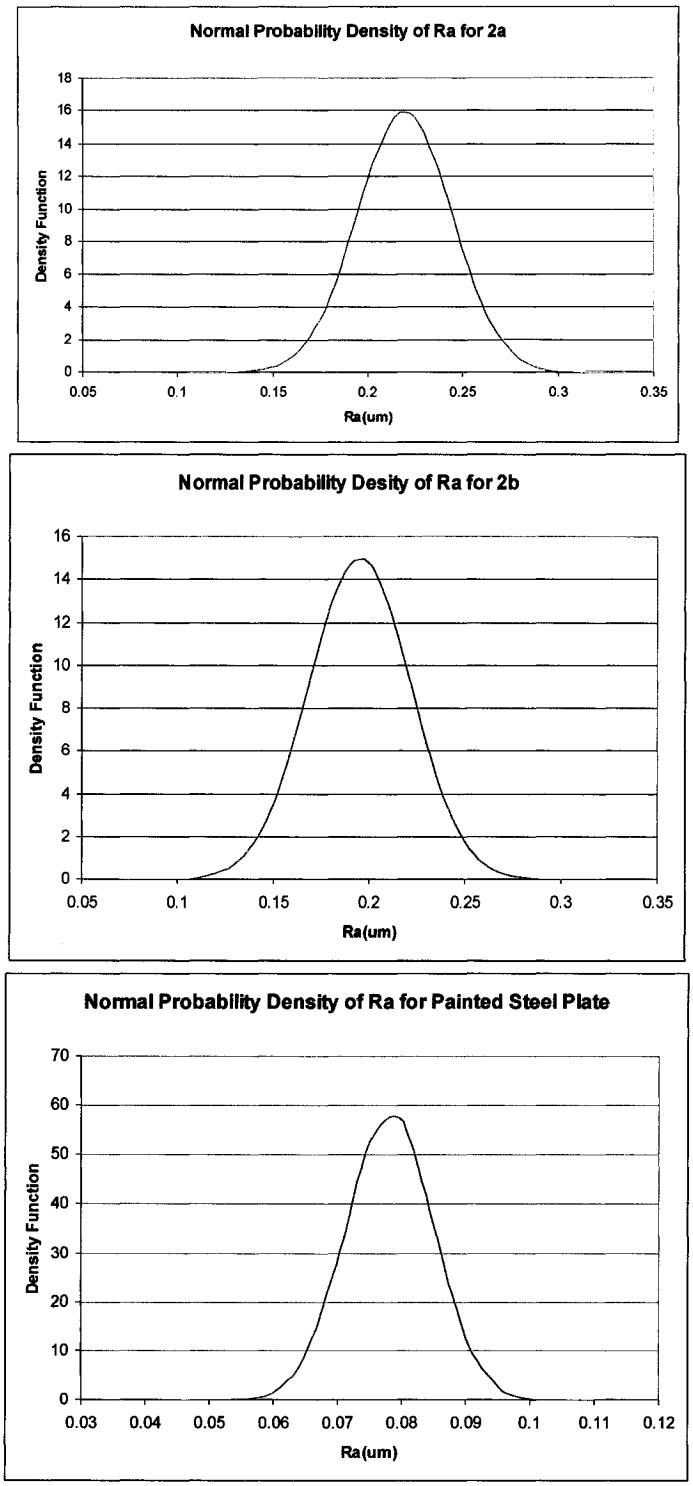

Fig. 4.1: The normal distribution profiles for the three plates

It can be seen that the normal distribution provides a means which does not seem to be able to easily distinguish plates 2a and 2b. This may be because the normal distribution allows only 2 degrees of freedom (mean and standard deviation) in fitting the data.

Based on above observation, Maximum Entropy Method is used to calculate probability density distribution of Ra on surfaces of composite plates. By using such method, distribution of Ra values on surface of composite panel can be computed and it is hoped that the results on surface of composite plate can be used to discriminate surface quality levels of composite plates having very close Ra values.

1. Maximum Entropy Method [96-98]

The Maximum Entropy Method is based on Jaynes' principle: The minimally prejudiced probability distribution is that which maximizes the entropy subject to constraints supplied by the given information.

- **Definition of entropy**

For a continuous random variable, entropy is defined as

$$S = -\int_R f(x)\ln[f(x)]dx \tag{4.1}$$

Or for a discrete random variable it is

$$S = -\sum_{i=1}^{n} f(x_i)\ln[f(x_i)] \tag{4.2}$$

Where $f(x)$ is the probability density function and $f(x_i)$ is the probability mass function.

- **Solution on probability density function**

To get maximum entropy for a density function, one can derive the basic formulae by applying Jaynes's principle.

$$S = -\int_R f(x)\ln[f(x)]dx = Maximum; \tag{4.3}$$

Subject to the constraints

$$\int_R f(x)dx = 1; \tag{4.4}$$

$$\int_R x^i f(x)dx = m_i \quad \text{i=1 .. m;} \tag{4.5}$$

Where m is the number of moments to be used and m_i is the ith moment about the origin, determined numerically from the sample. To achieve a maximum, let $\overline{S}$ be the modified function and use Langrangian multiplier $\lambda_0, \lambda_{1,,,,} \lambda_m$.

One has (4.6)

$$\overline{S} = S + (\lambda_0 + 1)[\int_R f(x)dx - 1] + \sum_{i=1}^{m} \lambda_i [\int_R x^i f(x)dx - m_i] \tag{4.6}$$

One wishes to make the derivative $d\overline{S} / df(x)$ equal to zero.

From this, assume that *f(x)* takes the form

$$f(x) = \exp(\lambda_0 + \sum_{i=1}^{m} \lambda_i x^i) \tag{4.7}$$

This is the analytical form for the maximum entropy density function. The problem is how to determine the values of the λ's.

- **Determination of λ's values**

According to equation (4.4), one has

$$\int_R \exp(\lambda_0 + \sum_{i=1}^{m} \lambda_i x^i)dx = 1 \tag{4.8}$$

Taking log of the both sides yields

$$\lambda_0 = -\ln[\int_R \exp(\sum_{i=1}^{m} \lambda_i x^i)dx] \tag{4.9}$$

or

$$\exp(-\lambda_0) = \int_R \exp(\sum_{i=1}^{m} \lambda_i x^i) dx \tag{4.10}$$

Next, differentiate equation (4.9) and (4.10) with respect to λ_i,

$$\partial\lambda_0 / \partial\lambda_i = -\int_R x^i \exp(\sum_{i=1}^{m} \lambda_i x^i) dx / \int_R \exp(\sum_{i=1}^{m} \lambda_i x^i) dx \tag{4.11}$$

$$\partial\lambda_0 / \partial\lambda_i = -\int_R x^i \exp(\lambda_0 + \sum_{i=1}^{m} \lambda_i x^i) dx = -m_i \tag{4.12}$$

From equation (4.11) and equation (4.12), one has

$$\int_R x^i \exp(\sum_{i=1}^{m} \lambda_i x^i) dx / \int_R \exp(\sum_{i=1}^{m} \lambda_i x^i) dx = -m_i \qquad \text{i=1, . m} \tag{4.13}$$

Equation (4.13) represents m simultaneous equations to be solved for λ_1, λ_2 ..... λ_m. λ_0 is obtained from equation (4.9). The equations above are put in a form more convenient for numerical solution as follows:

$$1 - \frac{\int_R x^i \exp(\sum_{i=1}^{m} \lambda_i x^i) dx}{m_i \int_R \exp(\sum_{i=1}^{m} \lambda_i x^i) dx} = R_i \tag{4.14}$$

where the R_i's are the residuals that are reduced to near zero by a numerical technique. A solution can be obtained by using nonlinear programming to obtain the minimum of the sum of the squares of the residuals. Convergence is achieved when $|R_i| < \varepsilon$, where ε is the specified acceptable error. Equation (4.9) is used to obtain λ_0. Integrals in equation (4.13) are evaluated numerically, and it is apparent that the bounds of the unknown density function must be known or assumed. The most successful nonlinear programming technique for the problem was found to be one proposed by Jacobson and Oksman [96].

In this way, the analytical form for the maximum entropy density function (4.7) can be used to analyze Ra values.

2. Analysis of surface roughness by Maximum Entropy Method (MEM)

Let us first use an example to explain the advantage of MEM when doing surface roughness analysis. In most cases one assumes that measurement values have normal distribution. The advantage of the MEM as compared to the normal distribution function is shown in Figure 4.2. MEM can provide probability density function of real Ra values. This is the result from plate 2a (scan length of 8 mm). It can be seen that if measurement values are fitted using the normal distribution then normal distribution shows one peak while the MEM shows two peaks. The normal function is forcing the data to fit into a normal distribution while the MEM allows the data to follow its variation. The two peaks may indicate that there are two dominant amplitudes for roughness.

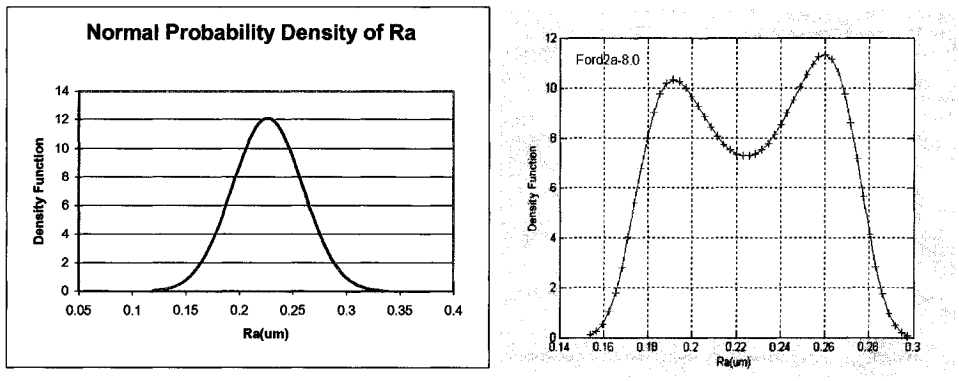

Fig. 4.2: Normal Distribution and Maximum Entropy Distribution

Assume $n = 4$, and use the data from table 3.2, the coefficients λ_0, λ_1, λ_2, λ_3 and λ_4 for painted steel plate, composite plates 2a and 2b, respectively, are obtained and are shown in Table 4.1. Distribution curves of probability density on Ra values for painted steel plate, composite 2a and 2b are shown in Fig. 4.3.

Table 4.1: Coefficients for steel plate and composite plates 2a and 2b

Samples / Coefficients	2a ($\lambda i*10^5$)	2b ($\lambda i*10^4$)	Steel ($\lambda i*10^7$)
λ_0	0.00724718948426	0.00786502057793	0.00023113909480
λ_1	0.13439269022056	0.14070263699347	0.01145891449462
λ_2	0.93098047794313	0.93536658614619	0.21234308548347
λ_3	2.86430230850958	2.88320549100634	1.74688422807841
λ_4	3.30130038208806	3.53934577102839	5.38586992695367

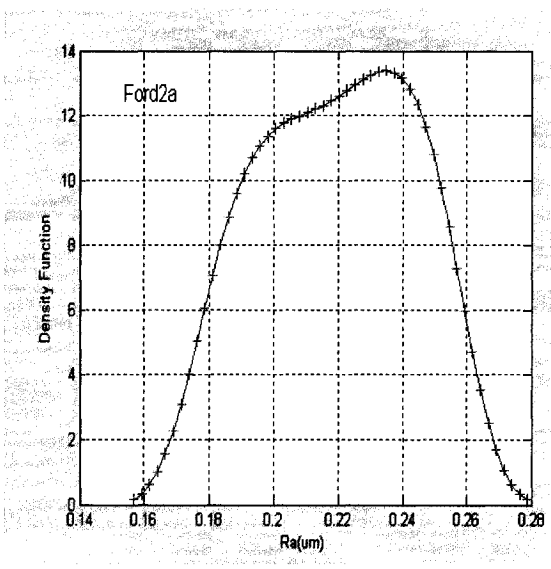

2a

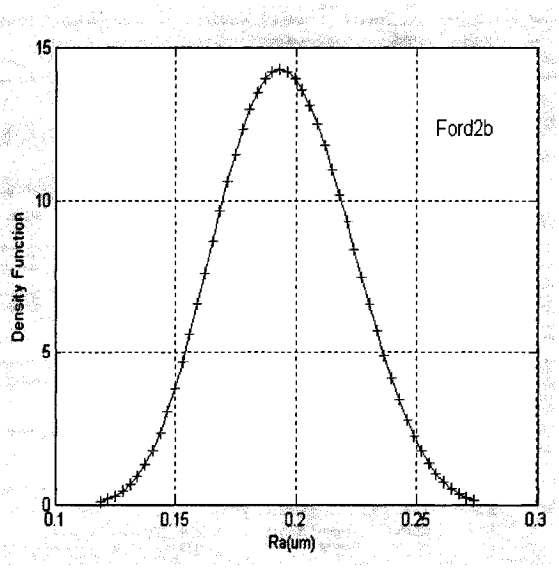

2b

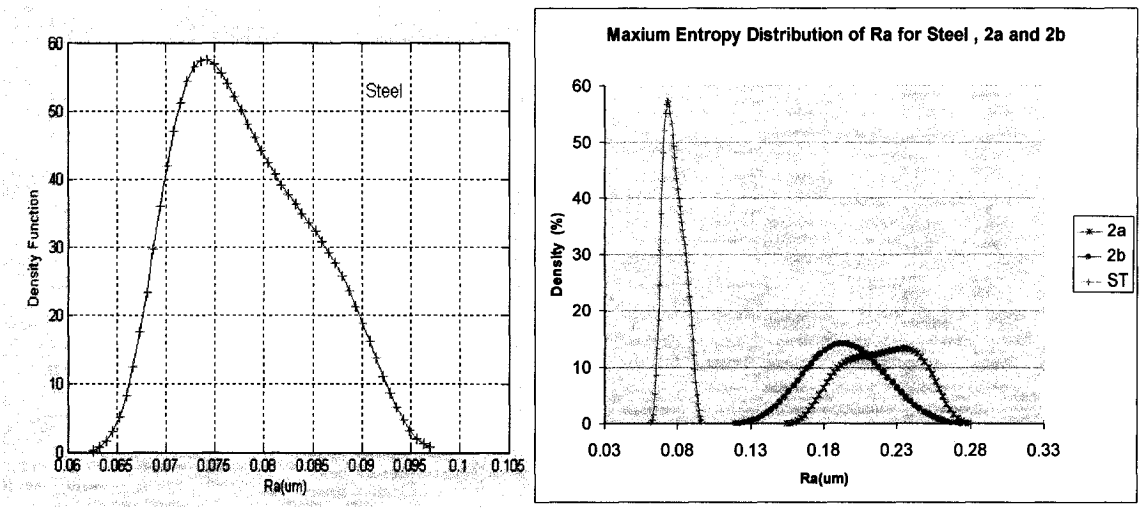

Steel **Steel, 2a and 2b**

Fig. 4.3: Probability distributions of R_a for 2a, 2b and painted steel plates (13.3 mm)

It is clearly seen from Fig. 4.3 that for composite plates 2a and 2b, though they have very close R_a values, their distribution curves have very different shapes. There are two concentration points for Ra values at 0.195μm and 0.22μm for plate 2a and Ra values of 2b has a uniform symmetrical distribution. The probability density function distribution of R_a of plate 2b is more uniform than that of plate 2a at 13.3 mm scan length. Therefore, it can be said that the surface smoothness of 2b is better that that of 2a.

Ra value of painted steel plate is very small. Its average value is 0.0782 μm and it highly concentrated around the expected value. Therefore, surface quality level of painted steel plate is much higher that those of composite 2a and 2b.

The probability density functions of R_a for different scanning lengths, 0.5mm, 1.0mm, 2mm, 4mm, 8mm, and 13.3mm, are shown in Fig. 4.4

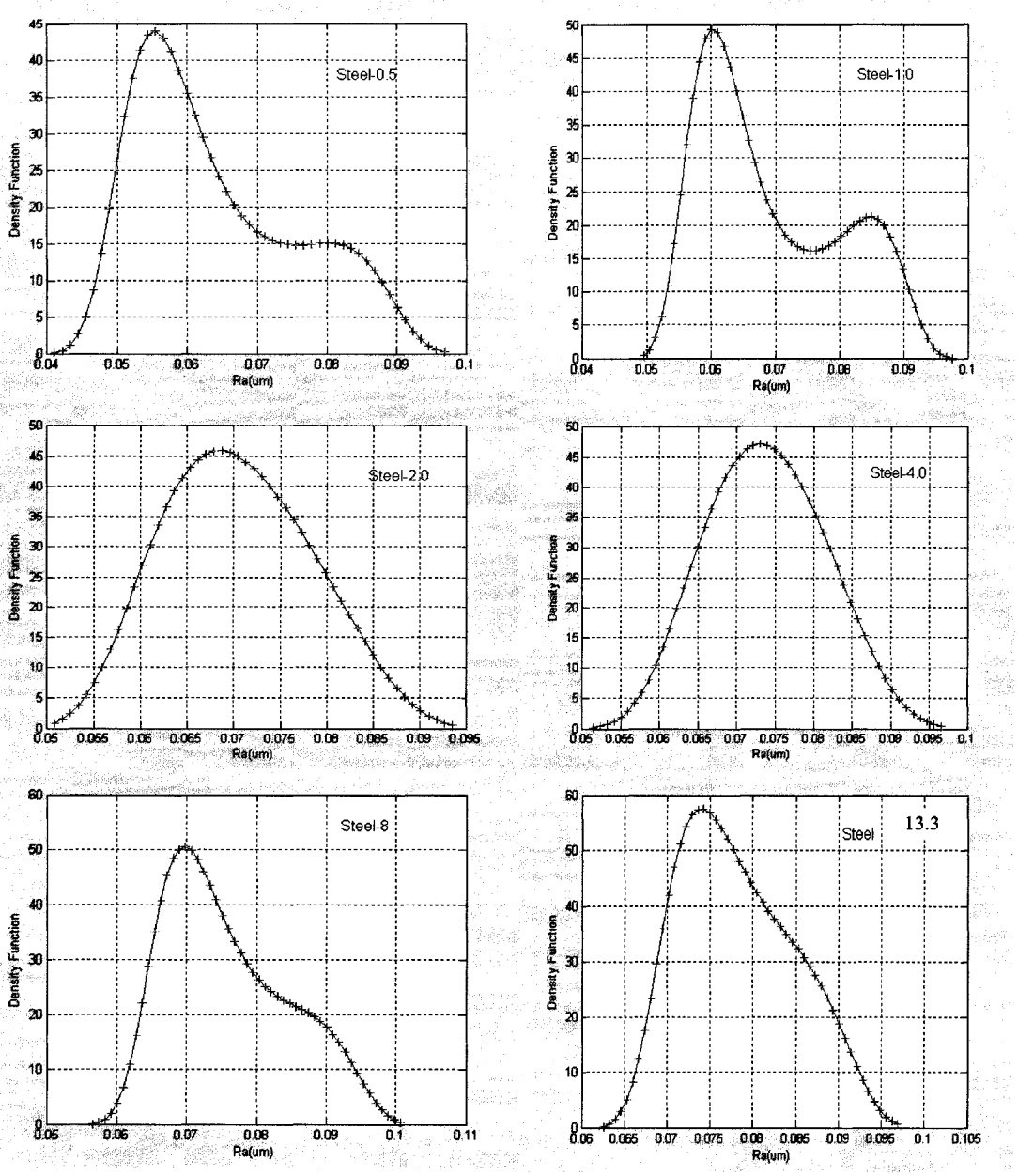
Steel-0.5
Steel-1.0
Steel-2.0
Steel-4.0
Steel-8
Steel 13.3
Density Function
Ra(um)

Steel

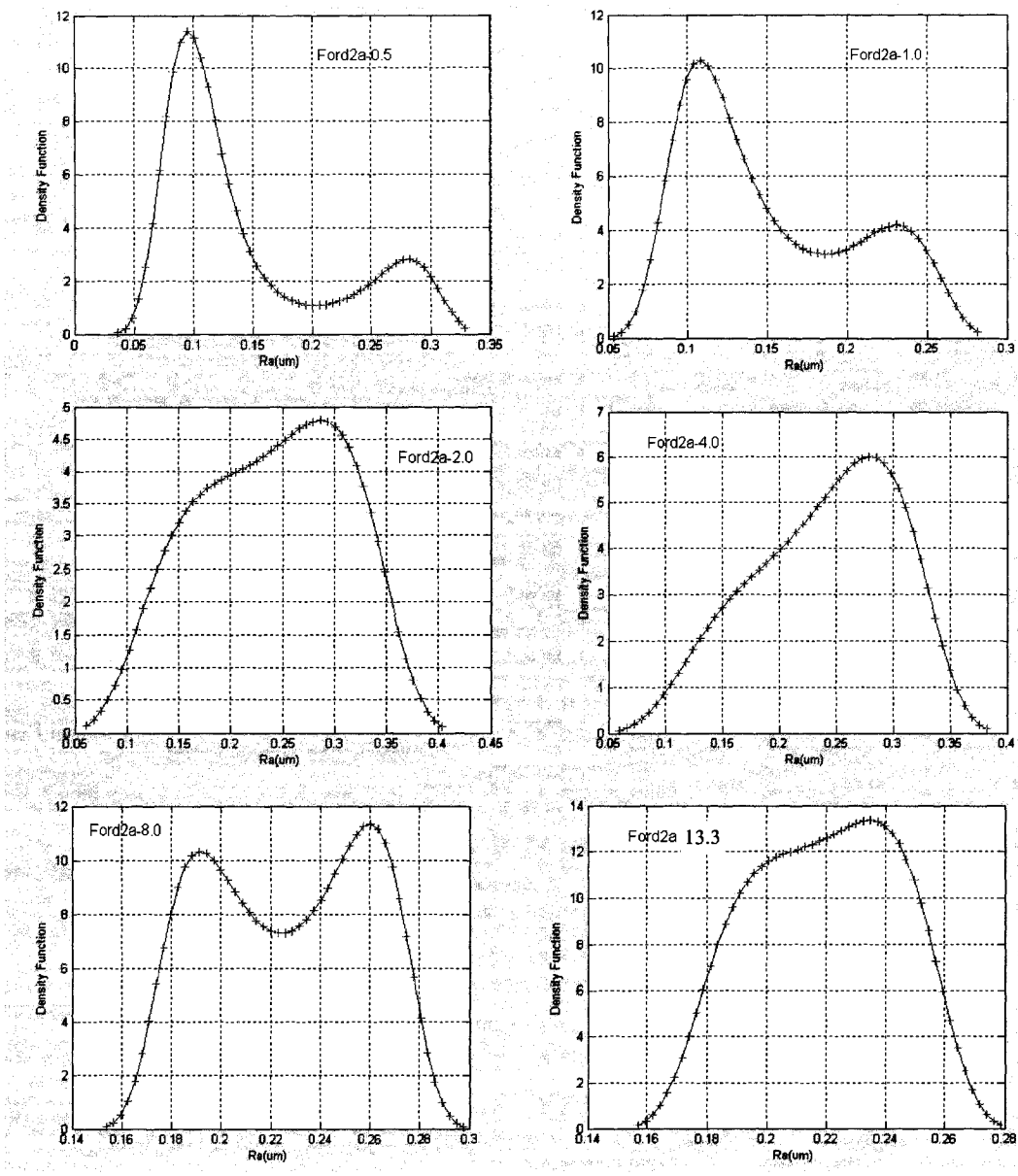
Ford2a-0.5
Ford2a-1.0
Ford2a-2.0
Ford2a-4.0
Ford2a-8.0
Ford2a 13.3
Density Function
Ra(um)

2a

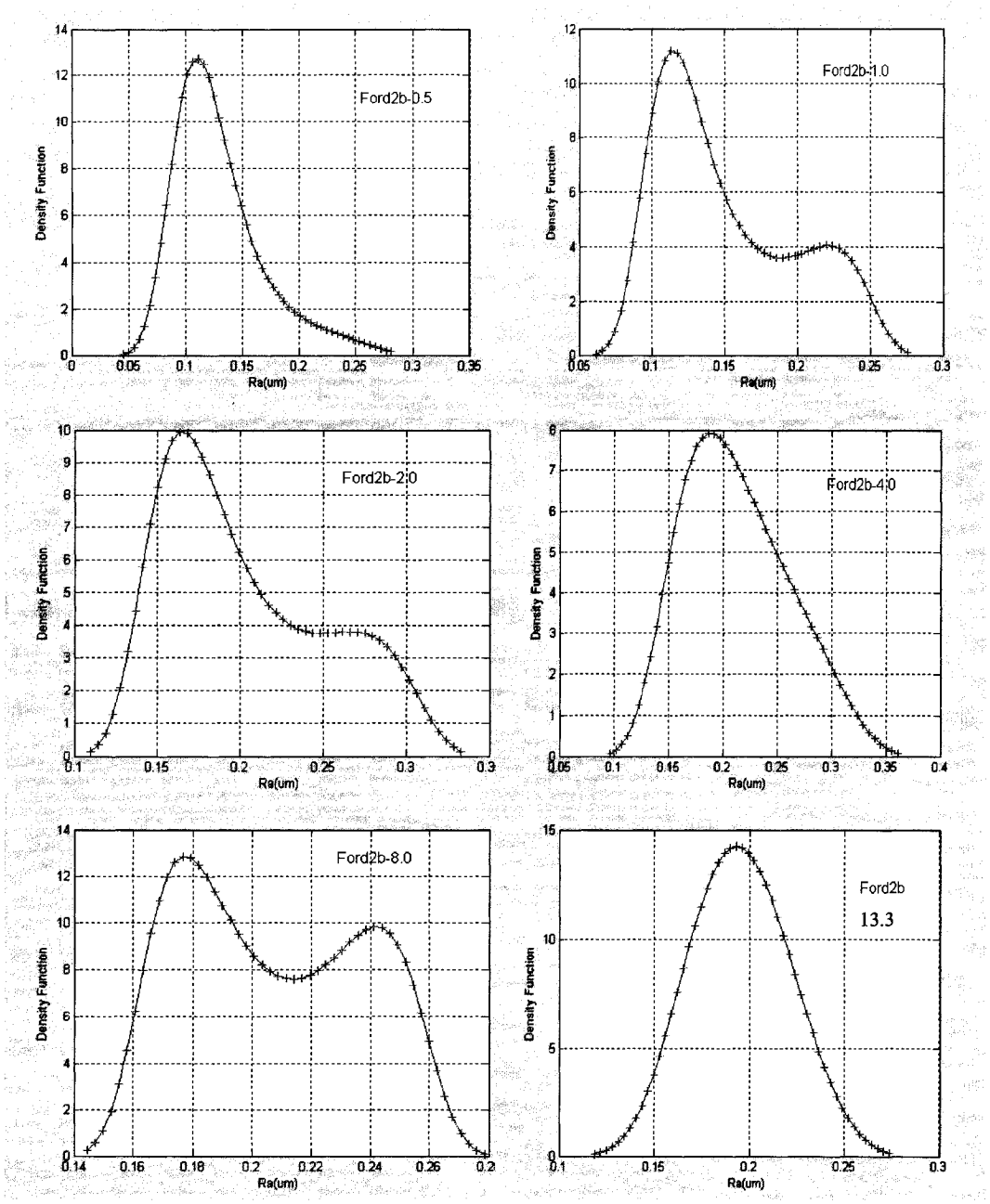

2b

Fig. 4.4: Probability density functions of Ra for scanning lengths 0.5, 1, 2, 4, 8, 13.3 mm for plates 2a and 2b and steel plate

Fig. 4.4 shows that the probability density functions vary with scan length. It is clear that dispersion degree of Ra values for the composite materials are much higher of that of painted steel plates. The variations in the distribution profiles demonstrate that surface profiles of composite material have much higher random characteristics than that of painted steel plate. So research of surface of composite material is more difficult than that of machined metallic material surface.

Due to lack of clear distinction between the profiles, it is not definite that MEM can provide a clear method for the evaluation of the surfaces.

4.2 PostStack software of Landmark Graphics Corporation

In chapter 2, new approaches that are used to distinguish approximation surface quality of composite plates have been proposed. The approaches can be also shown in Fig. 4.5.

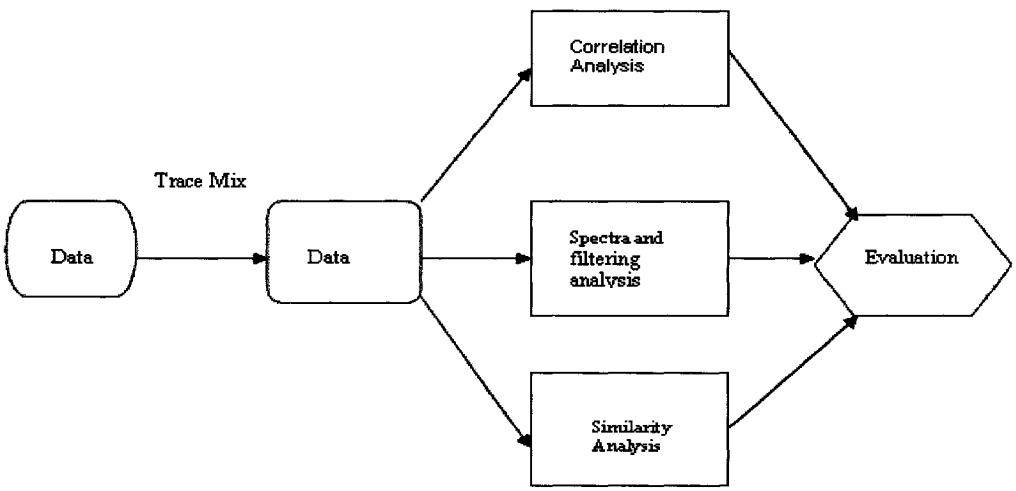

Fig. 4.5: The evaluation of surface quality of multiple attribute parameters

All calculation work was carried out using PostStack software of Landmark Graphics Corporation [99-100].

Landmark solutions integrate exploration, reservoir management, drilling, production, business-decision analysis and data management. There are more than 200 applications and processes in the package. PostStack is one of the processing application packages. The PostStack product family provides a suite of data processing & interpretation tools designed to extract information and, therefore, more value from data. It has been successfully used by oil companies [102-104].

PostStack is designed for seismic data optimization, attribute extraction, waveform classification, similarity processing, inversion and creating revealing attributes. The measured surface profile and raw data from a surface profilometer are very similar to seismic data. The main characters for both surface profile and seismic data can be described in amplitude, frequency and phase. PostStack package brings 124 processes. This includes Amplitude Statistics, Correlation Statistics, Complex Trace Statistics, Spectral Statistics, Sequence Statistics, Similarity Analysis, Waveform Classification and Data Enhancement, Filter, Deconvolution, etc [105]. For study of surface profiles, amplitude, frequency, filtering, correlation and similarity analysis are used to discriminate surface quality of composite panels.

The data from Surfpark measurement system was output in Excel format. Then it was transferred to SEG-Y (binary code) format in order to input to PostStack system. The data model used for surface profile is a three dimension dataset. The process of data can be expressed as a workflow that is shown in Fig. 4.6.

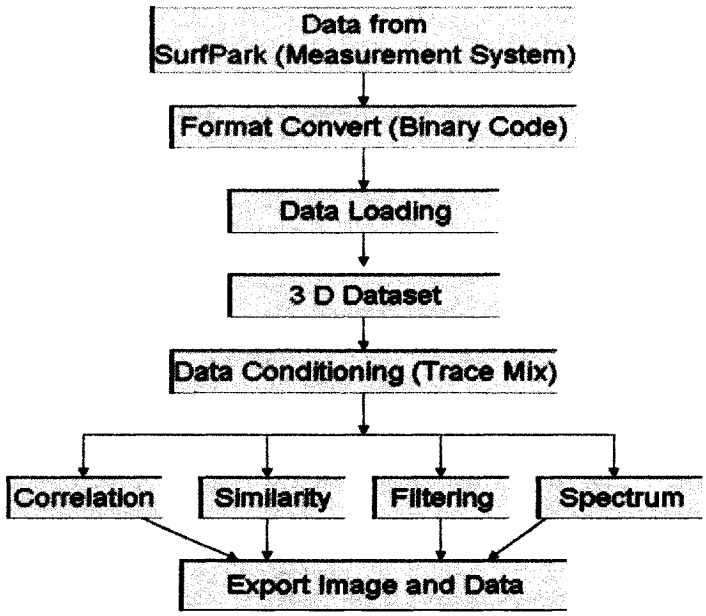

Fig. 4.6: The workflow of process of data

4.3 Spectral analysis and filtering analysis

1. Spectral analysis [106, 107]

In chapter 2 Fourier analysis has been discussed. Spectral analyses of the three panels were carried out by PostStack program. Fig. 4.7 shows that the spectrum characters of painted steel plate, composite plates 2a and 2b which is analyzed by DFT. It can be seen from Fig. 4.7 that painted steel plate has apparent characteristic peaks at 3, 162, 322, 355, 406Hz. Plate 2b also has these characteristic peaks but they are not as clear as painted steel plate. Characteristic peaks of plate 2a are weaker than that of plate 2b. The characteristic peaks of composite plate 2b may be more similar to that of painted steel plate than that of composite 2a. However, it is difficult to determine whether one spectrum is similar to the other one or not by using characteristic peaks.

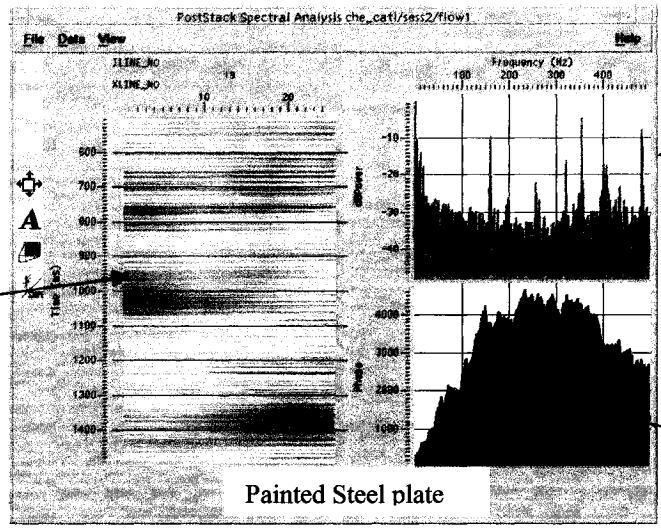
PostStack Spectral Analysis che_cat1/sess2/flow1
File Data View
Help
Frequency (Hz)
Spectrum
Traces
Phase
Painted Steel plate

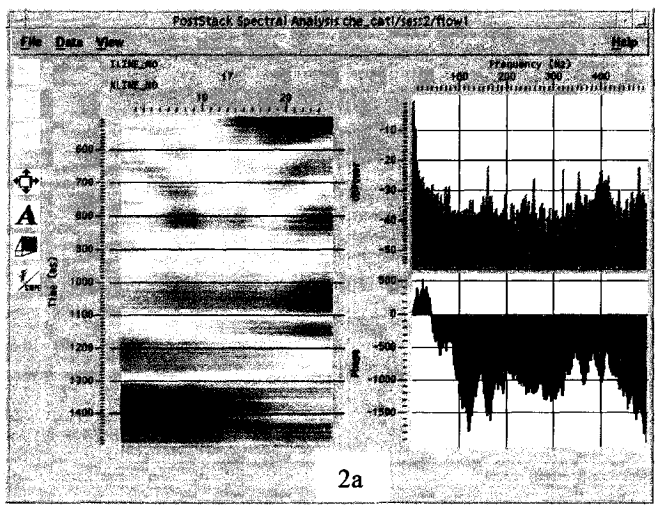
PostStack Spectral Analysis che_cat1/sess2/flow1
File Data View
Help
Frequency (Hz)
2a

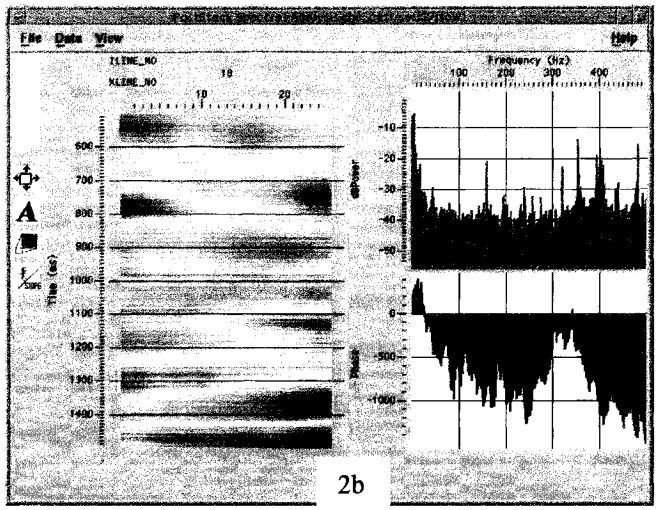

Fig. 4.7: The spectrum character of steel plate, plates 2a and 2b analyzed by DFT

2. Filtering analysis

The curves of amplitudes and displacement with low frequency would show the waviness of the surface signatures. The curves of amplitude and displacement with high frequency would reflect surface brightness. Therefore, filtering analysis is helpful to understand the properties for the surfaces of materials.

In the PostStack software Ormsby filter is used. The Ormsby filter is a trapezoidal filter defined by the four corner frequencies. Hanning windows (cosine tapers) are used to ensure smooth filter definition between the specified corner points, thereby reducing filtering artifacts [85]. Frequencies that fall within the bandwidth (in Fig. 4.8 the range is 10 - 50 Hz) are not attenuated. Frequencies that fall within the filter ramps (5 -10 Hz and 50 - 60 Hz) are increasingly attenuated away from the central bandwidth. Frequencies that fall beyond the cut points (<5 Hz or >60 Hz) are, in effect, eliminated.

PostStack applies the filter specified (by setting the four corner points) to each incoming trace. Fig. 4.8 is an example of an Ormsby filter.

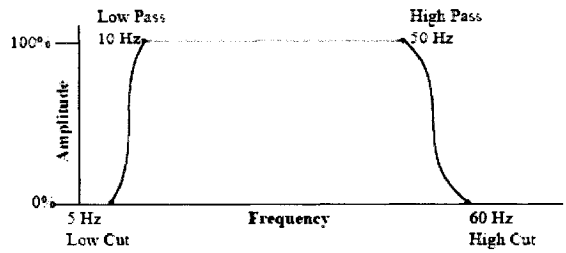

Fig. 4.8 Example of an Ormsby Filter

Based on analysis of characteristic peaks, low frequency and high frequency are performed in order to understand surface properties.

Fig. 4.9 shows low frequency components of surface signatures for these three panels. The approach can demonstrate surface waviness also.

Fig. 4.10 shows amplitudes with higher frequency components which would affect gloss and smoothness of the surface.

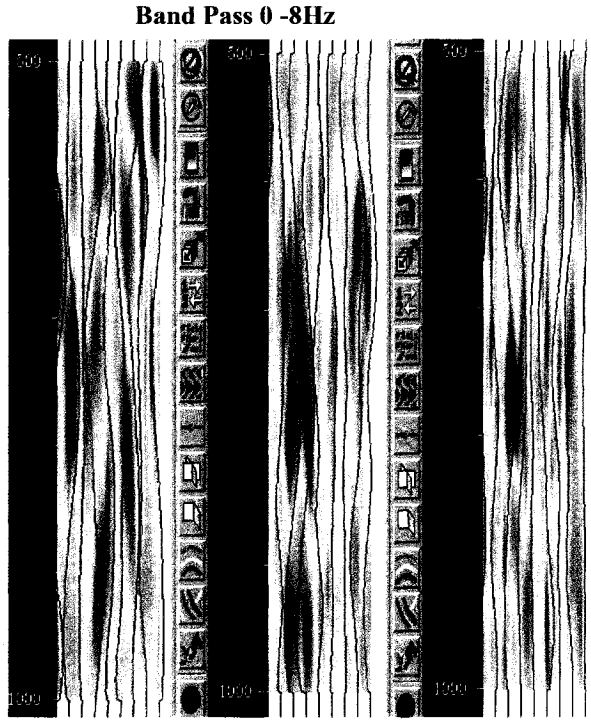

Fig. 4.9: Surface shape of the plates (0-8Hz) for painted steel plate, plates 2a and 2b

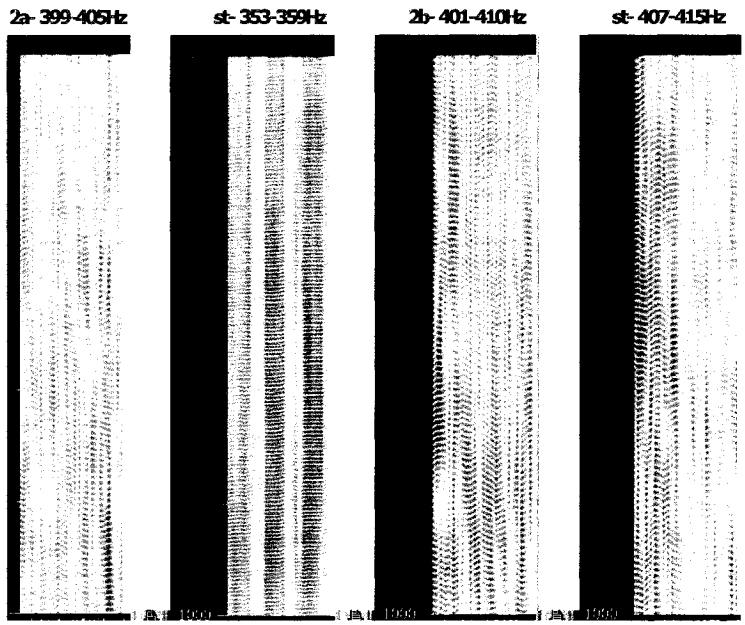

Fig. 4.10: Surface amplitudes (high frequencies) for painted steel plate, plates 2a and 2b

4.4 Correlation and similarity models

4.4.1 Introduction

Description and evaluation of surface finish of composite panels are a complex problem. However, as mentioned before, no standardized definition for a class-A-surface is available. In most cases, judgment of whether or not a surface is of Class A is made just by physical observation of experts [26, 27, 38].The only general definition could be: a panel made of composite material has a class-A-surface finish if its optical appearance is identical to an adjacent steel panel of class A surface finish.

On the other hand, a method of usual quantitative evaluation is using Ra value to evaluate surface quality levels. It is well known that Ra is widely used to evaluate surface

roughness in metals. However, it is not difficult to imagine that the same Ra value can be attained from total different waveforms. It is clear that different shapes of curve of surface profile would enable surfaces to have different characters. Ra value is not sensitive to waveforms which affect surface characters of panels. Therefore, measurements of surface quality levels should not depend on only one factor Ra.

How to solve this complex evaluation problem? Psychological and physiological studies have given many interesting facts about animal perception, but no understanding is sufficient to duplicate their performance with a machine. Everyday perceptual processes are carried out below conscious level, paradoxically, we are all experts at perception. Judging surface finish of Class A for composite panels is often perceptual process by visual observation.

Though lacking of a complete theory of perception, people still try to solve more modest problems. Many of these involve pattern classification. One has to seek to design and build a machine that can recognize pattern, such as speech recognition, fingerprint identification, optical character recognition, DNA sequence, and so on [109-111].

If the surface of a painted steel plate is defined as surface finish of class A, theory and method of correlation and similarity could be used to discriminate surface quality levels of composite plates.

For example, assume that A and B gauges are made in a tool shop. How to know which one has better accuracy? If A gauge and B gauge are compared to a standard gauge C, the answer will be attained quickly. It is clear that the gauge that has smaller value of A-C or B-C has better accuracy. Actually, it is a minimum distance principle. Better accuracy gauge is also said to have a greater similarity to standard gauge.

If a painted steel plate with Class A surface finish as a standard, composite panels can be compared to be A, B and C gauges and so on. By comparison reference surface of Class A surface finish with surfaces of many composite plates, respectively, the surface that has the greatest similarity to the surface of Class A should have the best surface quality. Meanwhile related quality levels in all materials can be set up.

This analysis of wavelets has a great advantage in that it can provide more information of the surface. This type of the information may be used to replace the physical observation of humans. Therefore, on the basis of this type of comparison between reference function and target function one may simulate human's perception for the surface of material to some extent. The comparison is different from the comparison between statistic average parameters. It is because statistical average parameters screen only characteristics of wavelets, such as total different wavelets may have the same Ra values and it may not indicate which surface has better surface quality.

On the basis of the idea of directly analyzing wavelets that contain large quantity of information of surface, a model of similarity analysis is developed to discriminate surface differences between reference function and target function.

Cross correlation analysis can be used to describe waveforms of similarity between reference surface and target surface. Distance coefficients can describe the adjacent extent between the reference point and the target point. If the reference point and the target point are shifted along a path, in terms of distance between the two points, similarity of the reference object and the target object can be described. Actually, the distance is absolute deviation between the reference point and target point. The description of the distances between the points of reference object and target object may

contain not only the information of amplitudes and but also the information of waveforms. The method may describe the similarity between the two objects better. In terms of the difference surface status of target object can be also discriminated and surface quality ranks of the materials can be achieved.

4.4.2 Models of cross correlation and similarity analysis

Analysis models of cross correlation and similarity analysis are developed to discriminate surface quality levels, in which the surface of painted steel plate is used as a reference function, and composite plates 2a and 2b are used as target functions. By comparison and analysis of their waveforms, surface quality levels of the composite plates having approximate Ra value can be discriminated.

Fig. 4.11 is a model which is presented in 3 dimensions. One coordinate represents materials, the other represents traces, and the third one associated with samples. In the model the relationship between materials, samples and traces is set up. In this way, the surfaces of two panels can be compared to each other by mathematical calculations and the data can be easily read by the computer. Cross correlations and similarity analysis between painted steel plate and plates 2a and 2b can be calculated [112].

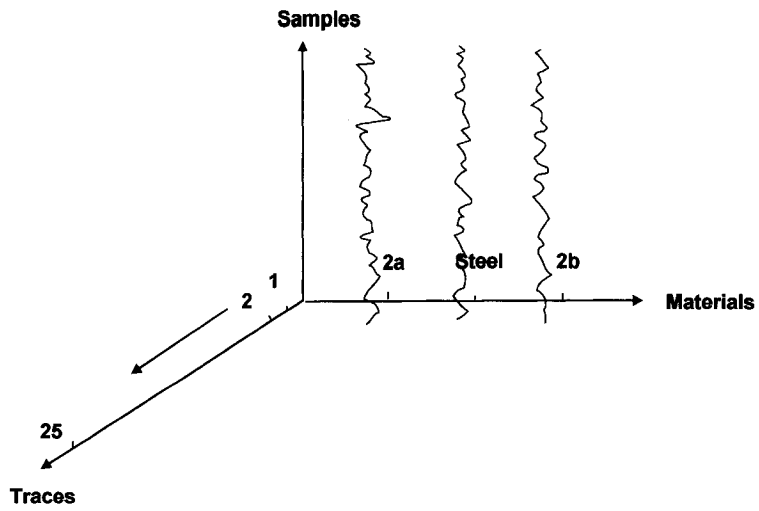

Fig. 4.11: 3-D data volume model for materials, traces and samples

1. Correlation analysis

- **Model of cross correlation coefficient[113, 114]**

Fig. 4.12 shows a schematic diagram for expectation function and variance of a random signal.

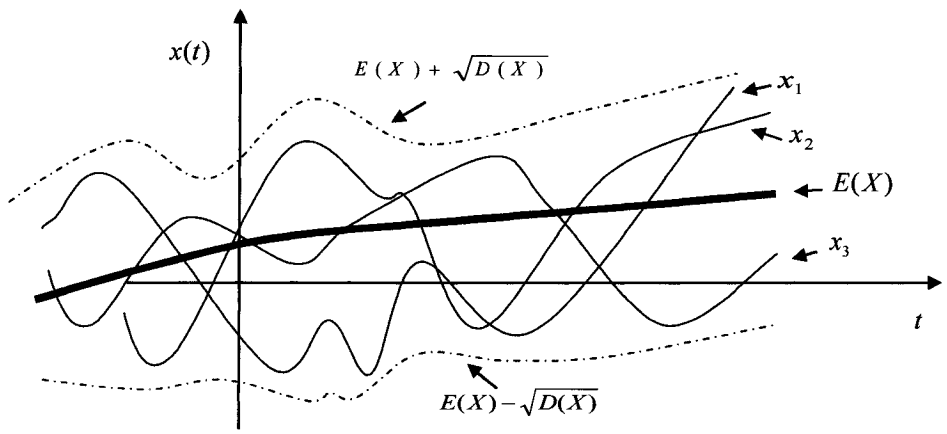

Fig. 4.12: A schematic diagram for expectation function and variance of a random process

If X_1 and X_2 represent two random variables, cross correlation coefficients between X_1 and X_2 can be calculated by equation (4.14)

$$\gamma_{12} = \frac{E\{[X_1 - E(X_1)][X_2 - E(X_2)]\}}{\sqrt{D(X_1)}\sqrt{D(X_2)}} = \frac{C_{12}}{\sqrt{C_{11}}\sqrt{C_{22}}} \tag{4.15}$$

γ_{12} is coefficient of cross correlation for random variables X_1 and X_2. It is also a normalized coefficient, which describes the extent of correlation between the two random variables.

In equation (4.15) *E(X)* is mathematical expectation that can be expressed as follows:

$$E(X) = \int x(t)p(x,t)dx \tag{4.16}$$

P(x, t) is probability density function.

For discrete data

$$E(X) = \frac{1}{N}\sum_{i}^{N} x_i(t) \tag{4.17}$$

D(X) represents variance that can be expressed as follows:

$$D(X) = E[(x(t)-E(X))^2] = \int (x(t) - E(X))^2 p(x,t)dx \tag{4.18}$$

For discrete data

$$D(X) = \frac{1}{N}\sum_{i}^{N} (x_i(t) - E(X))^2 \tag{4.19}$$

C_{12} represents covariance for X_1 and X_2. It can be written as:

$$C_{12} = E\{[X_1 - E(X_1)][X_2 - E(X_2)]\} \tag{4.20}$$

C_{12} represents covariance between X_1 and X_2.

Fig. 4.13 shows an example to be studied. 25 scan lines were done for each plate. Trace 1 for A plate is correlated to trace 1 for plate B and the first correlation coefficient can be

attained. Trace 2 for A plate is correlated to trace 2 for plate B and the second correlation coefficient can be attained. In this way, 25 correlation coefficients can be attained. This can describe the extent of correlation between the surface of plate A and the surface of plate B.

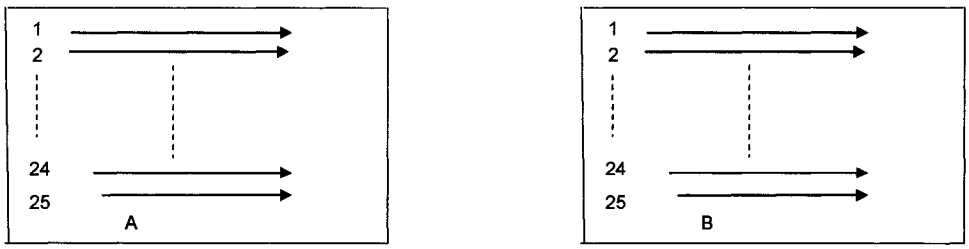

Fig. 4.13: Comparison of scan lines on surface A and surface B

Fig. 4.14 shows an example of a trace of plate A and plate B.

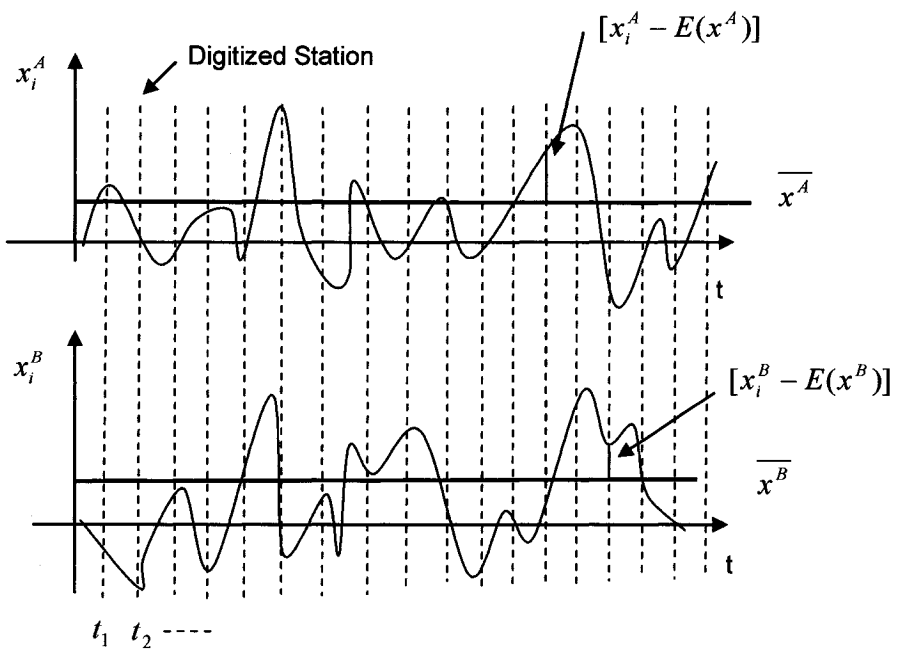

Fig. 4.14: The schematic diagram for the two traces for plate A and plate B

In the example, expected values for a trace of plate A and Plate B are

$$\overline{x^A} = \frac{1}{n}\sum_i^n x_i^A \qquad (4.21)$$

$$\overline{x^B} = \frac{1}{n}\sum_i^n x_i^B \tag{4.22}$$

respectively, where x_i^A and x_i^B are digitized values in the scan lines of plate A and plate B.

Their variances are

$$D^A = \frac{1}{n}\sum_i^n (x_i^A - \overline{x^A})^2 \tag{4.23}$$

$$D^B = \frac{1}{n}\sum_i^n (x_i^B - \overline{x^B})^2 \tag{4.24}$$

respectively.

Therefore, correlation coefficient of the two traces of plate A and plate B is

$$\gamma_{AB} = \frac{\frac{1}{n}\sum_i^n (x_i^A - \overline{x^A})(x_i^B - \overline{x^B})}{\frac{1}{n}\sum_i^n (x_i^A - \overline{x^A})^2 \frac{1}{n}\sum_i^n (x_i^B - \overline{x^B})^2} = \frac{\frac{1}{n}\sum_i^n (x_i^A - \overline{x^A})(x_i^B - \overline{x^B})}{D^A D^B} \tag{4.25}$$

In Fig. 4.11 one coordinate represents three materials, the other represents 25 traces, and the third one associated with samples. In this way, cross correlation coefficients between painted steel plate and samples 2a and 2b can be calculated by equation (4.25), respectively.

$$[\gamma_{ik}] = \frac{E\{[X_i - E(X_i)][X_k - E(X_k)]\}}{\sqrt{D(X_i)}\sqrt{D(X_k)}} = \frac{C_{ik}}{\sqrt{C_{ii}}\sqrt{C_{kk}}} \tag{4.26}$$

i, k= 1,2,3.....25.

For each material one can do calculation of correlation with a reference function, painted steel plate by using equation (4.26). For each material there are twenty five traces. Therefore, twenty five cross correlation coefficients can be attained, for instance, trace 1

for reference function can correlate to trace 1 for target function, trace 2 for reference function can correlate to trace 2 for target function and so on. For the case under study, 25x3 cross correlation coefficients can be obtained.

- **Calculation of cross correlation coefficient**

Similarity of painted steel plate, reference function, with either of the two composite plates can be calculated using above models and data measured.

a) Treatment of amplitudes of original data and by using Trace Mix

Before similarity analysis is performed, the data is processed by LandMark PostStack system [113, 114]. The acquisition data from Surpark are converted to binary format and inputted to LandMark PostStack software system.

Fig. 4.15 shows pictures of original data for the three plates.

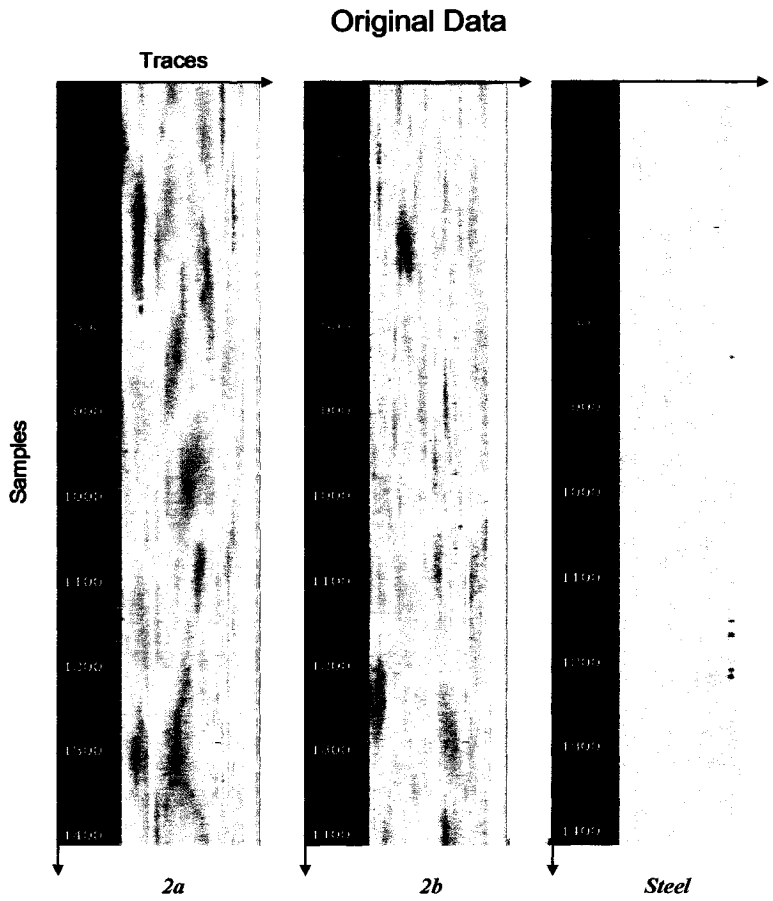

Fig. 4.15: Pictures of original amplitudes of plates 2a and 2b and painted steel plate

Dark color stands for large amplitudes in Fig. 4.15.

Fig. 4.16 and Fig 4.17 show pictures of data after trace mix treatment. It can be seen from Fig. 4.16 and Fig. 4.17 that these data are smoothed. This smoothed surface still contains the character of the material.

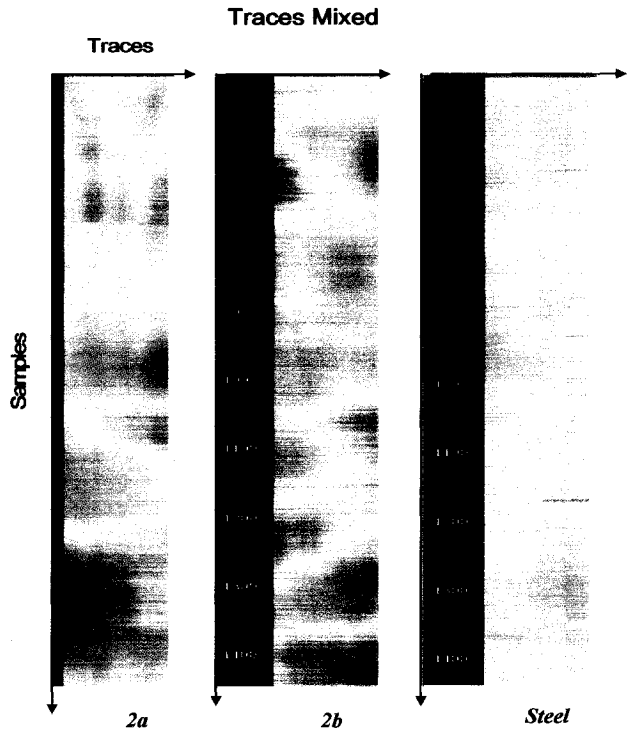

Fig. 4.16: Pictures of amplitudes of traces mixed data

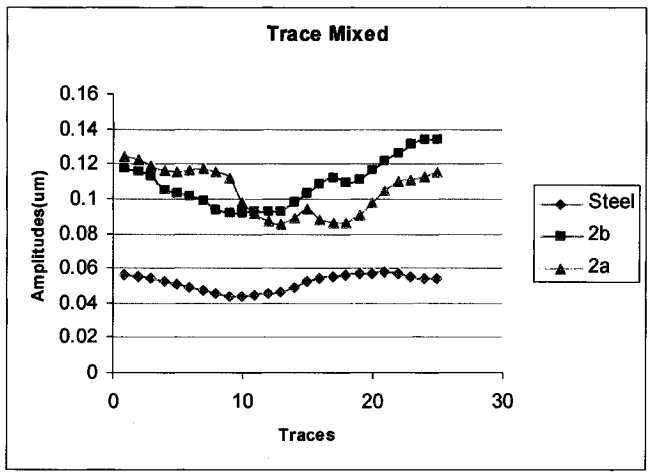

Fig. 4.17 Amplitudes of trace mixed data

b) Cross correlation analysis of the composite plates and painted steel plate

Correlation coefficients of reference surface (painted steel plate) and target surfaces (composite plate 2a and 2b) are calculated, respectively, and shown in Fig. 4.18.

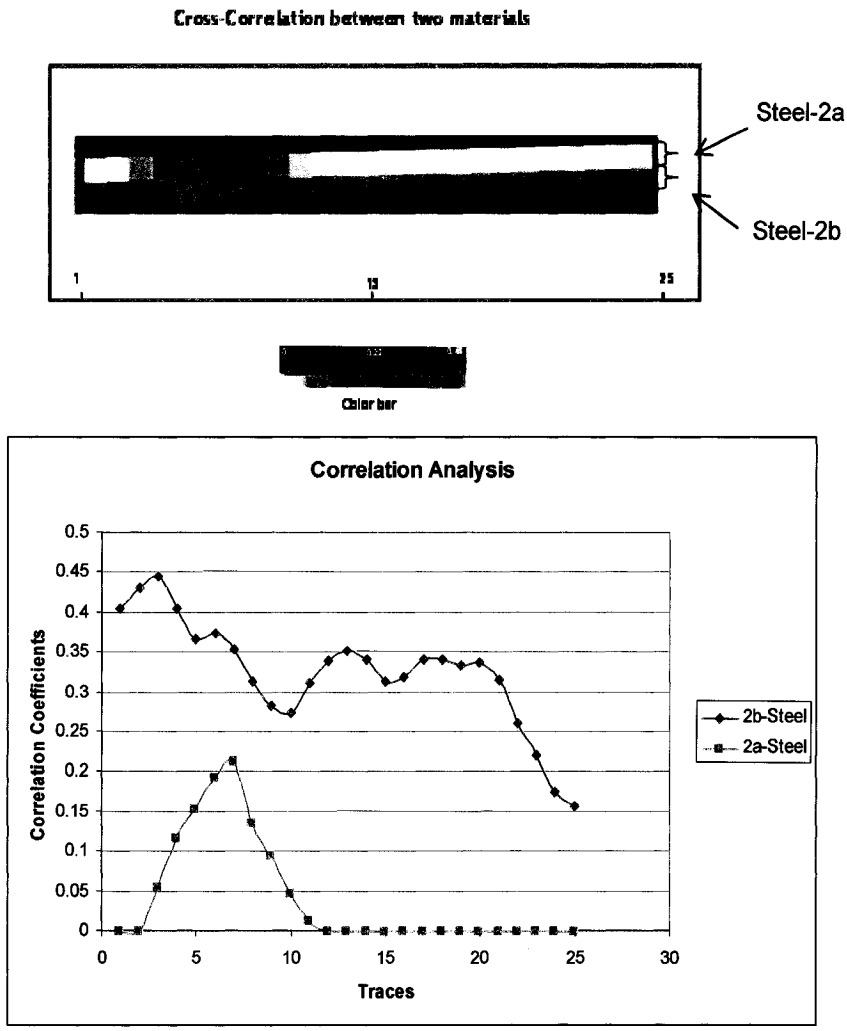

Fig. 4.18: Cross-correlation between painted steel plate and composite plates

The results calculated show composite plate 2b and painted steel plate have higher correlation coefficients than those between composite plate 2a and painted steel plate. Therefore, surface quality of composite plate 2b is more close to the surface quality of painted steel plate.

However, even for composite plate 2b, its average correlation extent with painted steel plate is only round 39%. This means surface quality level of composite plates still display a big gap with the surface quality level of painted steel plate.

2. Similarity analysis [88, 115]

As mentioned before, distance or distance coefficient is a very important parameter to describe similar extent between objects. In this model assume that the surface of the painted steel plate has class A surface finish. Therefore, it is used as a reference surface. Surface profiles of composite plates can be compared with the reference surface profile. In this way, it may be possible to distinguish surface quality between composite plates and can describe similar extents of composite plates and painted steel plate with class A surface finish.

- Manhattan Distance

Manhattan distance or City Block is an efficient statistical measurement of similarity/dissimilarity. For this situation, Manhattan distance uses two equal length wavelets with N time samples and sums the absolute value of the difference in corresponding samples for all samples. Manhattan distance is given by:

$$M = \sum_{i=1}^{N} |A_i - B_i| \tag{4.27}$$

where:

M is the Manhattan distance

A is the reference wavelet

B is the target wavelet guided by the horizon

N is the number of discretizations in each wavelet.

Two identical wavelets will result in a Manhattan distance value of 0 and wavelets that are not identical will result in a positive Manhattan distance.

In PostStack software the center trace window is compared to the target trace window using Manhattan distance (shown in Fig. 4.19).

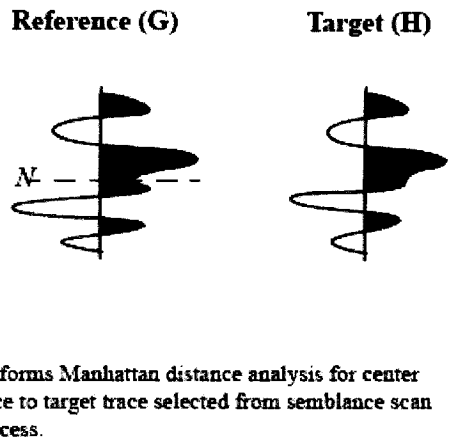

Fig. 4.19: A schematic diagram for similarity by Manhattan distance

The center trace is a reference function. Manhattan distance is the sum of the absolute value of the sample differences between the windows. This sum (numerator) is divided by the sum of the absolute values of each sample of the two traces within the specified window. The resulting values are numbered between 0 and +1. Number 0 expresses that the two trace are total similarity. It can be expressed as equation (4.28).

$$M_d = 100 \frac{\sum_{K=N-n/2}^{K=N+n/2} |G_k - H_{k+d}|}{\sum_{K=N-n/2}^{K=N+n/2} (|G_k| + |H_{k+d}|)} \qquad (4.28)$$

Where M_d is Manhattan distance for any pair of traces, G and H, n is the number of

digitizations in the wavelet, d is the integer sample shift, N is the center sample of the reference trace, 100 is scalar to facilitate display, G_k is Reference wavelet at k, H_k is Target wavelet at k.

In the PostStack program d is integer sample shift which would give a better match for the two traces. PostStack would search for a possible d automatically. For minimum similarity, the minimum value will be output.

- Semblance Value

In the PostStack program, semblance value for maximum similarity is also used to calculate similarity of wavelets. The formula for calculating semblance values is as follows:

$$S(t,d) = 100 \frac{\sum_{k=t-N/2}^{k=t+N/2} (G_k + H_{k+d})^2}{2 \sum_{k=t-N/2}^{k=t+N/2} (G_k^2 + H_{k+d}^2)} \tag{4.29}$$

where S is the semblance value calculated for any pair of traces, G and H, for scan distance t and dip d which is the shift along the scan line . N is the number of samples in the comparison window. The value 100 is used to scale the output to facilitate display.

This computation is repeated for every possible dip within the comparison limits, and the highest semblance value obtained is retained for the later selection of the target trace. Number 100 expresses that the two traces are total similarity. Fig. 4.20 shows the schematic diagram for the computation. In Fig. 4.20 (a) the semblance value of computation is 20, however, if a shift distance d value is used (shown in Fig. 4.20 (b)), the computation is repeated, the result is 90. The maximum value is output.

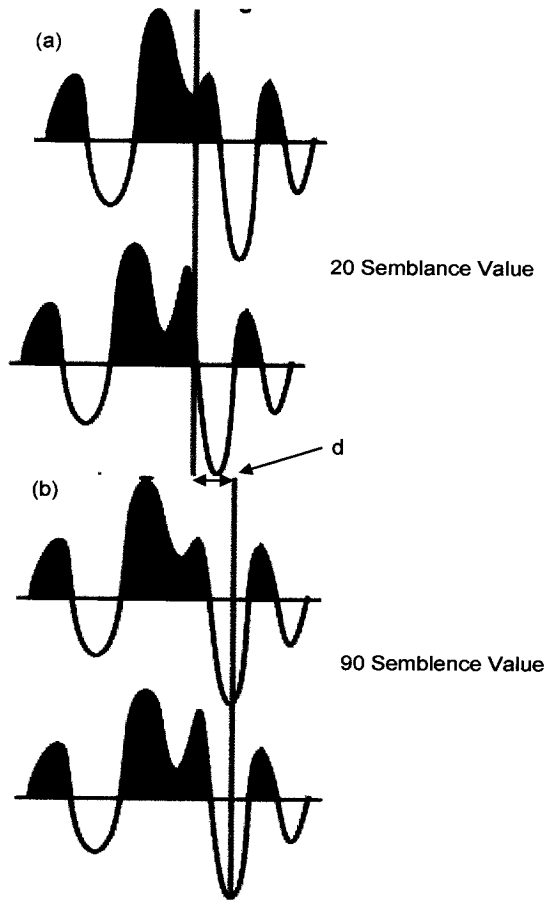

Fig. 4.20: A schematic diagram for computation dip

Fig. 4.21 is an example for similarity analysis by semblance value.

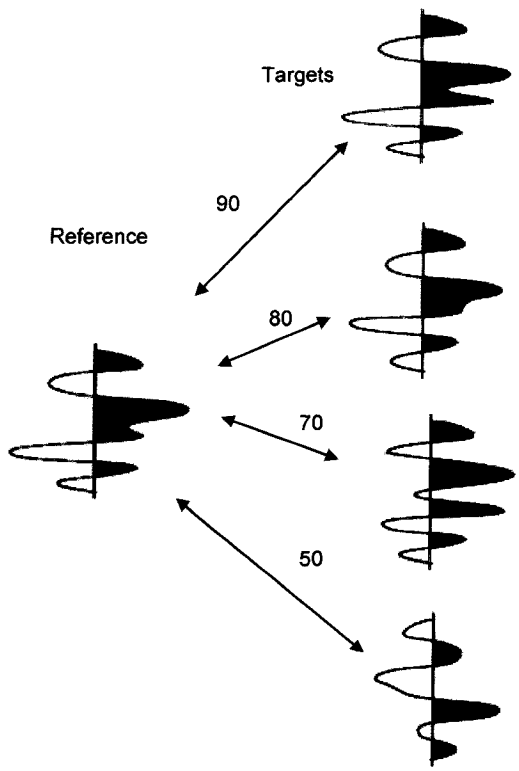

Fig. 4.21: An example for similarity analysis by semblance value

It can be seen that the semblance values can describe the extent of similarity between traces. For instance, in Fig. 4.21 if semblance value is 90, the two traces have the greatest similarity. Therefore, the bigger is semblance value, the more similarity is the two traces.

- Calculation of Similarity Analysis

In ESP (Event Similarity Prediction) calculations, semblance and Manhattan distance can be used to predict similarity. ESP 3D scans from one to eight nearest neighbor traces (Scan Pattern) using semblance to determine the minimum or maximum (Evaluation Statistic) similarity.

Unconstrained semblance scans of the center trace to each neighbor trace were used to analyze similarity for these materials. The Unconstrained option measures data similarity via a two trace semblance analysis. For each center trace, data within a fixed

displacement window is compared to data in a sliding time window on a neighbor trace. The best semblance value computed during the sliding process is retained for that neighbor. This process is repeated for each selected neighbor.

The scan pattern determines the number and arrangement of adjacent traces to be scanned by semblance analysis with the current center trace.

In the calculation, Ell-2 Traces program is used to compare the current trace with an adjacent inline and cross line trace. Fig. 4.22 is the result of semblance values that were calculated.

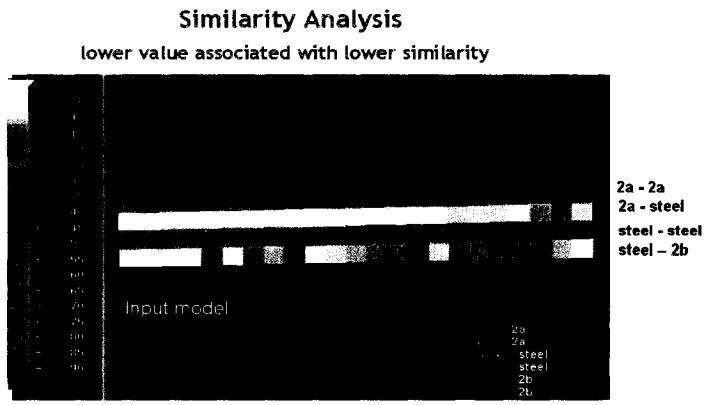

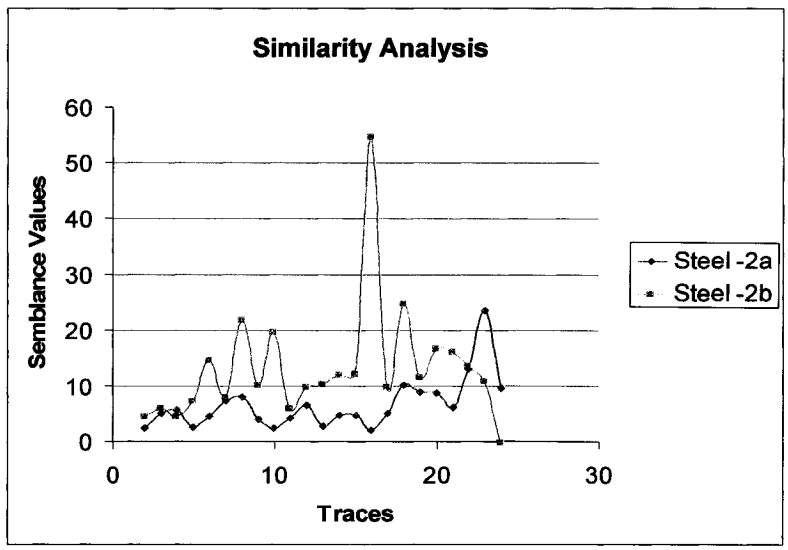

Fig. 4.22: Semblance values for painted steel-2b and painted steel-2a

It can be seen from Fig. 4.21 that surface profiles of 2b are more similar to those of painted steel plate than that of 2a. However, similarity extents of surface profiles of composite plates with the painted steel plates are very low. Average semblance values are 5.6 for plate 2b, 2.8 for plate 2a. This means there is a big gap between surface qualities of composite plates and painted steel plate.

4.5 Conclusion

It can be concluded from above analysis and discussion that it is possible to distinguish surface quality between composite plates 2a and 2b by comparing with painted steel plate (class A surface finish). Analysis of many characteristic parameters is helpful to distinguish surface quality of material.

The observations of optical microscopy shows that painted steel plate has the best surface finish, the surface finish of plate 2b is better than that of plate 2a.

Based on Ra, the Maximum Entropy Method was used to analyze Ra values distribution on surface of composite plate. This is able to discriminate surface quality in terms of distribution of Ra values in some extent.

Spectrum analysis does not show much correlation between frequency spectrum and quality of the surface.

The correlation analysis model shows composite plate 2b has stronger correlation with painted steel plate than composite plate 2a. But composite material surface still has low correlation extent with painted steel.

Similarity analyses model shows composite plate 2b and painted steel plate has greater similarity than composite plate 2a and painted steel plate.

Analyses of many parameters show that surface quality level of composite plate 2b is close to that of painted steel plate with class A surface finish. Therefore, surface quality of composite plate 2b is better than that of composite plate 2a.

Chapter 5

Validation of the proposed approaches

The above procedure was validated by using more plates. More composite plates fabricated at McGill University were measured and evaluated for validation of the proposed approach. In this chapter the results from seven plates are presented, in which the surface of painted steel plate is used as a reference function, the surfaces of six composite plates are used as target functions, in which sample 2a and 2b are from Ford Motor. Samples JU29, JL01, JL13 and JL15 are from McGill University. By comparison and analysis between their waveforms, under closely Ra values, surface quality levels of the six composite plates can be discriminated.

5.1 Composite Plates

Composite panels were made using RTM at McGill University. There are 3 main aspects of making a plate by RTM at McGill University [116].

1- Mold and pump preparation

2- Resin and fiber preparation

3- Resin filing and consolidation

Mold preparation

The Mold and pump were cleaned first using acetone, so that there was no residue on mold's surface from previous injection. The injection and vent ports were cleaned and plastic tubing was inserted in them for the new injection. The mold was then applied with a very thin layer of mold release agent (chemlease 41-90). The injection pump was also

applied with 4-5 layers of release agent. Picture frame was also applied with the release agent and was sealed using a sealing tape.

Fibers and resin preparation [116]

The F3P (Programmable Preform Process of Ford) preform consists of three layers of glass fibers as shown in Fig. 5.1.

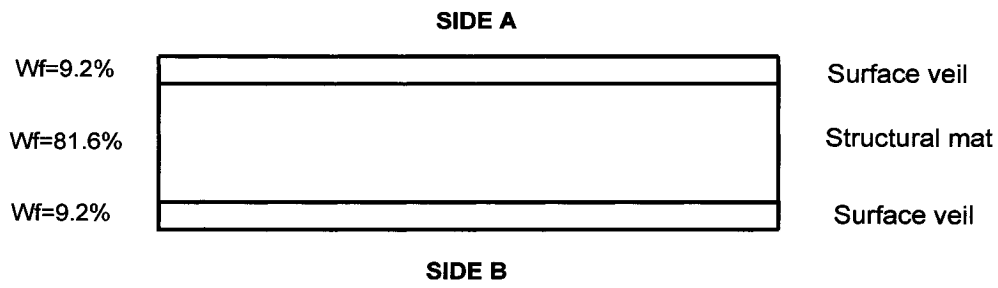

Fig. 5.1: Through thickness structure of the F3P glass fiber preform

The top layer (side A) had a surface veil consisting of thin continuous glass fibers of an average diameter of 20 μm. The center layer consisted of chopped fiber bundles and the bottom layer (side B) also had thin continuous glass fibers of an average diameter 20 μm. The difference between side-A and side-B was that relatively higher binder concentration was present on side-B of the preform which could potentially affect the surface quality of the sample. Hence, side-A was used for all the surface finish measurement. The weight fraction of surface veil was 9.2% and the weight fraction of structural mat was 81.6% in the preform. The F3P perform was cut to dimensions of the picture frame and resin was prepared about half an hour before the injection. The water heater was started two hours before the injection to heat the mold. The mold platens were kept away from each other during mold heating. Resin (Scott Basder PD9551 Standard) was prepared according to the formulation. The low profile additive used in the resin was Scott Bader PD94119.

Resin was mixed with the accelerator (cobalt 2-ethylhexanote), catalyst (tert-butyl peroxybenzoate), filler (OMYA BLR2 Calcium carbonate) and styrene (if required).

Resin filing and consolidation

The mold was heated for 2 hours before the injection could be done. The picture frame was inserted in the mold just before injection and mold platens were sealed together by the press. Resin was poured in the pump and injection was done at the required pressure. Water heater kept heating the mold during injection and curing. The pressure variation on the sensors was observed through the data acquisition system. When the pressure reached maximum value during curing, the plate was de-molded.

High pressure would keep the surface of mold in contact with the surface of composite plate, which would result in better surface finish. Resin with low profile additive (LPA) can push the composite plate against the mold cavity and compensate for the resin cure shrinkage in order to attain better surface finish.

5.2 Measurement results of samples from McGill

Four composite plates, JU29, JL01, JL13 and JL15 were examined. Ra values are shown in Table 5.1 and Fig.5.2.

Table 5.1: Ra of Samples (JU29, JL01, JL13 and JL15) from McGill University

Sample	JU29	JL01	JL13	JL15
Measurement Scans	Ra(μm)	Ra(μm)	Ra(μm)	Ra(μm)
1	0.142	0.13	0.114	0.154
2	0.162	0.134	0.13	0.13
3	0.132	0.131	0.14	0.137
4	0.175	0.146	0.15	0.161
5	0.212	0.134	0.13	0.14
6	0.168	0.168	0.133	0.139
7	0.13	0.174	0.13	0.147
8	0.131	0.159	0.158	0.133
9	0.121	0.187	0.152	0.13
10	0.127	0.145	0.121	0.149
11	0.123	0.155	0.124	0.141
12	0.141	0.137	0.141	0.131
13	0.128	0.166	0.169	0.136
14	0.163	0.162	0.114	0.148
15	0.129	0.125	0.141	0.147
16	0.143	0.141	0.121	0.123
17	0.138	0.133	0.13	0.146
18	0.139	0.125	0.139	0.144
19	0.17	0.148	0.145	0.148
20	0.144	0.168	0.12	0.13
21	0.131	0.152	0.131	0.151
22	0.125	0.135	0.115	0.163
23	0.128	0.132	0.118	0.137
24	0.139	0.211	0.114	0.142
25	0.134	0.13	0.124	0.17
Average(Ra)	0.143	0.149	0.132	0.143

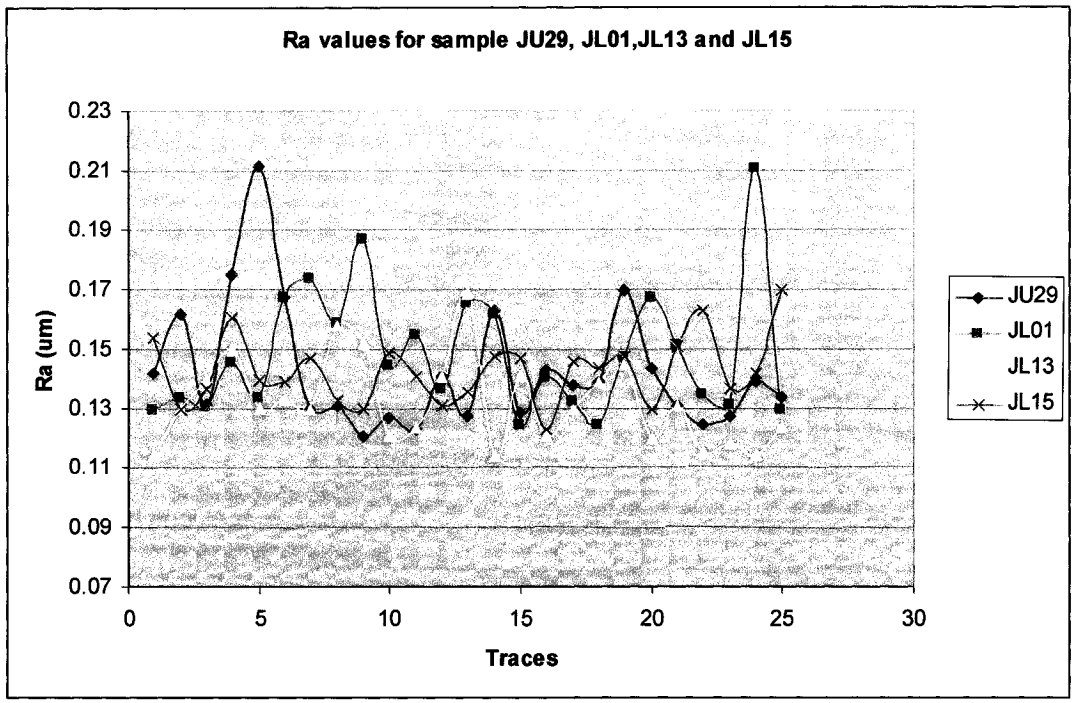

Fig. 5.2: Ra values of samples JU29, JL01, JL13 and JL15

Each trace was transferred to digital data to output in Excel format. All data outputted were transferred to binary data in order to input into Landmark analysis software system.

5.3 Evaluation of surface quality levels

1. Ra Values

Ra values of the seven materials are shown in Table 5.2 and Fig. 5.2.

Table 5.2: Average Ra values of composite plates and painted steel plate

Name	2a	2b	JU29	JL01	JL13	JL15	Steel
Ra(μm)	0.220	0.195	0.143	0.149	0.132	0.143	0.078

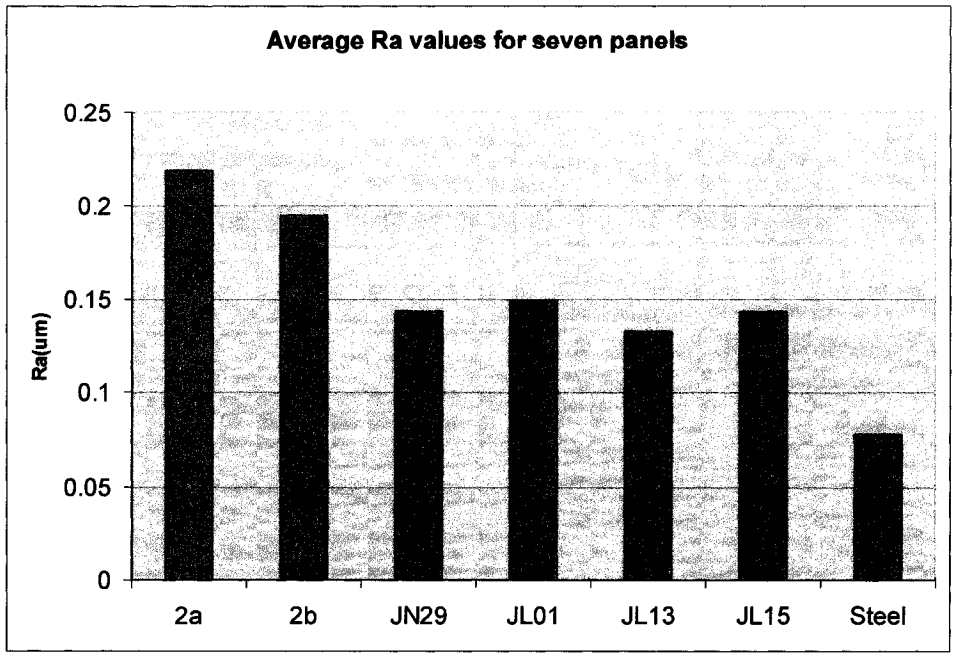

Fig. 5.3: Average Ra values for seven panels

It can be seen from Table 5.2 and Fig. 5.3 that samples from McGill University have very close Ra values. Their Ra values are smaller than that of composite samples from Ford Motor. In terms of Ra values, surface quality of samples from McGill University seems to be better than that of samples from Ford Motor. But it is difficult to discriminate surface quality between samples from McGill University from Table 5.2 and Fig.5.2. Table 5.3 shows a ranking for the seven panels based on Ra values.

Table 5.3: Rank of composite plates and painted steel plate by Ra values

Name	2a	2b	JU29	JL01	JL13	JL15	Steel
Ra(μm)	0.220	0.195	0.143	0.149	0.132	0.143	0.078
Rank	6	5	3	4	2	3	1

2. Visual observation and microstructures

Fig. 5.4 shows magnification photographs of the surfaces.

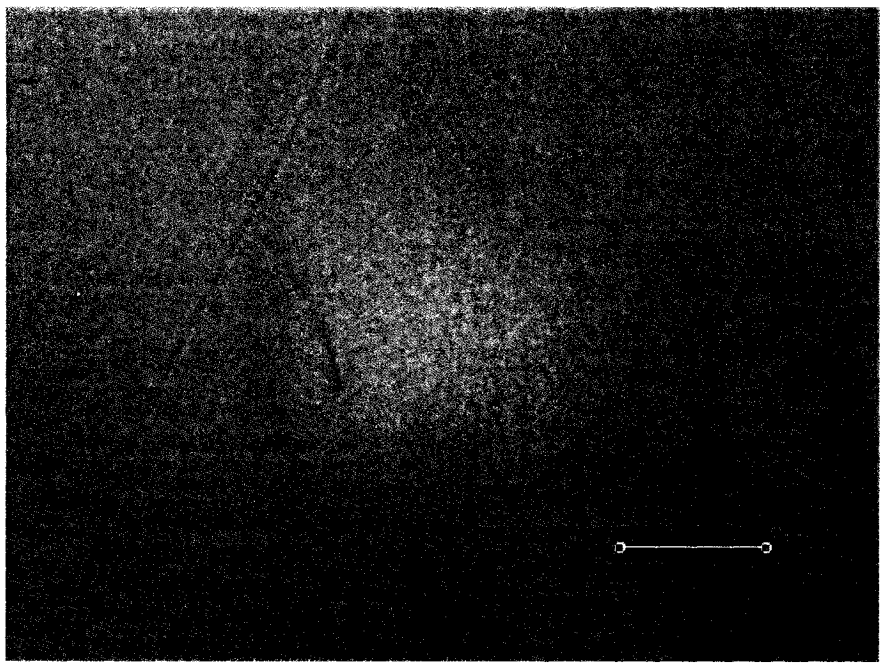

Painted steel plate

2a

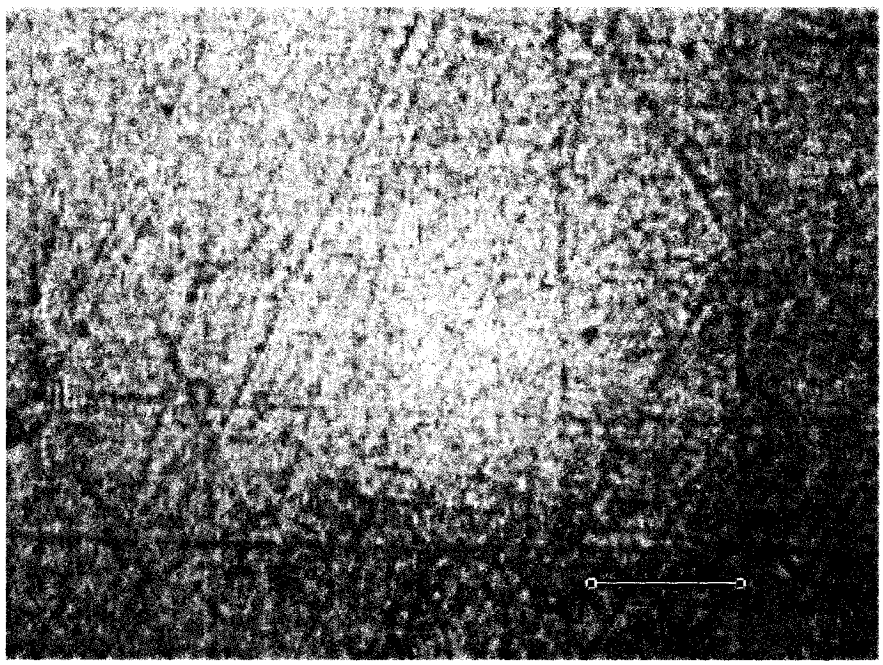

2b

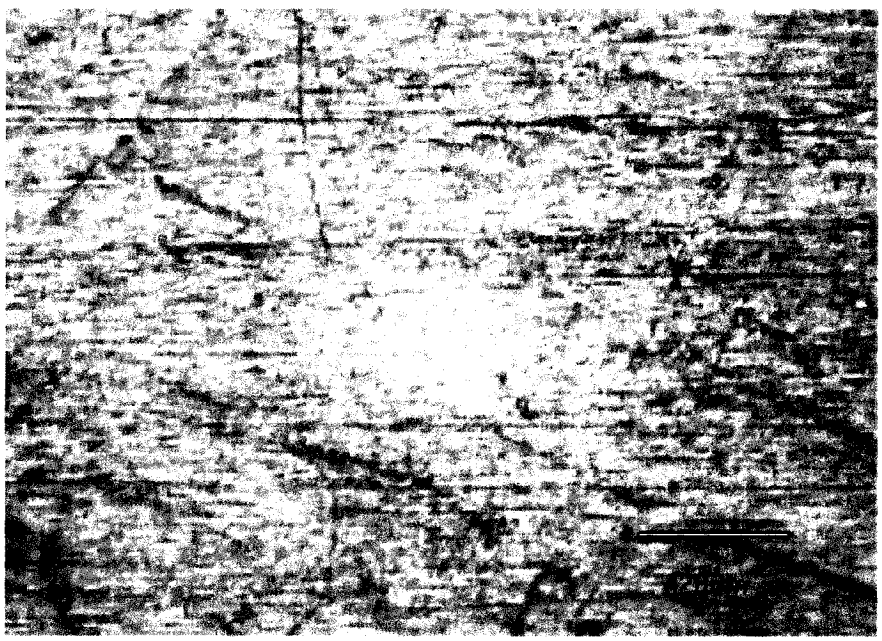

JU29

JL01

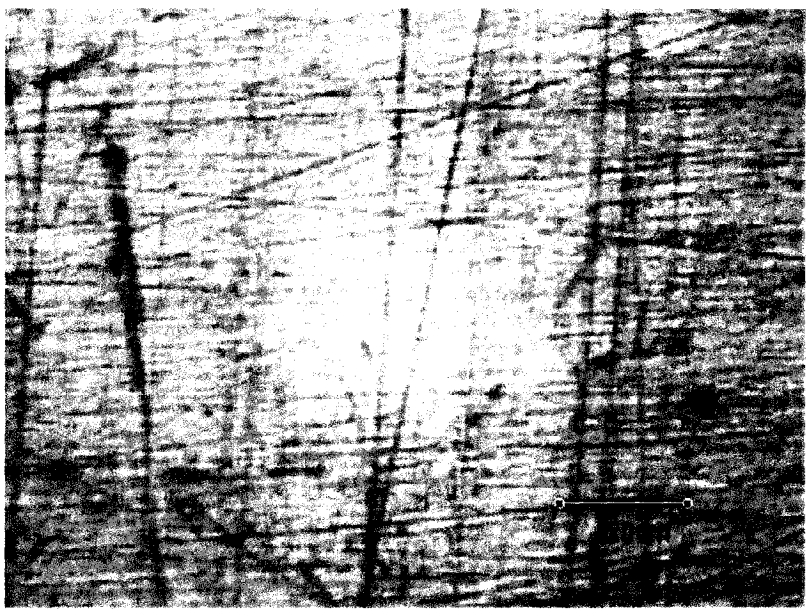

JL15

JL13

Fig. 5.4: Surface photographs of the seven panels

The ranking of quality of the seven surfaces was first done by visual observation. Twenty eight people were invited to observe the surfaces of panels. They gave surface quality's ranks of these panels in Table 5.4. Average rank of surface quality levels of the seven panels are shown in Table 5.5.

Table 5.4: Ranks of surface quality levels of the seven panels by 28 people

	ST	2a	2b	JU29	JL01	JL13	JL15
Ming Xie	1	5	2	4	7	6	3
Heng Wang	1	3	2	3	7	6	5
Linxin Wu	1	3	2	4	7	6	5
Kassan	1	7	2	3	6	4	5
Dousheng Xu	1	7	2	3	6	4	5
ShilianHu	1	7	2	3	6	4	5
Paul	1	6	2	3	7	4	5
EeileenHuang	1	7	2	3	6	5	4
Rahimzadeh	1	7	2	3	6	4	5
Kim	1	7	2	3	4	6	5
Y. Zhang	1	6	2	3	7	5	4
Ernest	1	3	2	4	7	5	6
Nick	1	6	2	3	7	4	5
Da Ying Liu	1	3	2	5	7	6	4
Arshad	1	6	2	3	7	5	4
Yuan Xu	1	7	2	3	6	5	4
Luckart	2	6	1	3	7	4	5
Akhlaqn	1	6	2	4	7	3	5
W. Liu	1	7	2	3	4	6	5
Fatseyeu	1	3	2	4	7	5	6
Vasil	1	4	2	3	7	5	6
Roxana	1	6	2	3	7	5	4
Allereng	1	3	2	6	7	5	4
Motamedi	1	3	2	4	7	5	6
You	1	5	2	4	7	3	6
Davide	1	6	2	3	7	5	4
Ama	1	6	2	3	7	4	5
Rabert	1	6	2	3	7	5	4

Table 5.5: Average rank of surface quality levels of the seven panels by visual observation

	ST	2a	2b	JU29	JL01	JL13	JL15
1	1	5	2	4	7	6	3
2	1	3	2	3	7	6	5
3	1	3	2	4	7	6	5
4	1	7	2	3	6	4	5
5	1	7	2	3	6	4	5
6	1	7	2	3	6	4	5
7	1	6	2	3	7	4	5
8	1	7	2	3	6	5	4
9	1	7	2	3	6	4	5
10	1	7	2	3	4	6	5
11	1	6	2	3	7	5	4
12	1	3	2	4	7	5	6
13	1	6	2	3	7	4	5
14	1	3	2	5	7	6	4
15	1	6	2	3	7	5	4
16	1	7	2	3	6	5	4
17	2	6	1	3	7	4	5
18	1	6	2	4	7	3	5
19	1	7	2	3	4	6	5
20	1	3	2	4	7	5	6
21	1	4	2	3	7	5	6
22	1	6	2	3	7	5	4
23	1	3	2	6	7	5	4
24	1	3	2	4	7	5	6
25	1	5	2	4	7	3	6
26	1	6	2	3	7	5	4
27	1	6	2	3	7	4	5
28	1	6	2	3	7	5	4
Average values	1.035	5.393	1.964	3.429	6.571	4.786	4.786
Rank	1	6	2	3	7	4	4

Ranking range is 1-7 in which 1 represents the best quality.

Optical microscope was used to observe the sections of the six composite plates. AFM was used to observe the surfaces of the composite plates. Microstructures of sections of the six composite plates are shown in Fig. 5.5.

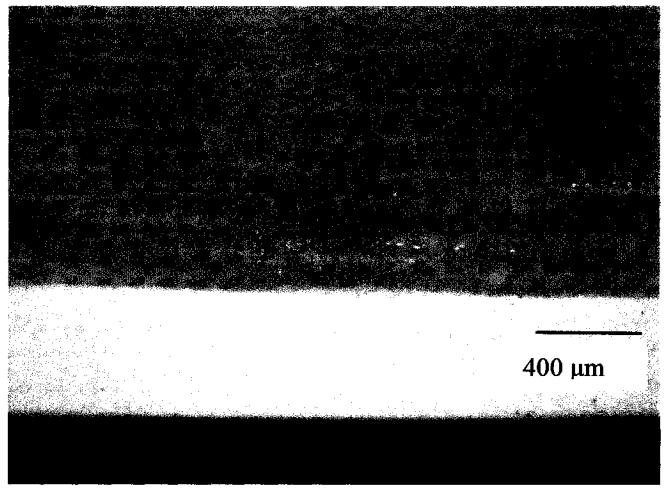

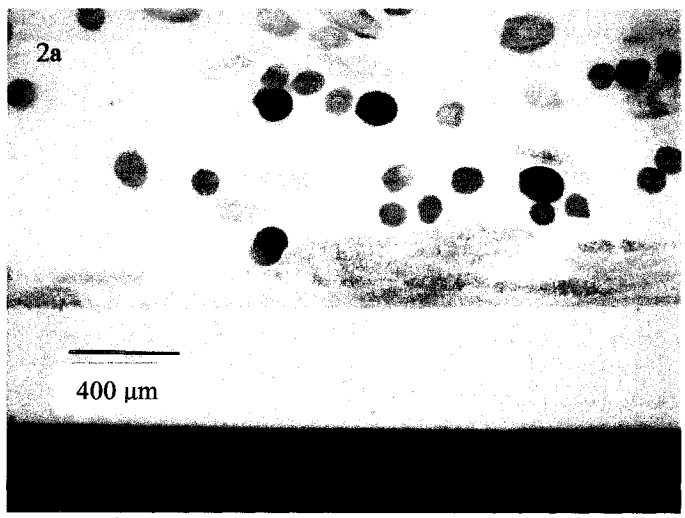

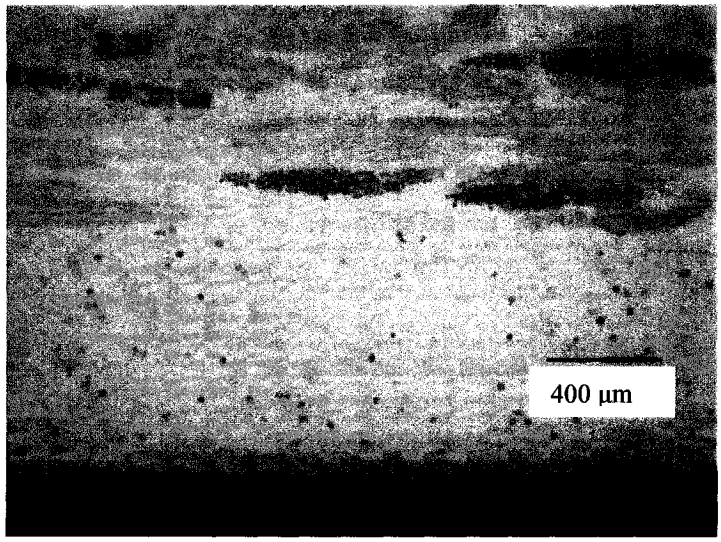
400 µm

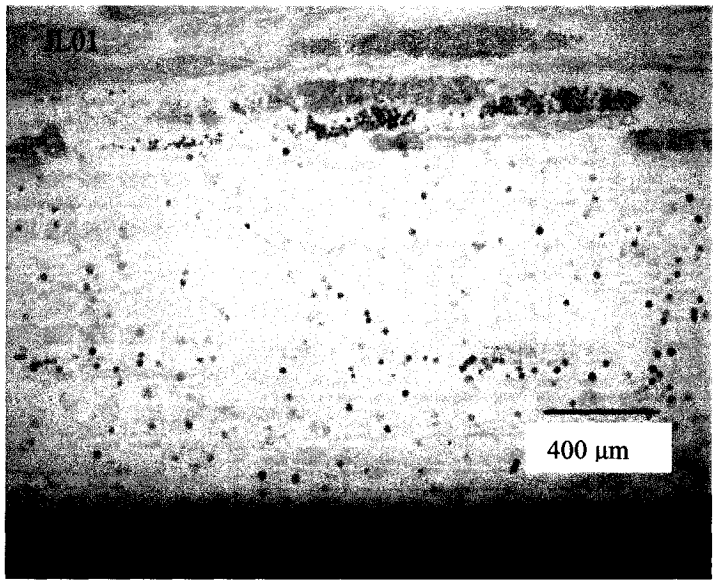
400 µm

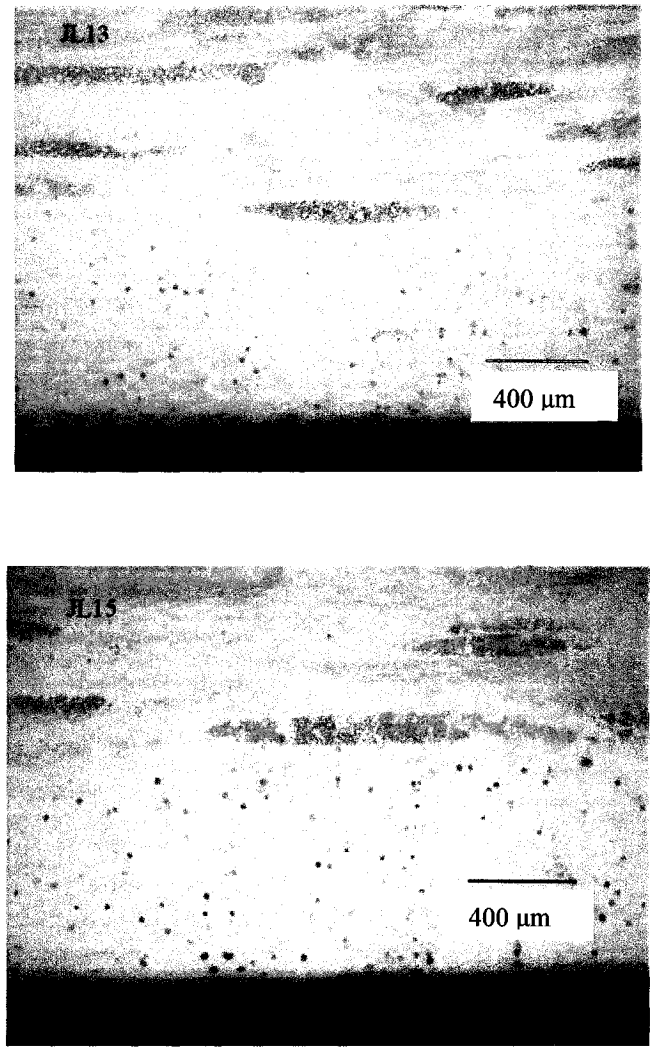

Fig. 5.5: Microstructures of sections of the six composite plates

It can be seen from Fig. 5.5 that there is a layer of resin on the surface of plate (lower part of the figures). The thickness of the layer is around 0.4-0.5mm. The resin layers of composite plates 2a and 2b are clearer than that of other plates. Composite plates made at McGill seem to mix fibers in the layer and the thickness of the layer for samples of McGill University is a little larger than that of samples of Ford Motor. Larger thickness of the layer is helpful to reduce fiber readout and textile-induced waviness [38].

AFM microstructures of the surfaces of the six composite plates are shown in Fig. 5.6. The microphotographs demonstrate surface topography of the samples using the same data scale. However, phase images are used to identify microconstituents with varying values of elastic modulus. Fig. 5.7 shows topography and phase images of the six composite plates.

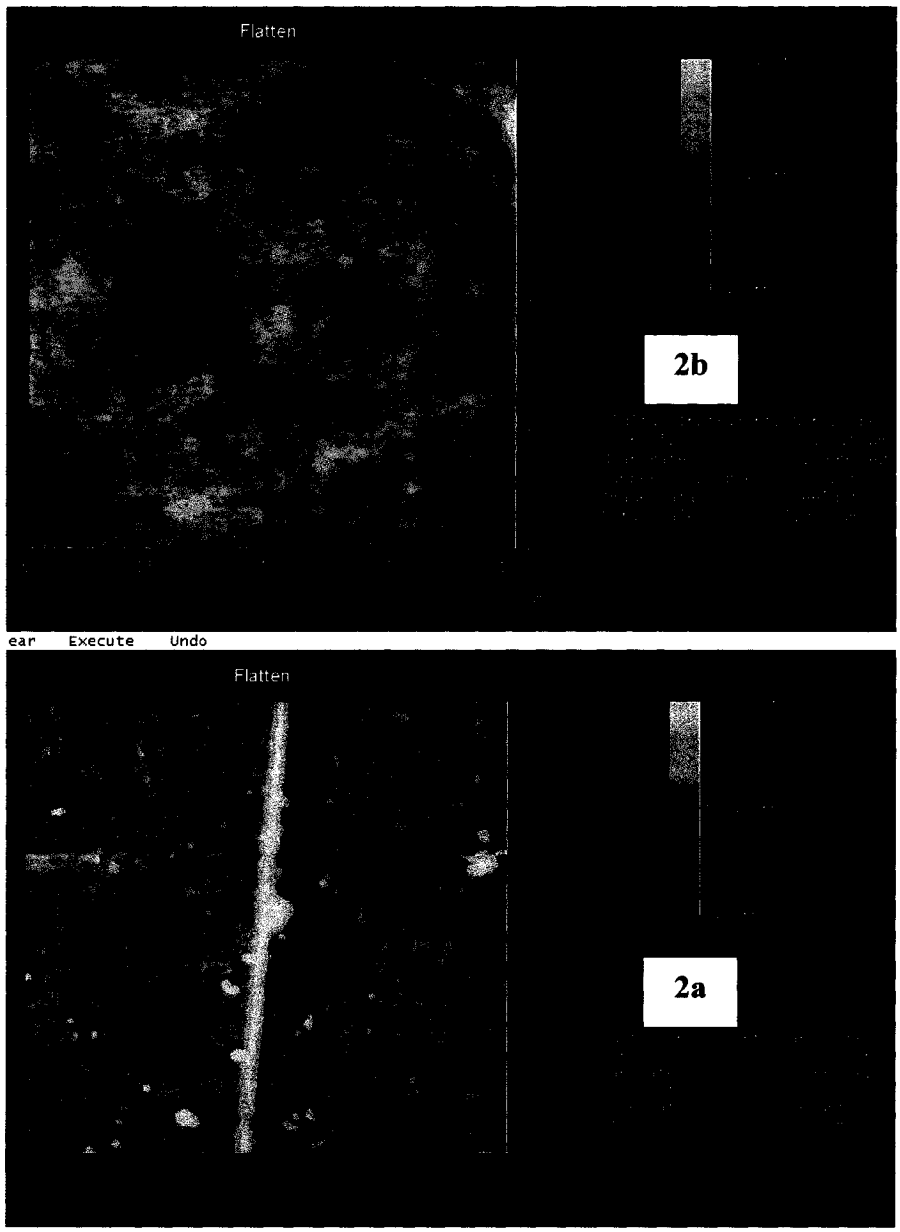

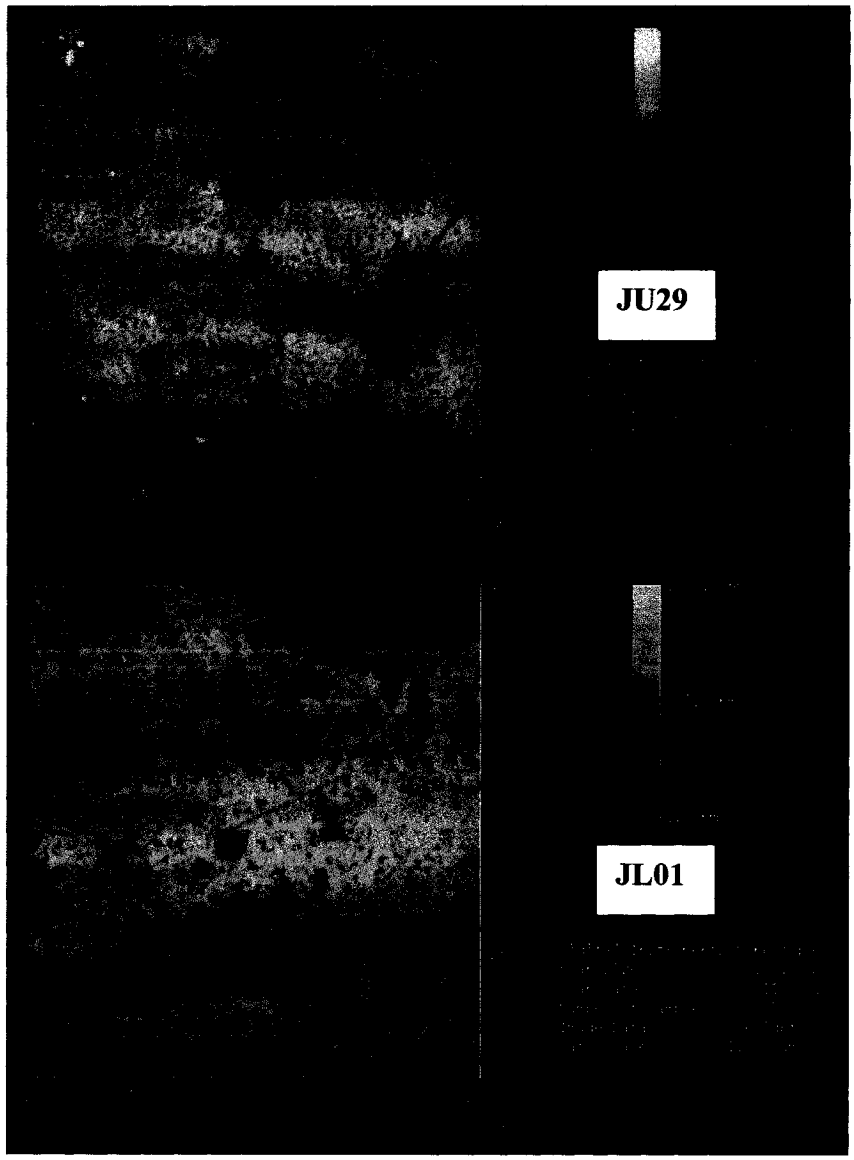
JU29
JL01

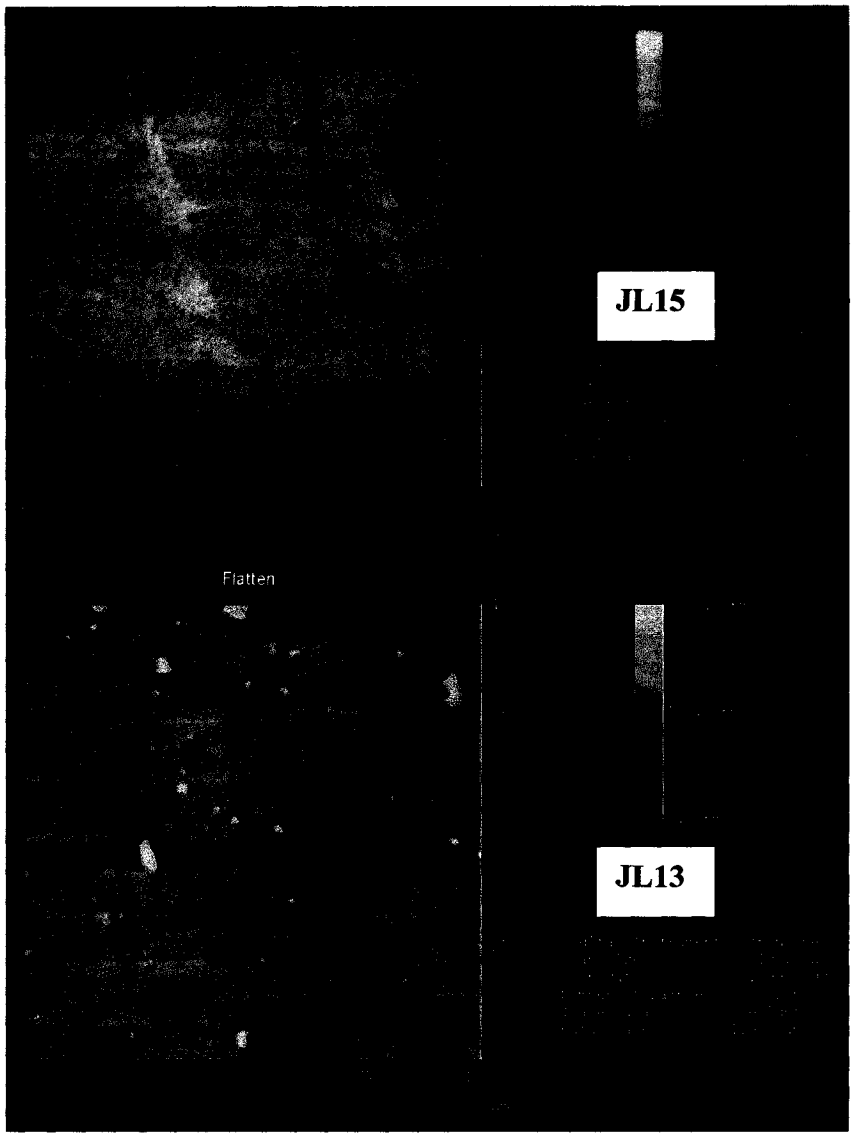

Fig. 5.6: The surface topography of the six composite plates

It can be seen from Fig. 5.6 that surface topography of plates from Ford are coarser than that of plates from McGill. Surfaces of Plate JL13 and JU29 are smoother than that of other plates.

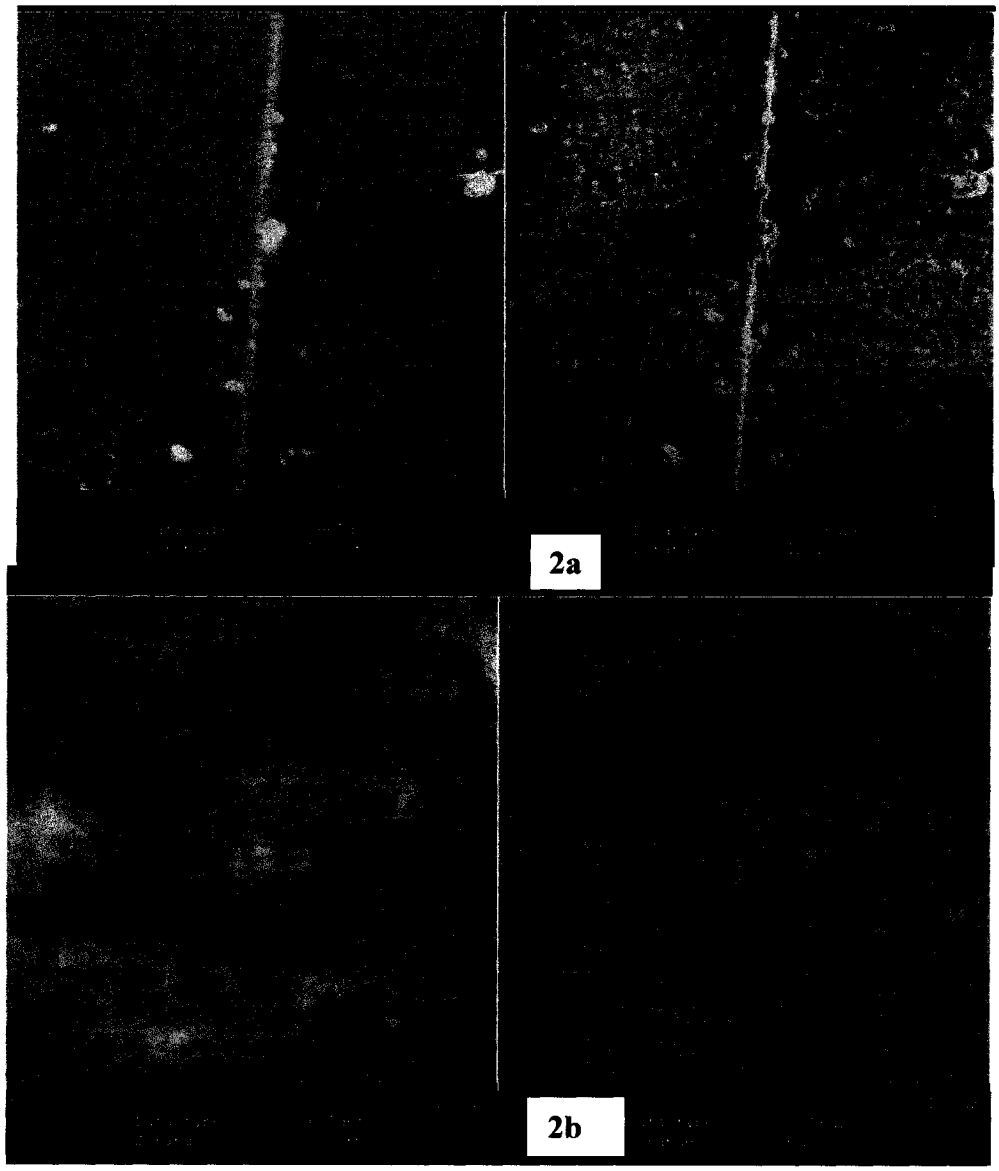
2a
2b

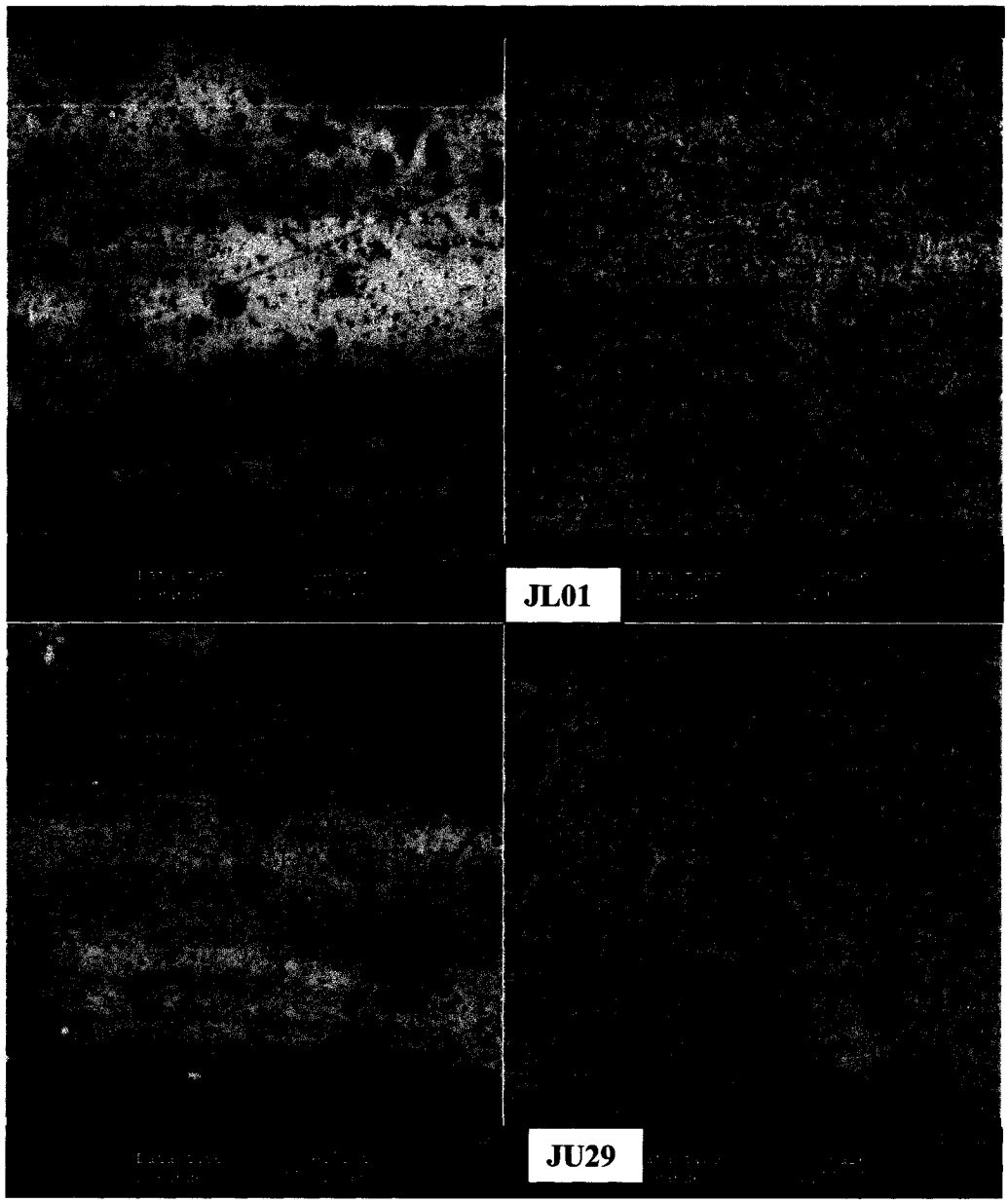
JL01
JU29

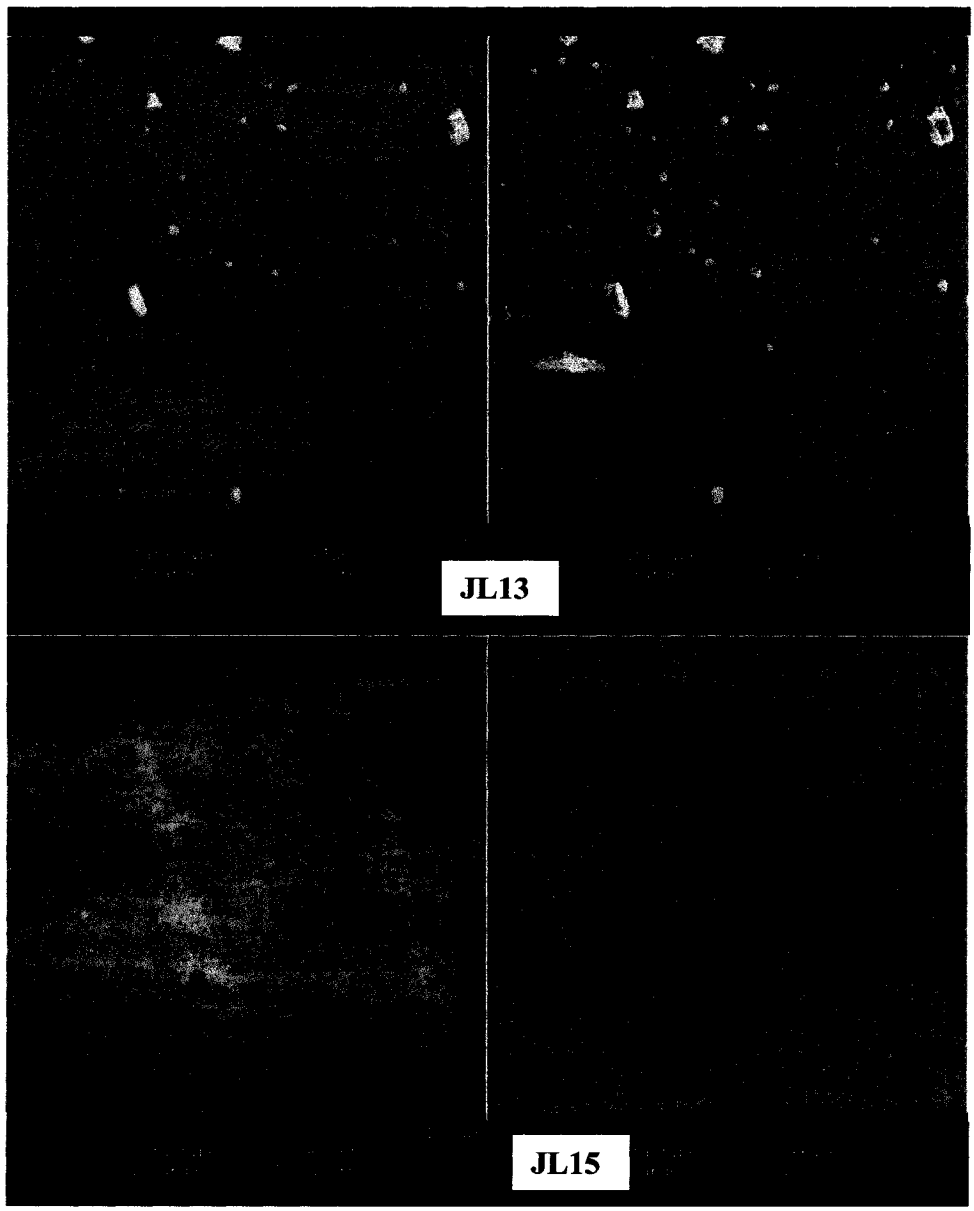

Fig. 5.7: Phase images of the surfaces of six composite plates

In Fig. 5.7 left pictures show topography and right pictures show their phase images. The phase image provides a high contrast due to differences in stiffness, viscoelasticity or adhesion, depending on the imaging conditions, thus allowing to distinguishing the different components of a composite. Moreover, the phase image provides a higher resolution than the height image [117]. As mentioned above, there is a layer of resin on

the surface of the composite plate. Some $CaCO_3$ powders are mixed in the resin. It is not difficult to see that the extent of dispersion of particles and sizes or segments of the particles will affect the topography of the surface. Therefore, it is very important to use fine particles and enable them to be more uniformly mixed in the resin. If nano powders are used to replace the coarse particles and they may be dispersed in the resin, surface quality of composite plate may be improved. Nanoclay has been used to control shrinkage of low profile unsaturated resin [118].

3. Maximum Entropy probability distribution profiles

Maximum Entropy Method was used to determine the distributions of Ra of surface signatures of the seven panels. The probability density distribution of Ra values for the seven panels are shown in Fig. 5.8. Fig. 5.9 shows the probability density distribution of Ra values of samples from McGill University.

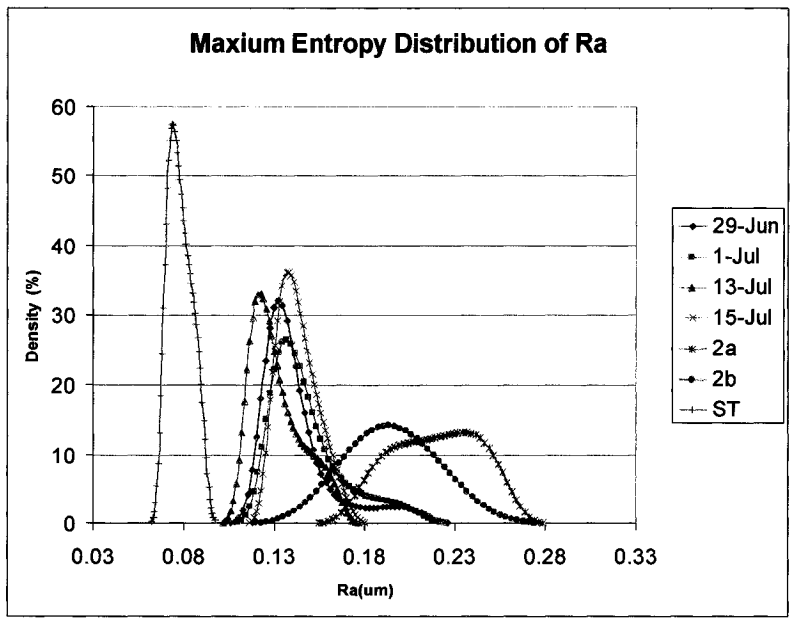

Fig. 5.8: Probability density functions of Ra values for the seven panels

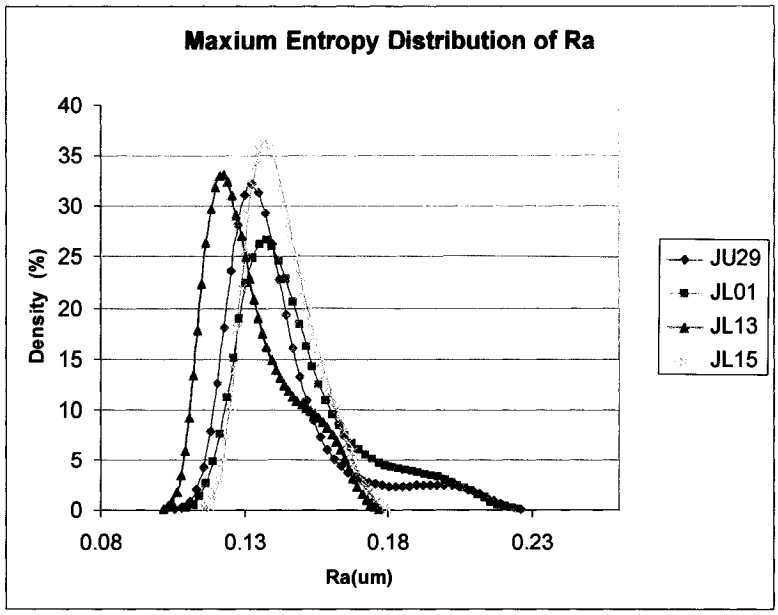

Fig. 5.9: Probability density functions of Ra values of samples from McGill University

It should be noted that based on evaluation standards of Ra painted steel plate has the best surface finish, surface finish of samples from McGill University are better than that of samples from Ford Motor. In samples from McGill University, sample JL13 seems to have the best surface finish. JU29 and JL15 seem to have the same surface finish and their surface finish may be a little better that of JL01.

It is obvious from Table 5.5, Fig. 5.8 and Fig. 5.9 that there are differences between evaluation using probability distribution based on Ra and visual observation.

Table 5.6 shows the ranking using MEM.

Table 5.6: Rank of surface quality levels of the seven panels using MEM

	ST	2a	2b	JU29	JL01	JL13	JL15
Rank	1	6	5	3	4	2	3

Note that the results in Table 5.6 are the same as Table 5.3.

4. Models of cross correlation and similarity analysis

In models using cross correlation and similarity analysis the surface of painted steel plate is used as a reference function, the six composite plates are used as target functions, in which samples 2a and 2b are from Ford Motor, samples JU29, JL01, JL13 and JL15 are from McGill University. By comparison and analysis between their waveforms, surface quality levels of the six composite plates may be discriminated.

Fig. 5.10 shows 3-D data arrangement, three coordinates representing materials, traces and samples, respectively. Each material has 25 scans, which is referred to as 25 traces. The surfaces of each panel can be compared to each other by mathematical calculations and the data are read by the computer.

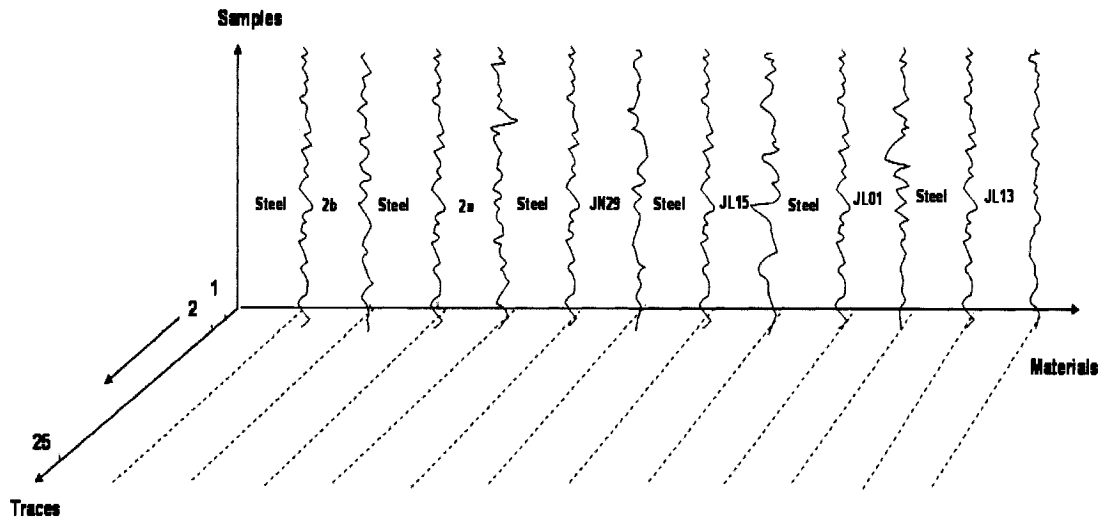

Fig. 5.10: 3D data volume model of the seven panels

a) Amplitudes of original data and Trace Mix

The data used for analysis was processed by LandMark system. The acquisition data from Surpark were converted to binary format and inputted to LandMark software system.

Fig. 5.11 shows pictures of original data for the seven materials. Painted steel has the smallest amplitude. For other material it is difficult to say which one is smoother or better.

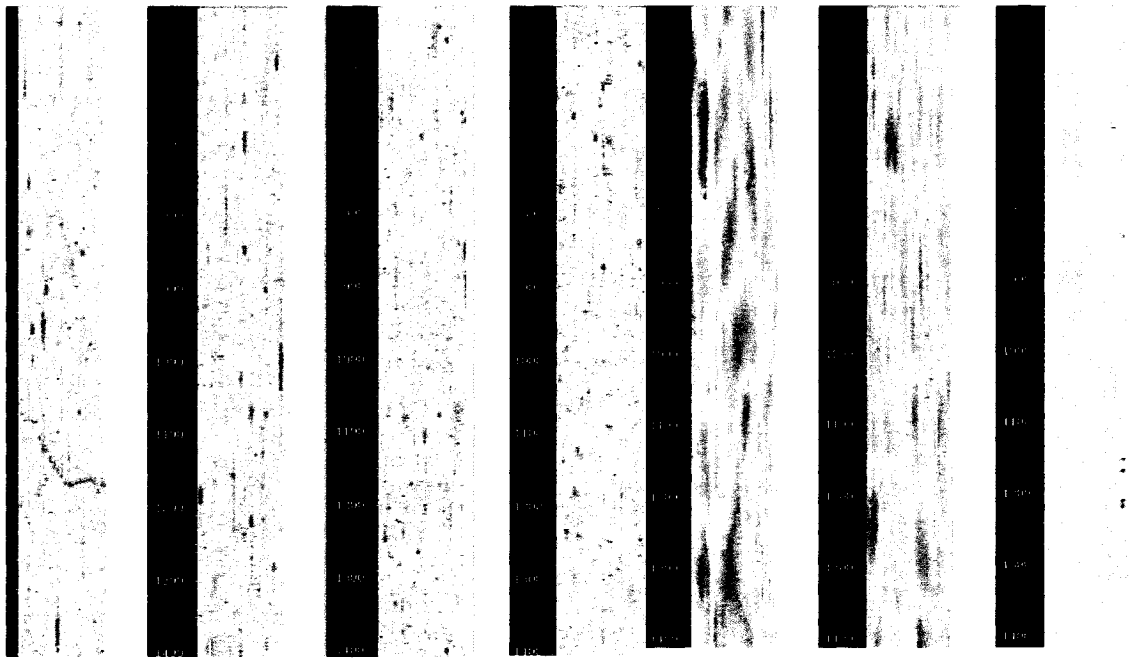

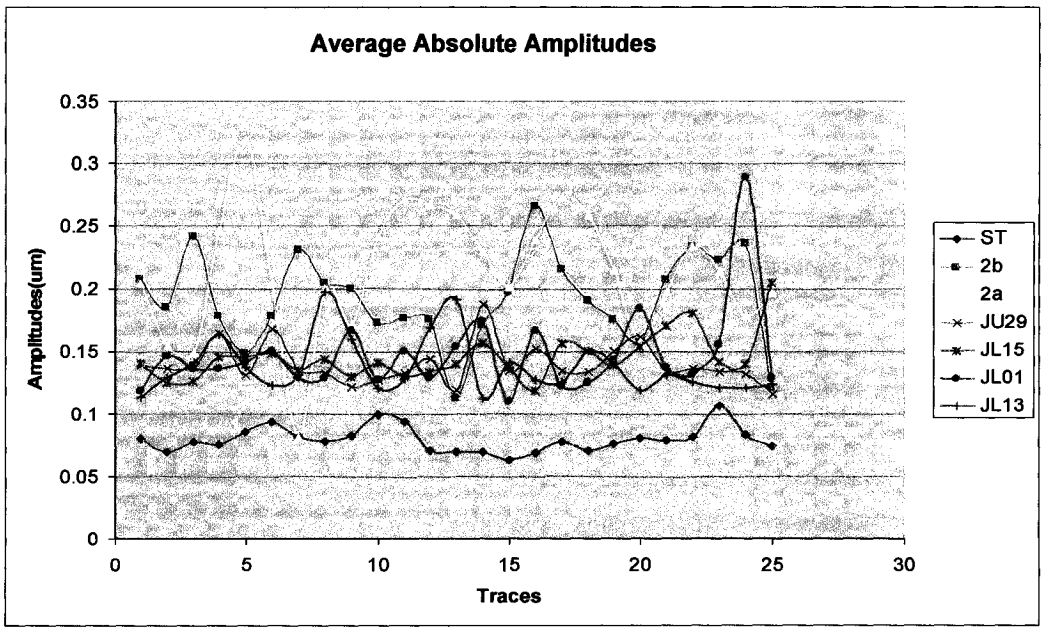

Fig. 5.11: Average absolute amplitudes of seven panels

As mentioned before, in terms of Ra values the surface finish of the samples from McGill University seems to be better than the surface finish of composite the samples from Ford Motor. Each panel has 50000 sample points. Fig. 5.12 shows the amplitudes histogram statistics of the seven panels.

Original Amplitudes

Histogram

ST

Data between 0 – 2.26
The majority Amps are in 0.063 – 0.116

AMPLITUDE RANGE LOW VALUE - HIGH VALUE	# SAMPLES IN RANGE	% IN RANGE	CUMULATIVE PERCENT	HISTOGRAM
0.100E-02 to 0.190E-02	495	0.814	0.814	**********
0.200E-02 to 0.380E-02	793	1.583	2.407	**********
0.390E-02 to 0.704E-02	1582	3.179	5.986	**********
0.794E-02 to 0.140E-01	3271	6.572	12.559	**********
0.150E-01 to 0.300E-01	6307	12.674	24.902	**********
0.316E-01 to 0.621E-01	11457	22.981	47.973	**********
0.631E-01 to 0.119E+00	15919	31.986	79.959	**********
0.126E+00 to 0.241E+00	9482	19.052	99.011	**********
0.251E+00 to 0.491E+00	467	0.938	99.950	**********
0.501E+00 to 0.990E+00	12	0.024	99.974	**********
0.100E+01 to 0.226E+01	13	0.026	100.000	**********

2b

Data between 0 – 1.81,
The majority Amps are in 0.126 – 0.241 and 0.251-0.491

AMPLITUDE RANGE LOW VALUE - HIGH VALUE	# SAMPLES IN RANGE	% IN RANGE	CUMULATIVE PERCENT	HISTOGRAM
0.100E-02 to 0.190E-02	167	0.335	0.335	**********
0.200E-02 to 0.380E-02	342	0.686	1.020	**********
0.390E-02 to 0.704E-02	644	1.291	2.311	**********
0.794E-02 to 0.140E-01	1438	2.882	5.193	**********
0.150E-01 to 0.300E-01	2749	5.510	10.704	**********
0.316E-01 to 0.621E-01	5256	10.535	21.239	**********
0.631E-01 to 0.116E+00	9455	18.952	40.190	**********
0.126E+00 to 0.241E+00	14827	29.920	70.110	**********
0.251E+00 to 0.491E+00	12366	24.787	94.897	**********
0.501E+00 to 0.990E+00	2533	5.077	99.974	**********
0.100E+01 to 0.181E+01	13	0.026	100.000	**********

2a

Data between 0 – 3.61,
(67 samples fall in 1 – 3.61)
The majority Amps are in 0.126 – 0.241 and 0.251 – 0.491, similar as 2b

AMPLITUDE RANGE LOW VALUE - HIGH VALUE	# SAMPLES IN RANGE	% IN RANGE	CUMULATIVE PERCENT	HISTOGRAM
0.100E-02 to 0.190E-02	155	0.311	0.311	**********
0.200E-02 to 0.380E-02	315	0.631	0.942	**********
0.390E-02 to 0.704E-02	630	1.263	2.205	**********
0.794E-02 to 0.140E-01	1380	2.766	4.970	**********
0.150E-01 to 0.300E-01	2660	5.331	10.302	**********
0.316E-01 to 0.621E-01	5085	10.191	20.493	**********
0.631E-01 to 0.116E+00	8967	17.972	38.465	**********
0.126E+00 to 0.241E+00	13779	27.616	66.081	**********
0.251E+00 to 0.491E+00	13223	26.502	92.582	**********
0.501E+00 to 0.990E+00	3634	7.283	99.866	**********
0.100E+01 to 0.361E+01	67	0.134	100.000	**********

JU29

Data between 0 – 3.51,
(33 samples fall in 2.0 – 3.51)
majority Amps are in 0.126 – 0.241 and 0.063 – 0.116

AMPLITUDE RANGE LOW VALUE - HIGH VALUE	# SAMPLES IN RANGE	% IN RANGE	CUMULATIVE PERCENT	HISTOGRAM
0.100E-02 to 0.190E-02	243	0.487	0.487	**********
0.200E-02 to 0.380E-02	532	1.067	1.554	**********
0.390E-02 to 0.704E-02	935	1.996	3.550	**********
0.794E-02 to 0.140E-01	1976	3.963	7.513	**********
0.150E-01 to 0.300E-01	3792	7.605	15.119	**********
0.316E-01 to 0.621E-01	7377	14.796	29.914	**********
0.631E-01 to 0.116E+00	12491	25.053	54.967	**********
0.126E+00 to 0.241E+00	15158	30.422	85.389	**********
0.251E+00 to 0.491E+00	6356	12.768	98.157	**********
0.501E+00 to 0.990E+00	800	1.621	99.777	**********
0.100E+01 to 0.199E+01	78	0.156	99.934	**********
0.200E+01 to 0.351E+01	33	0.066	100.000	**********

JL01

Data between 0 – 12.1
(only 16 samples fall in 2.00– 12.1)
The majority Amps are in 0.126 – 0.241 and 0.063 – 0.116 the similar as JU29, JL13, JL15

AMPLITUDE RANGE LOW VALUE - HIGH VALUE	# SAMPLES IN RANGE	% IN RANGE	CUMULATIVE PERCENT	HISTOGRAM
0.100E-02 to 0.190E-02	242	0.485	0.485	**********
0.200E-02 to 0.380E-02	499	1.001	1.486	**********
0.390E-02 to 0.704E-02	1023	2.052	3.538	**********
0.794E-02 to 0.140E-01	1934	3.879	7.416	**********
0.150E-01 to 0.300E-01	3845	7.711	15.128	**********
0.316E-01 to 0.621E-01	7355	14.751	29.878	**********
0.631E-01 to 0.116E+00	12421	24.911	54.789	**********
0.126E+00 to 0.241E+00	14634	29.349	84.138	**********
0.251E+00 to 0.491E+00	6601	13.239	97.377	**********
0.501E+00 to 0.990E+00	1176	2.359	99.735	**********
0.100E+01 to 0.199E+01	116	0.233	99.968	**********
0.200E+01 to 0.397E+01	6	0.012	99.980	**********
0.398E+01 to 0.121E+02	10	0.020	100.000	**********

JL15

Data between 0 – 3.68,
(15 samples fall in 2.00 – 3.68)
The majority Amps are in 0.126 – 0.241 and 0.063 -0.116 the similar as JU29, JL13 and JL01

AMPLITUDE RANGE LOW VALUE - HIGH VALUE	# SAMPLES IN RANGE	% IN RANGE	CUMULATIVE PERCENT	HISTOGRAM
0.100E-02 to 0.190E-02	284	0.570	0.570	**********
0.200E-02 to 0.380E-02	488	0.979	1.549	**********
0.390E-02 to 0.704E-02	1002	2.010	3.559	**********
0.794E-02 to 0.140E-01	1927	3.866	7.425	**********
0.150E-01 to 0.300E-01	3746	7.515	14.940	**********
0.316E-01 to 0.621E-01	7410	14.865	29.805	**********
0.631E-01 to 0.116E+00	12545	25.167	54.972	**********
0.126E+00 to 0.241E+00	14981	30.054	85.026	**********
0.251E+00 to 0.491E+00	6579	13.198	98.225	**********
0.501E+00 to 0.990E+00	797	1.599	99.823	**********
0.100E+01 to 0.199E+01	73	0.146	99.970	**********
0.200E+01 to 0.368E+01	15	0.030	100.000	**********

JL13

Data between 0 – 3.32,
(34 samples fall in 2.00 – 3.32)
The majority Amps are in 0.126 – 0.241 and 0.063 -0.116 the similar as JU29, JL15 and JL01

AMPLITUDE RANGE LOW VALUE - HIGH VALUE	# SAMPLES IN RANGE	% IN RANGE	CUMULATIVE PERCENT	HISTOGRAM
0.100E-02 to 0.190E-02	262	0.526	0.526	**********
0.200E-02 to 0.380E-02	516	1.035	1.561	**********
0.390E-02 to 0.704E-02	1070	2.147	3.708	**********
0.794E-02 to 0.140E-01	2160	4.334	8.043	**********
0.150E-01 to 0.300E-01	4206	8.440	16.482	**********
0.316E-01 to 0.621E-01	7951	15.955	32.437	**********
0.631E-01 to 0.116E+00	13216	26.520	58.957	**********
0.126E+00 to 0.241E+00	14558	29.212	88.169	**********
0.251E+00 to 0.491E+00	5147	10.328	98.497	**********
0.501E+00 to 0.990E+00	630	1.264	99.761	**********
0.100E+01 to 0.199E+01	85	0.171	99.932	**********
0.200E+01 to 0.332E+01	34	0.068	100.000	**********

Fig. 5.12: The amplitudes histogram statistics of the seven panels

The amplitudes of painted steel plate are between 0-2.26 μm and the majority amplitudes are in the range 0.063 - 0.116μm.

The amplitudes of 2b are between 0 – 1.81μm, like ST the majority amplitudes are in the range 0.126 – 0.241μm and 0.251 – 0.491μm.

The amplitudes of 2a are between 0 – 3.61. 67 sample points fall in the range 1-3.61μm. The majority of amplitudes are the range 0.126 – 0.214 and 0.251 – 0.491 μm, similar to 2b.

The amplitudes of JU29 are between 0 – 0.3.51 μm. 33 sample points fall in the range 2.0-3.51μm. The majority of amplitudes are in the range 0.126 – 0.241 μm and 0.063 – 0.116 μm.

The amplitudes of JL13 are between 0 – 3.32μm. 34 sample points fall in the range 2.00 – 3.32 μm. The majority of amplitudes are in the range 0.126 – 0.241 μm and 0.063 – 0.116 μm, the similar to JU29, JL15 and JL01.

The amplitudes of JL15 are between 0 – 3.68 μm. 15 sample points are in the range 2.0 – 3.68 μm. The majority amplitudes are in the range 0.126 – 0.241 μm and 0.063 –0.116 μm, similar to JU29, JL13 and JL01.

The amplitudes of JL01 are between 0 – 12.1μm, 16 sample points are fall in the range 2.0 – 12.1μm. The majority of amplitudes are in the range 0.126 – 0.241μm and 0.063 – 0.116μm, similar to JU29, JL13 and JL15.

The analysis shows that it is difficult to discriminate surface status only by amplitude analysis.

Fig. 5.13 shows pictures of mixed traces for the seven panels by equal weighting model.

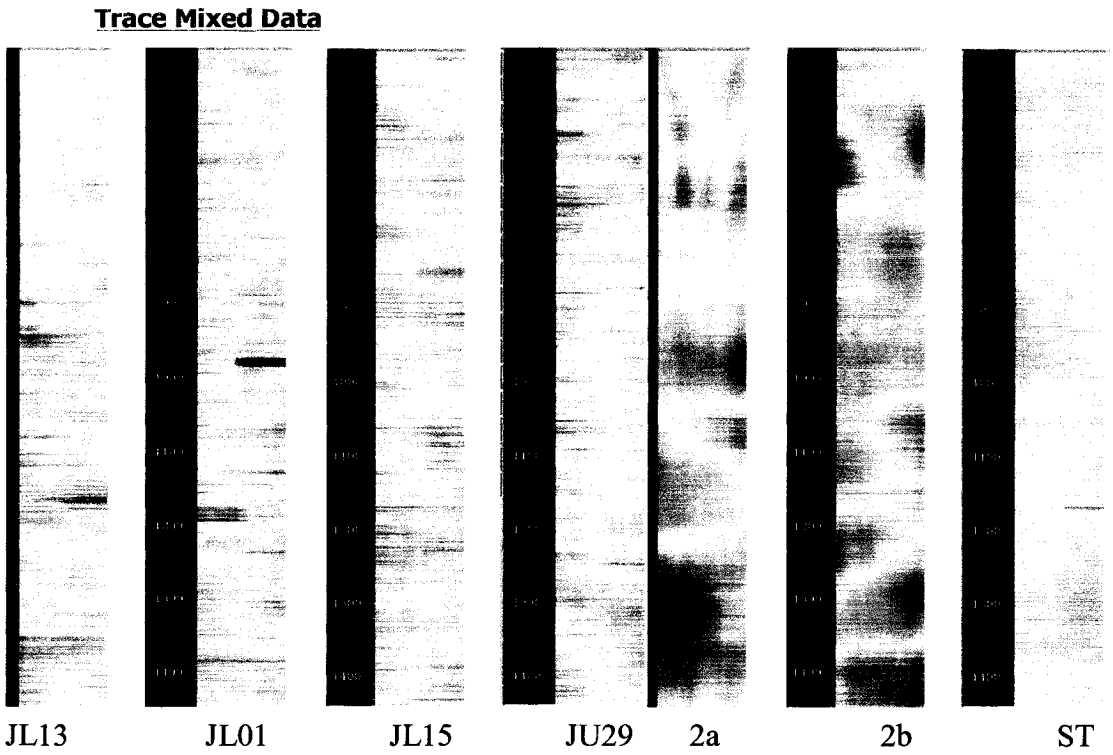

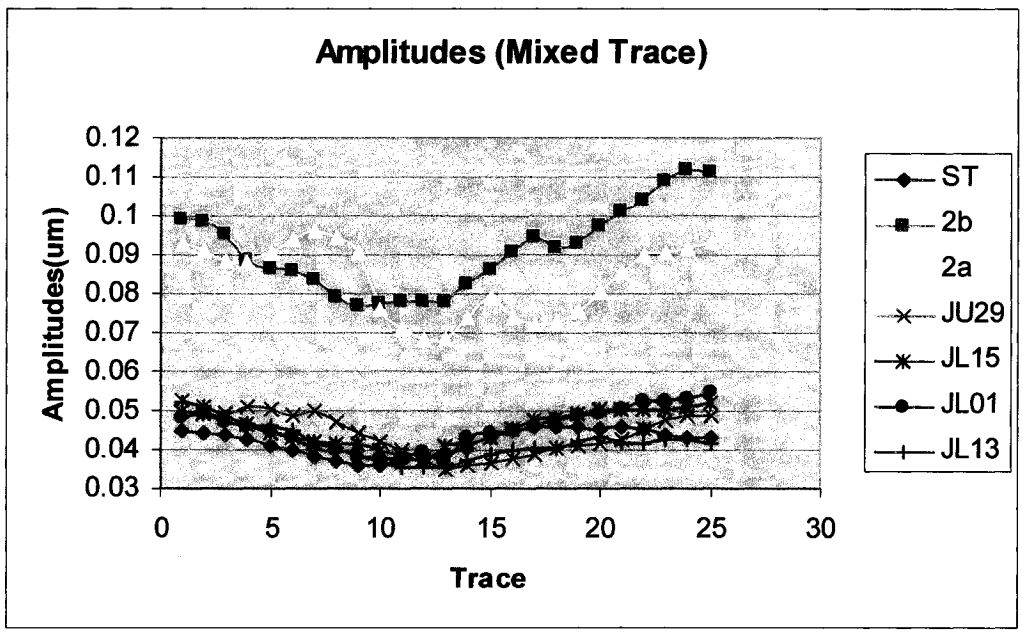

Fig. 5.13: Pictures of mixed traces for the seven panels

It can be seen from Fig. 5.13 that these data are smoothed. This smoothed surface still contains the characters of the material.

b) Cross correlation analysis of the six composite plates and painted steel plate

Correlation coefficients with painted steel plate for plates 2a, 2b, JU29, JL01, JL13, JL15, respectively are calculated and shown in Fig. 5.14.

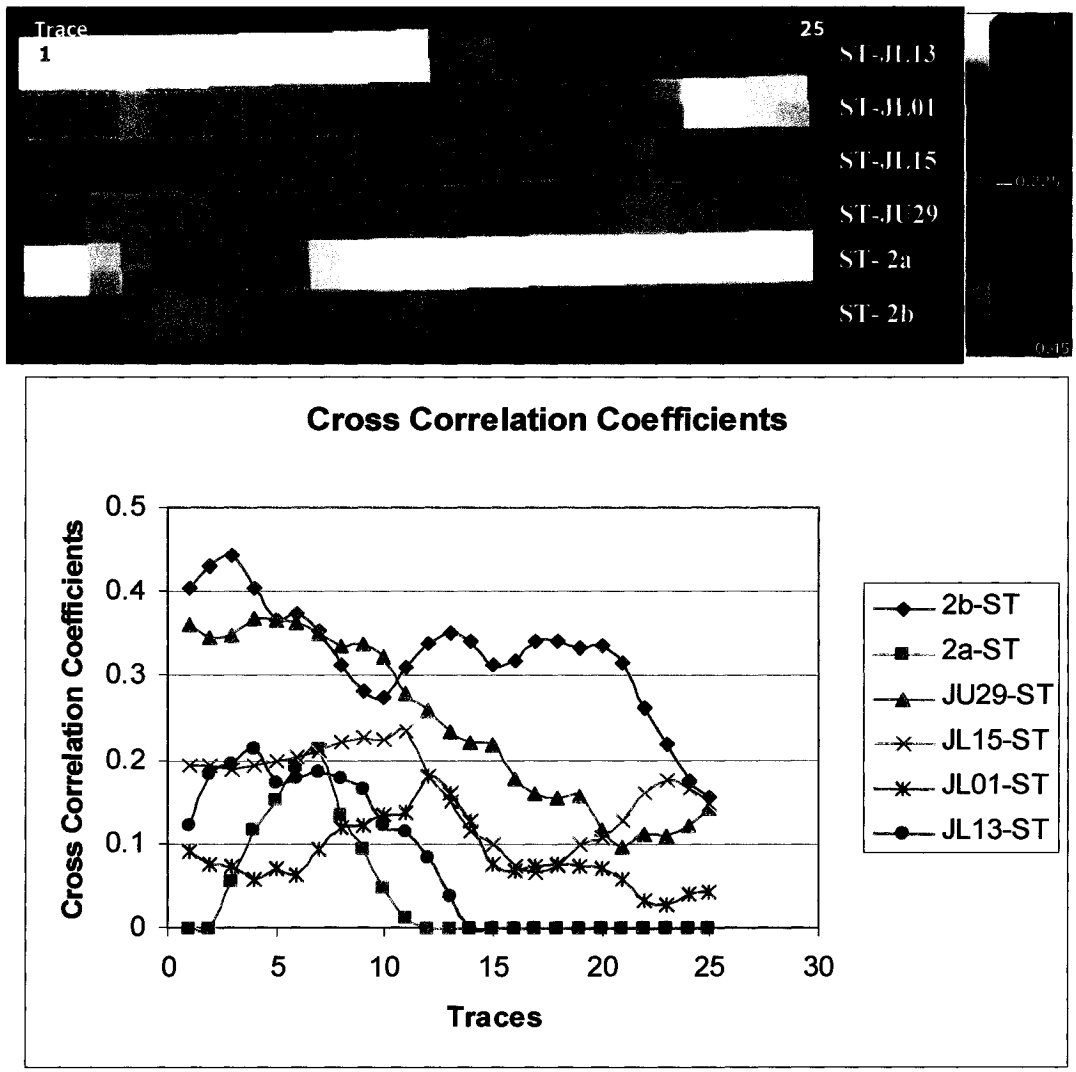

Fig. 5.14: Correlation coefficients between composite plates and painted steel plate

Fig. 5.14 shows coefficients of cross correlation between the six composite plates and painted steel plate. In this model trace of painted steel plate is reference trace, target traces are other six composite materials.

The results calculated show composite plate 2b and painted steel plate have the best correlation coefficients in all materials. Sample JU29 has the next best correlation with painted steel plate. Table 5.7 shows average values of cross correlation coefficients for the six composite plates.

Table 5.7: Average cross correlation coefficients

	2a-ST	2b-ST	JU29-STl	JL01-ST	JL13-ST	JL15-ST
Cross Correlation Coefficients	0.041	0.325	0.240	0.087	0.078	0.162
Rank	6	1	2	4	5	3

Other composite plates have lower correlation with painted steel plates. Therefore, surface quality of composite plate 2b is the closest to surface quality of painted steel plate in all materials.

Though Ra values of 2b is a little higher than those of samples from McGill University, in extent of surface correlation with painted steel plate 2b has the greatest correlation with the steel plate of Class A surface finish because its waveforms are more similar to that of painted steel plate. The second one in rank is sample JU29. Surface correlation of sample 2a with painted steel plate is lowest.

However, sample 2a has almost the same amplitude distribution and magnitudes as sample 2b, why do they have different correlation coefficients with the reference function, the surface profile of painted steel plate? This is because they have different waveforms

compared to the waveform of the painted steel plate. Cross relation coefficient represents the extent of similarity between waveforms.

However, even for composite plate 2b, its average correlation extent with painted steel plate is only round 33%. This means surface quality level of composite plates still is far away from surface quality level of painted steel plate.

This analysis shows differences between waveforms of surfaces of the materials. If amplitudes of waveforms are very close, surface characters can be distinguished by the methods.

c) Similarity analysis

Minimum similarity is used to calculate semblance values. Fig. 5.15 is results of semblance values that were calculated for painted steel & for samples 2a, 2b, JU29, JL01, JL13 and JL15 respectively.

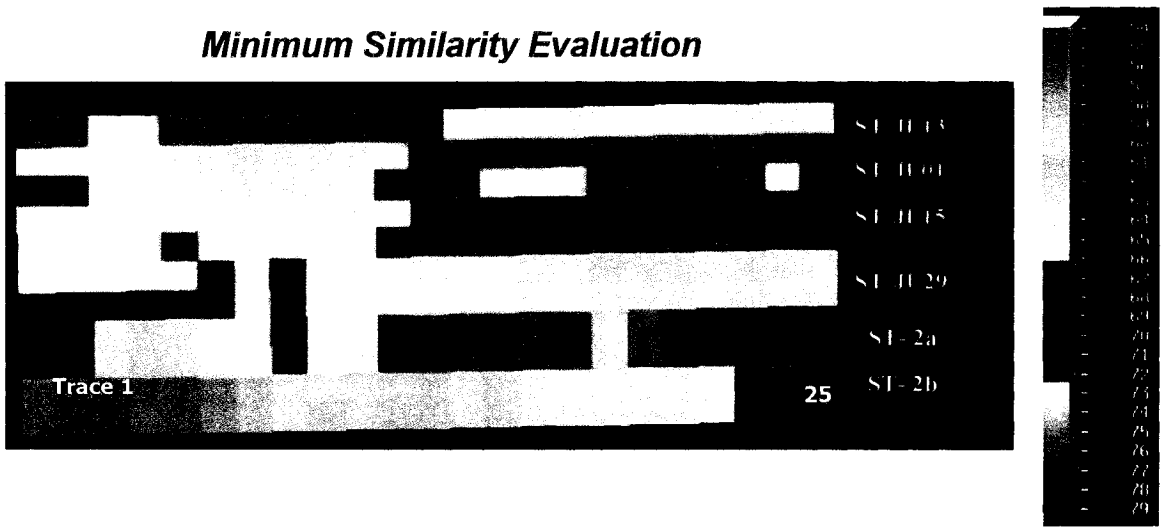

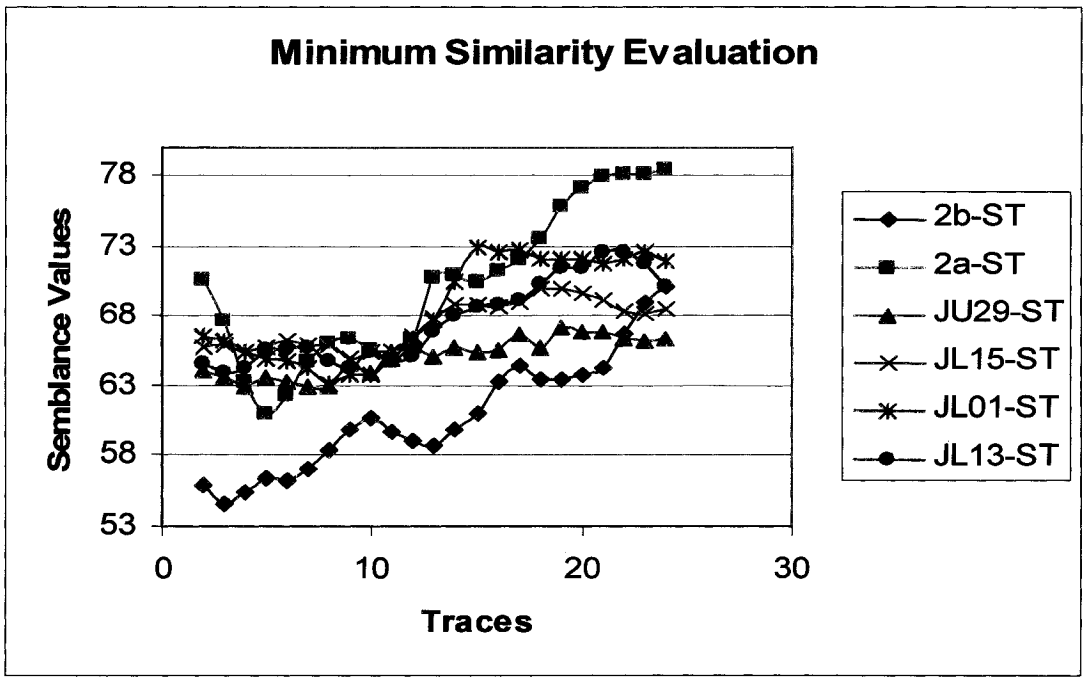

Fig. 5.15: The minimum similarity calculation for the seven panels

(The higher value indicates the higher dissimilarity.)

Fig. 5.15 gives the results of similarity of the six composite plates and painted steel. The calculated results are basically identical with results calculated by correlation model. Sample 2b has the greatest similarity to painted steel plate in all panels. Sample JU29 has the next best similarity to steel surface.

Table 5.8 shows average semblance values of the six panels.

Table 5.8: Average Semblance values (minimum similarity) of the six panels

	2a-ST	2b-ST	JU29-ST	JL01-ST	JL13-ST	JL15-ST
Semblance Values	70.2	60.9	65.1	68.5	67.7	67.4
Rank	5	1	2	4	3	3

Sample JL01 and 2a have low similarity to surface of painted steel plate in the panels. JL13 and JL15 have almost same similarity to painted steel plate.

This type of analysis method describes similarity between objects. It not only considers surface waveforms, but also considers amplitudes of waveforms. It can be seen from Tables 5.3, and 5.7 that in Table 5.8 plate JL13 is a little better than plate JL01, which may be caused because amplitudes of plate LJ13 are lower than that of plate JL01.

5. Spectrum analysis and filtering analysis

a) Fourier analysis of Surface profiles of panels

The purpose of the section is to study surface characteristics of materials in frequency domain. Characteristic peak amplitude for the frequency could show surface characters of the materials. Different frequency parts would show different surface characters.

Fig. 5.16 shows spectra of the seven panels, each panel has 25 traces, as calculated by DFT.

Spectrum of 2b and ST

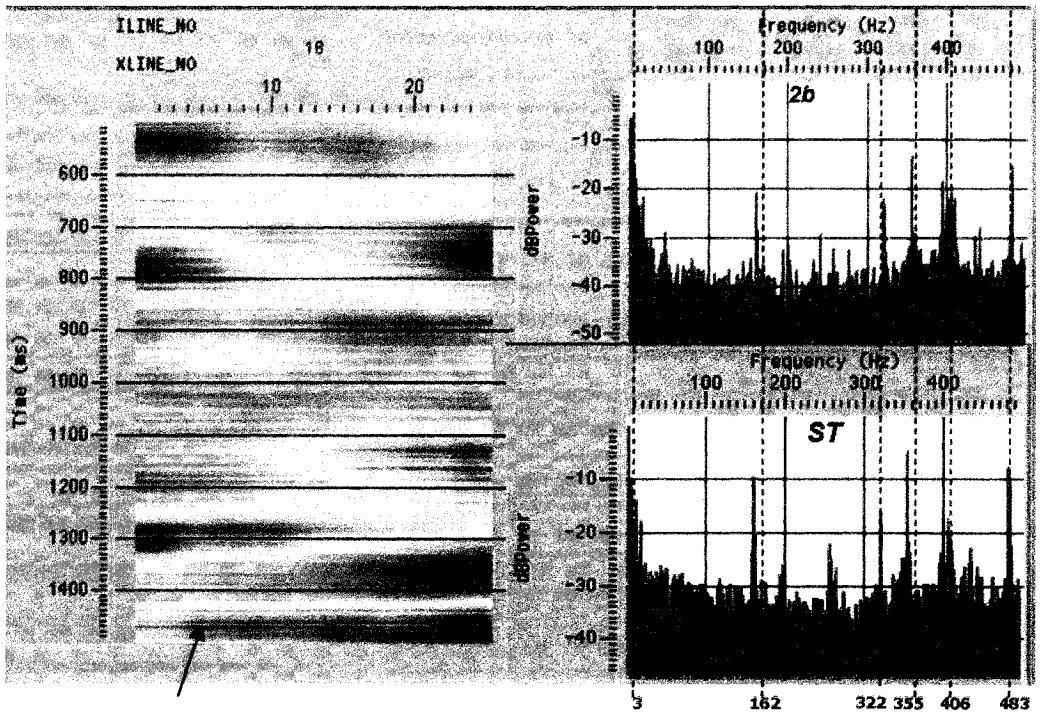

traces

Spectrum of 2a and ST

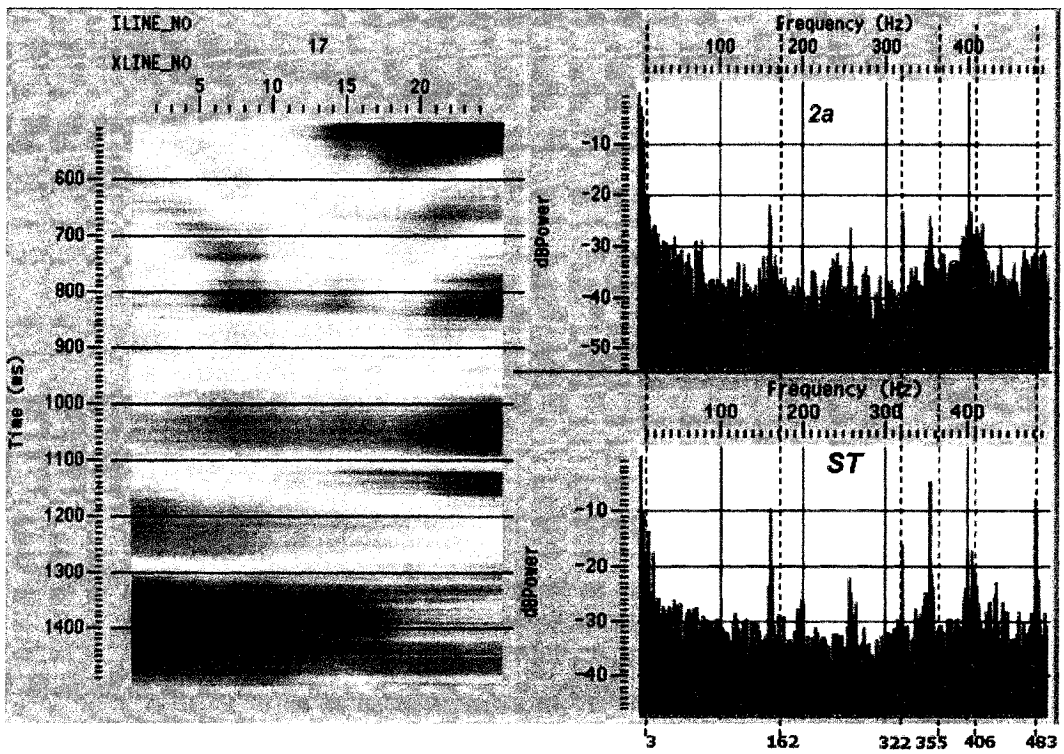

Spectrum of JU29 and ST

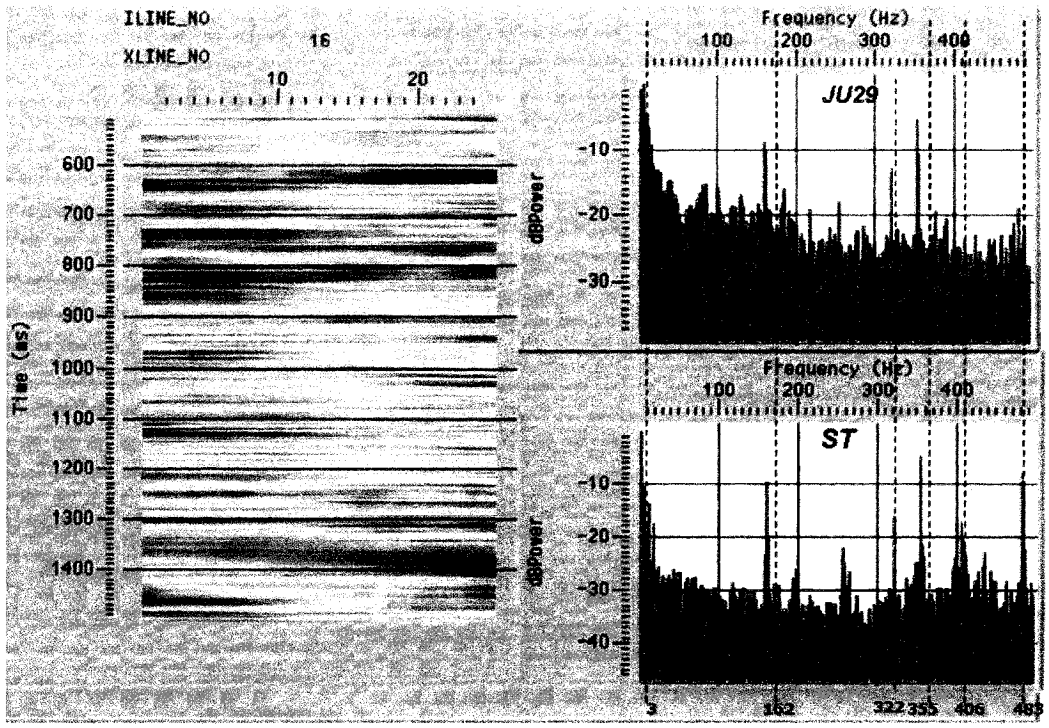

Spectrum of JL01 and ST

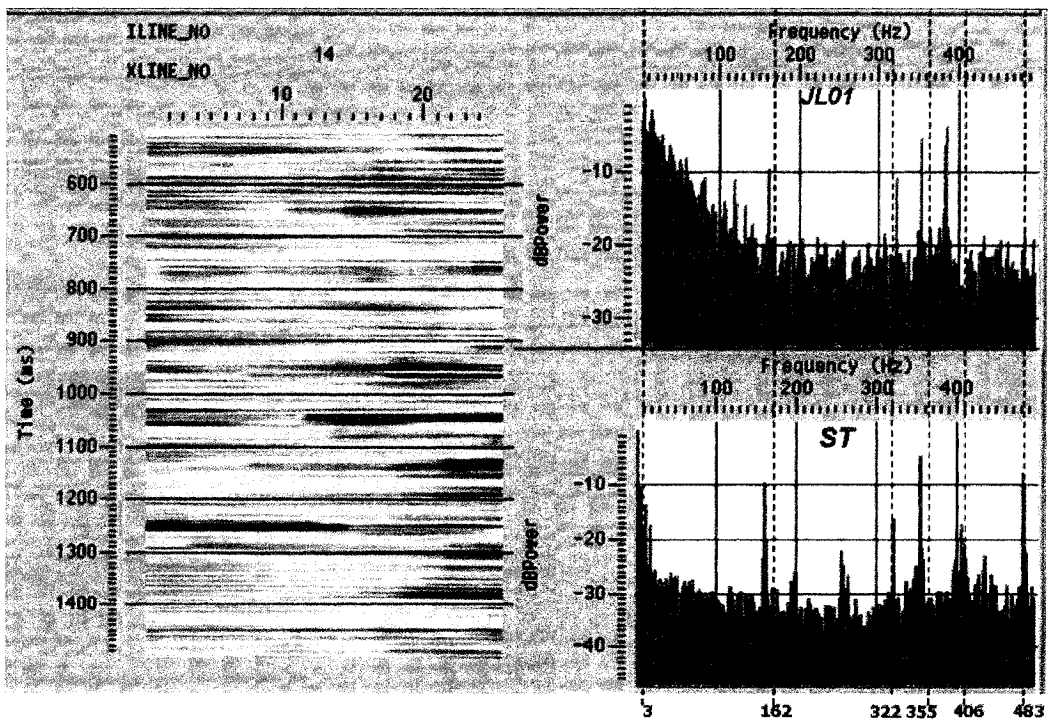

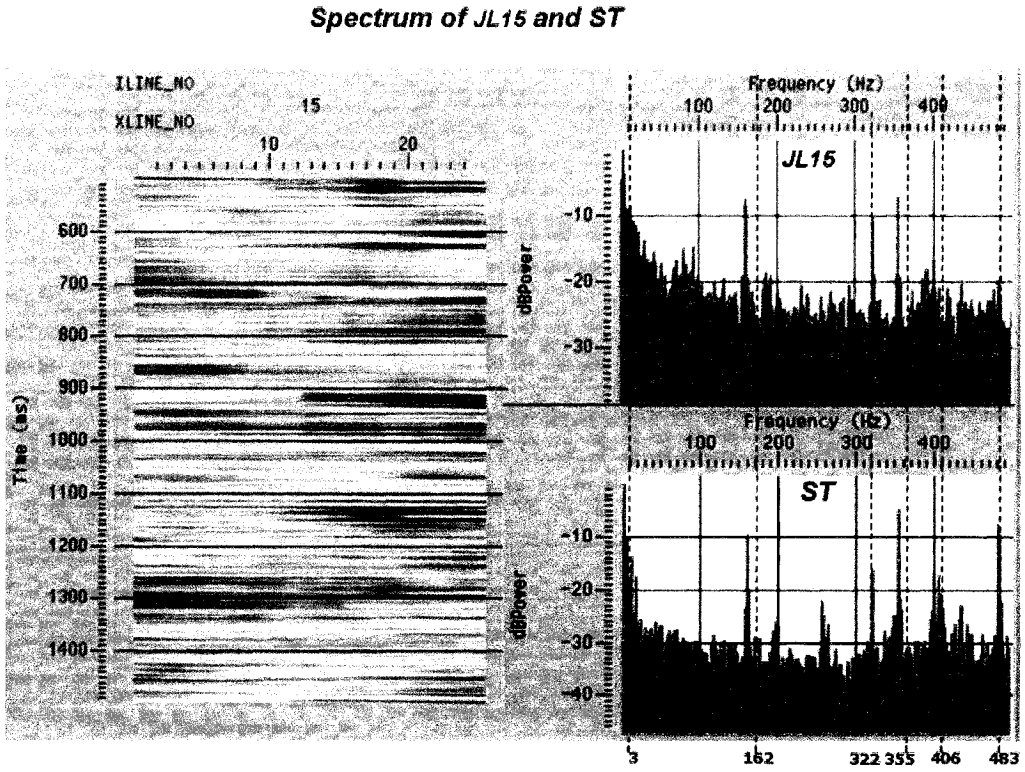

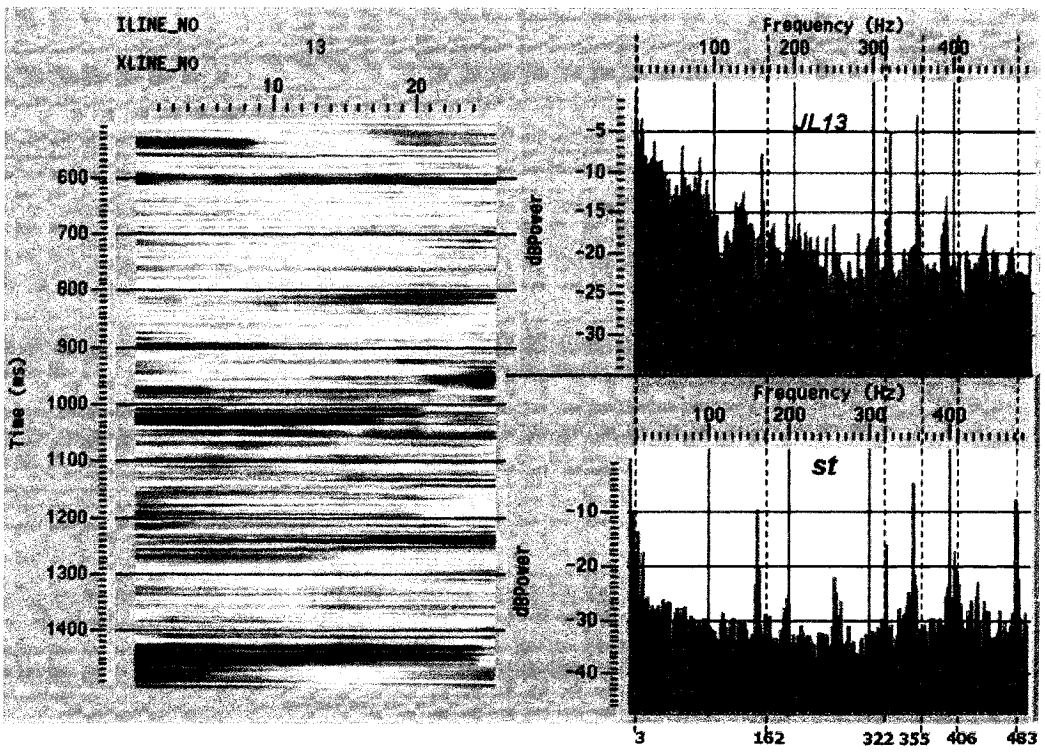

Fig. 5.16: Frequencies and spectra of seven panels

It can be seen from Fig. 5.16 that painted steel plate has characteristic peaks of more uniform distribution, at 160Hz, 322Hz, 355 Hz, 406Hz and 483Hz, respectively. This shows characteristics of resin on the surface and is also characteristics of the surface with Class A surface finish in frequency domain. For 2b, it has the characteristic peaks as painted steel plate at 160Hz, 322Hz, 406Hz and 483 Hz, respectively; for 2a, there are no clear characteristic peaks at these frequencies. For JU29, it has the characteristic peaks as steel plate at 160 Hz, 322 Hz, and 355Hz, not apparent peaks at 406 Hz and 483Hz. For JL15, it has the characteristic peaks as steel plate at 160 Hz 322Hz and 355Hz, and not apparent peaks at 406 Hz and 483Hz. For JL13, it has the characteristic peaks as steel plate at 160 Hz, 322Hz, 355Hz and 406, but not apparent peaks at 483Hz. For JL01, it has no clear peak at 160Hz and peak at 322Hz, 355Hz that are the same as steel plates, and has a peak at 390Hz, but not apparent peaks at 483Hz.

Analysis of Fig. 5.16 shows that composite plate 2b may be more similar to painted steel plate in frequency domain, composite plate 2a has the same characteristic peaks as painted steel plate, but these peaks are not sharply as that of composite plate 2b. Composite plates JL15, JL13 and JL01 have almost the same characteristic peaks as painted steel plate within 160 Hz -355Hz, but not parent peaks at 406Hz and 483 except JL13 at 406Hz.

Spectrum analysis shows composite plate 2b has the most similar spectrum to the spectrum of painted steel plate among the six composite plates. However, it is difficult to determine surface quality levels by frequency spectrum.

Table 5.8 shows the rank by frequency spectrum.

Table 5.9: Rank of surface quality levels of the six panels by spectrum analysis

	ST	2a	2b	JU29	JL01	JL13	JL15
Rank		2	1	2	2	2	2

b) Filtering analysis

By filtering, characteristic curves of the surface at frequency range can be shown. It would reflect surface shapes of the material in particular views.

Low frequency means large wavelength. Therefore, curves of amplitudes and displacement at low frequencies would give the surface shape of plates. The curves of amplitude and displacement at high frequencies would reflect surface brightness of plates because the resolution of human eyes is around 0.15mm. When tiny amplitude changes occur at high frequency, human eye would not make out the changes and feel the surface is smooth. Now high frequency components have not been studied very well. Research work mainly is focused on the waviness, low frequency components. Filtering analysis is helpful to understand the characters for panels.

It can be seen from Fig. 5.16 that there are many characteristic peaks in these panels. Filter can separate the characteristic frequencies. In low frequency window 3-5Hz, the curves of characteristic amplitudes of the surfaces of the seven panels can be obtained and shown in Fig. 5.17.

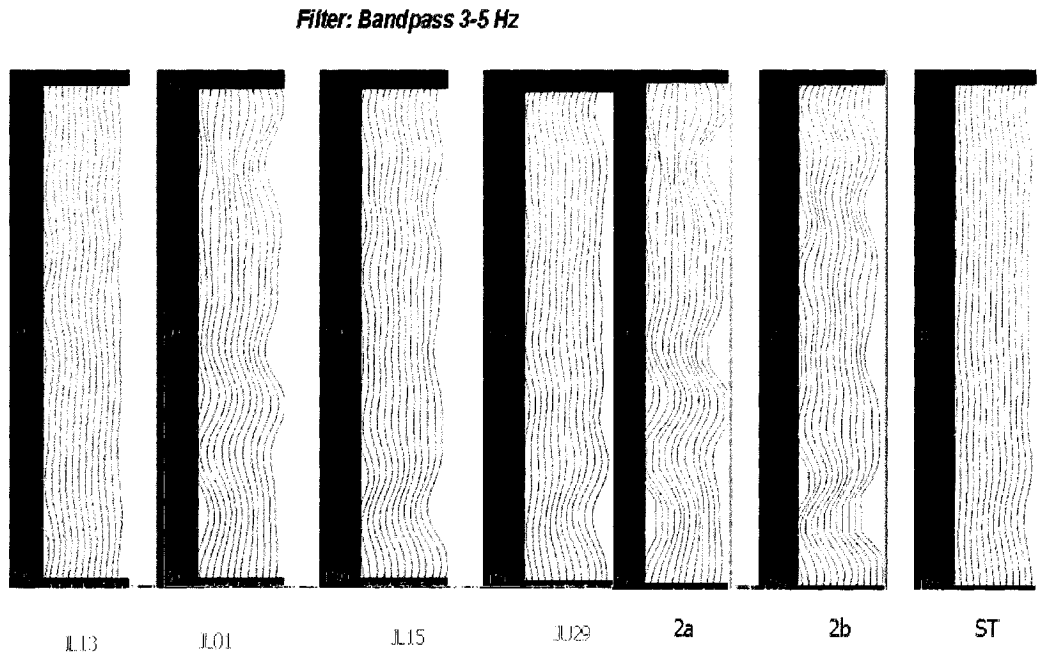

Fig. 5.17: The surface shapes of the seven plates for filtering in bandpass 3-5 Hz

It is clearly seen from Fig. 5.17 that painted steel plate has the best flatness. Composite plates JL13 and JU29 have also better flatness. Composite plates 2b, 2a, JL15 and JL01 have bigger waviness in low frequency. General speaking, the waviness of samples from Ford are larger than that of samples from McGill University. Therefore, for these samples there is a need to reduce the waviness in order to improve surface quality.

Due to uninform and anisotropic properties for composite material, the contraction in forming the plate would affect on the waviness of materials. Waviness of composite plate 2b with LPA is more uniform than that of composite plate 2a without LPA. So adding LPA is helpful to reduce waviness of surface. Processing techniques of JU29 and JL13 may be helpful to improve surface quality level of 2b.

The results of filtering show that to improve surface quality of composite one needs to reduce the waviness. Therefore, it is very important for designing a reasonable arrangement of materials, and using low contraction materials in order to have the least contraction. Top coating would also improve surface quality.

Results of filtering in bandpass 355-357 Hz are shown in Fig.5.18. It is clearly seen from these results that surface amplitudes of the materials all have more uniforms distribution, which is more pleasing to the eyes. However, painted steel plate has higher characteristic frequencies. The surface of painted steel pate has the highest brightness.

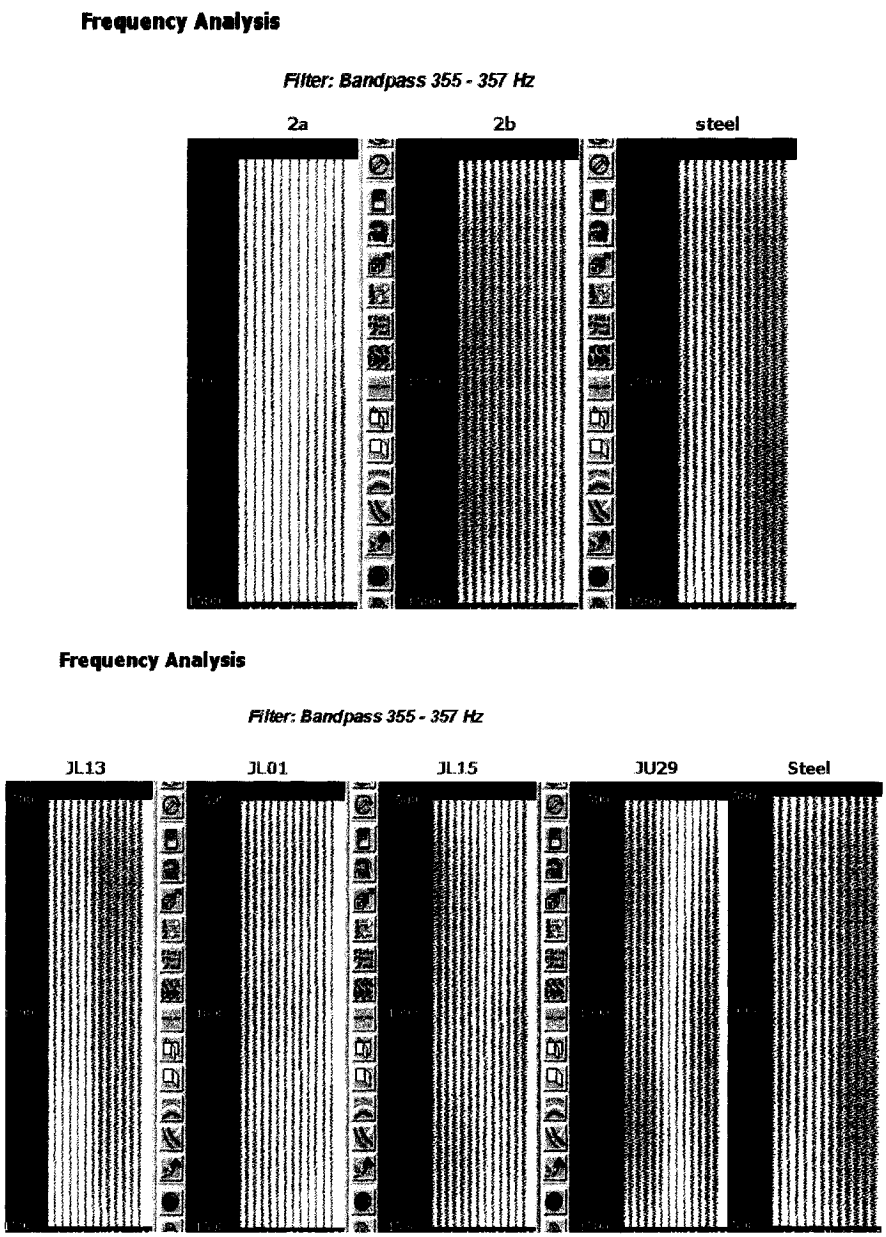

Fig. 5.18: Surface shapes of the seven plates for filtering in bandpass 355-3575 Hz

Table 5.10 shows the ranking by filtering analysis.

Table 5.10: Rank of surface quality levels of the seven panels by filtering analysis

	ST	2a	2b	JU29	JL01	JL13	JL15
Rank	1	6	5	3	4	2	3

c) Summary

- The surface profiles of seven panels are analyzed in frequency domain. The characteristic spectra of these seven panels are attained.
- The filtering technique is used to analyze surface profiles of the seven panels. In low bandpass 3-5Hz and high bandpass 355-357Hz surface profiles of seven panels are examined.
- The results of spectra show that the painted steel plate has more uniform distribution of characteristic frequency peaks from low frequency to high frequency. They are 160, 322, 355, 406 and 483Hz, respectively.
- The spectrum of composite plate 2b is more similar to that of the painted steel plate. But characteristic frequency peaks of plate 2a are not as sharp as the spectrum of composite plate 2b.
- The spectra of composite plates JL01, JL13 and JL15 are similar to the spectrum of the painted steel plates in 160-355Hz, however, there are no characteristic frequency peaks at 406 and 483Hz. This may effect on surface brightness.
- The filtering analysis shows that in bandpass 3-5Hz the waviness of the painted steel plate is very small, so the steel plate has good flatness; the waviness of composite plates made from McGill University are smaller than that of composite plates made from Ford, in which the waviness of composite plate 2b with LPA is smaller than that of composite plate 2a without LPA. In bandpass 355-357Hz there are no parent differences between these panels.
- Analyses in frequency domain show that samples made from Ford should have reduced waviness and samples made from McGill University should have

improved high characteristic frequency. In this way surface quality of composite plate may be close to surface quality of painted steel plate.

6. Comparison of calculation results with visual observation

Evaluation results by 28 people and calculation results of models are summarized in Table 5.11.

Table 5.11: Evaluation results by 28 people and calculated results from models

	ST	2b	JU29	JL13	JL15	2a	JL01
Visual observation (Average)	1(Reference) (1.035)	1 (1.964)	2 (3.429)	3 (4.786)	3 (4.786)	4 (5.393)	5 (6.571)
Ra (μm)	1(Reference) (0.078)	4 (0.195)	2 (0.143)	1 (0.132)	2 (0.143)	5 (0.219)	3 (0.149)
MEM	1(Reference)	4	2	1	2	5	3
Spectrum Analysis	1(Reference)	1	2	2	2	2	2
Filtering Analysis	1(Reference)	4	2	1	2	5	3
Cross Correlation coefficients (Average)	1(Reference)	1 (0.35)	2 (0.24)	4 (0.078)	3 (0.16)	5 (0.041)	4 (0.087)
Similarity (Average)	1(Reference)	1 (60.9)	2 (65.1)	3 (67.7)	3 (67.4)	5 (70.2)	4 (68.5)

Fig. 5.19 shows numbers of agreement with visual observation for the techniques.

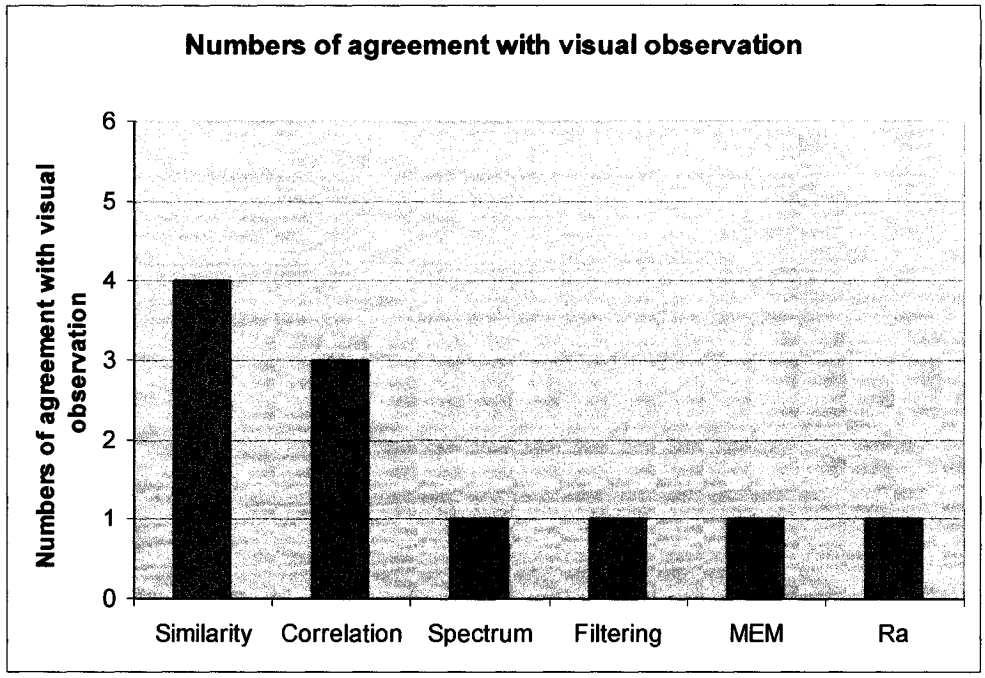

Fig. 5.19: Comparison agreement with visual observation

It can be seen from Table 5.11 that there are big differences in the evaluation between visual observation and Ra, MEM, spectrum and filtering analysis. When MEM, spectrum and filtering analysis are used to determine surface quality levels, it is difficult to distinguish by these analysis curves. However, the information of long and short wavelengths for composite plates can be achieved by spectrum and filtering analysis. This will be helpful to point out the way of the improvement of surface quality.

It can also be seen from Table 5.11 that results of calculation by similarity model are very close with evaluation results by 28 people except for sample 2a and JL01. For Samples JL13 and JL15 the ranks by visual observation gave are the same, i.e, by visual observation, they are of the same quality level. Results of calculation by similarity model also show that they have almost the same surface quality levels.

Results of calculation by cross correlation model are almost identical with results by similarity model. The results of calculation seem to show the same quality level for

sample JL01 and JL13. However, correlation coefficients describe similarity of waveforms, waveform of JL01 may be a little better that that of JL13. However, Ra value (0.132 μm) of JL13 is smaller than that (0.149 μm) of JL01. Therefore, when effects of amplitudes are considered, semblance values of JL13 in similarity model are a little better than that of JL01.

The methods that agree most with visual observation are similarity and cross correlation methods.

5.4 Conclusion and recommendation of new procedure

1. Conclusions

- Visual observation shows that in most cases it is difficult to distinguish surface quality of composite plates only by Ra values.
- Microstructure examination shows that a thick top coating layer is helpful to reduce fiber readout and textile-induced waviness. The extent of dispersion and size of filler particles may affect the surface quality.
- Maximum Entropy Method has some limitation to discriminate approximate surface quality based on Ra values.
- The method of mixed trace is used as pre-processing of the data. The method can reduce random fluctuation of the data. The surface data of different materials can be easily processed and analyzed.
- A new comparison analysis method is proposed: The surface finish with class A of painted steel plate is used as a reference surface and different surfaces of composite plates are compared to the reference surface. In this way, the differences between surface quality levels of composite plate can be distinguished.

- A 3D data arrangement is proposed, in which 3 coordinates represent materials, samples and traces respectively. The data arrangement establishes relationships between the three parameters. On the basis of the model, mathematical methods can be used to analysize surface quality levels. Through these mathematical methods, differences between the reference function and the target function can be found. By analysis of differences, surface quality levels between composite plates can be differentiated.
- A 3 D cross correlation model is proposed to analyze surface profiles between reference surface profiles and target surface profiles. The method can be used to discuss the similarity of waveforms between reference function and target function.
- A 3D similarity model is proposed to analyze surface profiles between reference surface profiles and target surface profile. The method can be used to analyze the similarity between the reference function and the target function.
- On the basis of correlation and minimum similarity models. The surface profiles of six composite plates are compared to the reference function. Calculation results show that the results of cross correlation and similarity can agree with results from visual observation, in which minimum similarity analysis can match results of visual observation very well.
- Spectrum analysis and filtering analysis show that the steel plate has the best flatness and waviness of plates from Ford is greater than that of plates from McGill University.

2. Recommendation of new procedure for evaluation surface quality

For evaluation of surface quality of composite plate, a new procedure is suggested as follows:

1) The surface of class A surface finish is defined as a reference surface.
2) 3 D data arrangement is established, in which the relationship of materials, traces and samples is set up. The Data are processed by trace mix.
3) Cross correlation and similarity analysis models can be used to calculate correlation coefficients and semblance values.
4) Spectrum analysis and filtering analysis can be performed to analyze the information of long and short wavelengths.

Chapter 6

Conclusions, contributions and recommendation for future work

6.1 Conclusions

The main conclusion is:

A new method for the differentiation of surface quality of composite plates has been developed: that of using cross correlation and similarity analysis based on a reference surface. The reference surface has the quality of class A. This method can not only differentiate surfaces of approximate quality, but it can also determine the quality of the surface, as to how close or how far it is away from the reference class A surface. As to the knowledge of the writer, this is the first time such a technique is available. This can be used to replace the determination by visual observation with an objective, systematic approach.

Based on the research conducted in the dissertation, following conclusions can be made:

- The model of Maximum Entropy Distribution for Ra value is proposed. It is used to analyze surface roughness of composite plates when they have approximate Ra values. Due to the limitation of Ra, sometimes the results from the method are not definite.
- Trace mix is proposed to process raw data. A 3D data arrangement related with materials, samples and traces is established.

- A method of comparison is developed so that differences between reference surface and target surface are used to distinguish surface quality. In this method more than two surfaces are used to compare with the reference surface. Based on their differences, the order of surface quality levels can be attained.
- Calculations of cross correlation, similarity for seven panels show that the results are almost identical with the results that evaluated by 28 people.
- Spectra analyses show that characteristic frequency peaks for the surface of class A surface finish is different from that of composite surfaces.
- Filtering analyses show that long and shot wavelengths of surfaces can be achieved by filtering. The surface of class A surface finish has the best flatness.

6.2 Contributions of the research

The goal of the thesis is to propose an innovative method to evaluate and distinguish surface quality of composite plate through quantitative analysis. The method uses mathematical method to develop multiply evaluation parameters, by which surface qualities of composite plate can be evaluated. Through these studies, several contributions are made. They can be summarized as follows:

- Proposed the use of target function and reference function to distinguish surface quality levels of composite materials. The differences between the surfaces to be evaluated and reference surface can be used to distinguish the surface quality levels.
- Developed models for cross correlation and similarity to analyze differences between the reference function and target functions.

- These kinds of research methods and models have not only very important theoretical value, but also powerful potential application values in engineering. In production line automatic recognition and evaluation quality for composite material can be made if possible. The method can be used to exhibit effects of processing parameters on surface quality.
- Investigated the use of the model of maximum entropy distribution to analyze distributions of Ra values on the surfaces of materials.
- Investigated the use of spectra and filtering analysis to study surface profiles. Characteristic frequency peaks of reference surface with surface finish of class A and target surface are researched. The filtering of low frequency is used to research wariness of surfaces and filtering of high frequency is also used to research surface profiles of materials.
- Published papers

(1) S. Hu, S.V Hoa and R. Ganesan, "A new evaluation method of surface finish of composite automotive panels using waveform analysis", submitted to Journal of Composite Materials, November 2006.

(2) S. Hu, R. Ganesan, S. V. Hoa, F. Trochu and M. DeBolt, "Probabilistic Analysis of Surface Finish for Automobile Composite Panels", Proceedings of the Fifth Joint Canada-Japon Workshop on Composites, September 2004, pp125-132.

(3) S. Hu, S.V. Hoa and R. Ganesan., "Evaluation of surface finish of composite automobile panel", The 21st Annual Technical Conference of the American Society for Composites, The University of Michigan, Dearborn Michigan, September17-20 2006.

(4) S. Hu, S.V Hoa and R. Ganesan, "Surface Finish of Composite Automobile Panels", 16th International Conference on Composite Materials (ICCM-16), Kyoto, Japan, July 2007.

6.3 Recommendations for future work

The thesis presents a new method for distinguishing composite plates of approximate quality. Based on above research work, it is recommended that the following future studies be undertaken to further explore the validation and application of the proposed methodology.

- Use the method to study effect processing parameters on surface finish.
- Implement an on line control and feedback system using proposed methodology.

References

[1] D. Hull and T.W. Clyne, "An Introduction to Composite Materials", 2nd ed., Cambridge Solid State Science Series, Cambridge: The University of Cambridge, 2001.

[2] M.W. Hyer, "Stress Analysis of Fiber-Reinforced Composite Material", The McGraw-Hill Companies, Inc., 1998.

[3] P. Ferabolia, A. Masinib, "Development of carbon/epoxy structural components for a high performance vehicle" Composites: Part B 35, 2004, pp. 323–330.

[4] G. Shook, "Reinforced Plastics for Commercial Composites Source Book", ASM, Metals Park, OH, 1986.

[5] U.S. Department of Agriculture Forest Service, "Wood Handbook: Wood as an Engineering Material, Agricultural Handbook No. 72", Washington, DC, 1987.

[6] "Introduction to Composites", 4th Edition, Composites Institute, Society of the Plastics Industry, New York, NY, 1998.

[7] D. V. Rosato, "Designing with Reinforced Plastics", Hanser / Gardner, Cincinnati, Ohio, 1997.

[8] Austin Verne, "Material and process innovation to develop Class 'A' surfaces on structural RIM and RTM" Society of the Plastics Industry, Reinforced Plastics/Composites Institute, Annual Conference - Proceedings, Feb. 1-5, 1988, pp. 10C.1-10C.2.

[9] C. N. Cucuras, "Computer generated Class A composites", Society of the Plastics Industry, Reinforced Plastics/Composites Institute, Annual Conference - Proceedings, Feb. 1-5, 1988, pp. 13B.1-13B.4.

[10] S.A Edwards, M. Provatas and N.R. Choudhury, "Surface finishes in injection moulding of polymeric materials and composites" International Journal of Materials and Product Technology, Vol. 19, No. 3-4, 2003, pp. 228-246

[11] C. F. Johnson, "Resin transfer molding", Composite Materials Technology-Process and Properties, P. K.Mallick and S. Newman, ed., Hanser Publisher, New York, 1990.

[12] L. R. Thomas, AK Miller and AL Chan, "Fabrication of complex high performance composite structures at low cost using VARTM", In: International SAMPE symposium and exhibition (proceedings), Vol. 47 (II); 2002, pp. 1317–29.

[13] S. G. Advani, E. M. Sozer, "Liquid Molding of Thermoset Composites", In: Talreja R, Manson J-AE, editors. Polymer matrix composites.Editor in Chief Kelly A, Zweben C, Amsterdam, Elsevier ScienceLtd., 2001, pp. 807–44.

[14] L Ascani, "Recent advancements and technical needs in structural concepts, fabrication, and joining flight-vehicle materials, structures, and dynamics – assessment and future directions", vol. 1. New York, USA: ASME; 1994.

[15] C. Dutiro, R.N. Alaka and F.L. Matthews, "Factors controlling surface finish in resin transfer molding", SAMPE Journal, Vol. 33, No. 5, Sep.-Oct., 1997, pp. 19-23.

[16] J. Seefried, "SMC-Außenhautteile in Class-A," Proceedings SMC Automotive, DaimlerChrysler Sindelfingen, 1998.

[17] G. Schlesinger, "Surface Finish", Machinery, Vol. 55, 1940, p. 721.

[18] M. L. Herring, "Surface Analysis for the Comparison of Quickstep and Autoclave Surface Finish", Report, School of Engineering and Technology, Deakin University, Australia, 2003.

[19] G. Schmalz, "Uber Glatte und Ebenheit als physikalisches und physiologishes

Problem", Verein Deatscher Ingenieure, Vol. 73, Oct.12, 1929, pp. 1441.

[20] G. Schmalz "Technische Oberflaechenkunde", Springer, Berlin, 1936, p. 66 and 269.

[21] J. Abbott and A. Firestone, "A New Profilograph Measures Roughness", Autom. Ind., 1933, p. 204.

[22] K. F. Sherwood and J. R. Crookall, "Surface Finish Measurement", Proc. Inst. Mech. Eng. Vol. 182 pt 3k (1967/68).

[23] R. E. Reason, "Biographical Memoirs by D. J. Whitehouse", Me. Proc. Roy. Soc., Vol. 36, 1990, p. 437

[24] M. Stedman, "Mapping the Performance of Surface Measuring Instruments", Proc. SPIE. Vol. 803, 1987, p. 138.

[25] D. J. Whitehouse, "Handbook of Surface Metrology", Inst. Phys. Pub., Bristol, 1994.

[26] M. Osterhold, "Influence of Substrate Structure on the Coating Appearance and the Relevant Characterization Methods", Materialwissenschaft und Werktoffechnik, Vol. 29, Issue 3, 1998, pp.131-136

[27] M. Coulthard and P. Kania "On-Line Measurement of Paint Appearance on Car Bodies", Metal Finishing, Vol. 91, No. 10, 1993, p. 45.

[28] J. F. Archard, "Elastic Deformation and the Laws of Friction", Proceedings Royal Society London A 243, 1957, pp. 190-205.

[29] W. A. Shewher, "Economic Control of Quality of Manufacturing Products", Van Nostrand, Princeton, 1931.

[30] D. Whitehouse, "Surface and their Measurement", Hermes Penton Litd., 2002.

[31] T. R. Thomas, "Rough Surfaces", 2nd ed., Imperial College Press, London, 1999.

[32] C.Y. Poon, and B. Bhushan, "Comparison of Surface Roughness Measurements by Stylus Profiler, AFM, and Non-contact Optical Profiler", Wear, 190, 1995, pp. 76-88

[33] T. R. Thomas, "Trends in Surface Roughness", International Journal of Machine Tools and Manufacture, 38, Issues 5-6, 1998, pp. 405-411

[34] M. O. Nicolls, "The Measurement of Surface Finish", Metrology and Inspection, No. 5, 1975.

[35] T. Asakara, "Roughness Measurements of Metal Surface using Laser Speckles", Optical Society of USA, Vol. 67, No.9, 1977.

[36] R. J. Whitefield, "Non-contact Optical Profilometer", Applied Optics, No. 10, 1975

[37] www.techlab.fr/Surface.htm

[38] M. Neitzel, M. Blinzier, K. Edelman and F. Hoecker, "Surface Quality Characterization of Textile-Reinforced Thermoplastics", Polymer Composites, Vol. 21, No. 4, Aug.2000, p. 630.

[39] www.proscan.co.uk/products.htm

[40] www.ubmusa.com/product/nanosurf.htm

[41] www.microphotonics.com/profilomenu.html

[42] www.mahr.com/index.php?NodeID=2409&SourceID=1737&LayerMenuID=3

[43] www.mitutoyo.co.jp/eng/products/keijyou_hyomen/hyomen_01.html

[44] K. J. Gasvik, "Optical Metrology", John Wiley & Sons Ltd., 1995.

[45] A. Wagner, "Class A Surface Aspect of Parts Molded By Resin Transfer Molding", Report the Term Project at Swiss Federal Institute of Technology Zurich, 2000.

[46] J. Peterson and H. Robertson, "Modeling of RTM Process", University of Michigan, Proc. New Developments Advanced Composite Materials, Detroit, Michigan, USA, Sep. 30-Oct. 1, 1991.

[47] P.W. Vaccarrella and J.E. Jensen, "Class A Surface by Resin Transfer Molding", Proc. Annual Conference, Composite Institute of Society of Plastic Industry, Cincinnati, Ohio, Session 23-C, 1987, p. 42.

[48] S. Hu, R. Ganesan, S. V. Hoa, F. Trochu and M. DeBolt, "Probabilistic Analysis of Surface Finish for Automobile Composite Panels", Proceedings of the Fifth Joint Canada-Japan Workshop on Composites, September 2004, pp. 125-132.

[49] J. F. Song and T. V. Vorburger, "Surface Texture", ASM Handbook 18, p. 334. 16010C.

[50] H. Zahouani, R. Vargiolu and J. L. Loubet, "Fractal Models of Surface Topography and Contact Mechanics", Mathl. Comput. Modeling, Vol.28, No.4-8, 1998, pp 517-534.

[51] L. He and J. Zhu, "The Fractal Character of Processed Metal Surface", Wear, 208, 1997, pp. 17-24.

[52] X. Kuang, Z. Zhu, G. Carotenuto and L. Nicolais, "Fractal Analysis and Simulation of Surface Roughness of Ceramic Particles for Composite Material", Appl. Compos. Mater., Vol. 4, 1997, p. 69.

[53] T. Schuller, W. Beckert, B. Lauke, " A Finite Element Model to Including Interfacial Roughness into Simulations of Micromechanical Test", Computer Materials Science Vol. 5, 1999, pp. 357-366.

[54] Y. Kuga, J. S. Colubum and P. Phu, " Millimetre-Wave Scattering from One Dimensional Surface of Different Surface Correlation Functions", Wave in Random Media, Vol. 3, 1993, pp. 101-110.

[55] T. Yoshinobu, A.Iwamoto, K. Sudoh and Iwasaki, "Scaling of Si/SiO_2 Interface Roughness", J. Vac. Sci. Technol., B 13(4), Jul/Aug., 19995, p.1630.

[56] H. Jeong, B. Kahng, S. Lee, C.Y. Kwak, A. L. Barbasi and J. K. Furdyna, "Monte Carlo Simulation of Sinusoidally Modulated Supperlattice Growth", Physical Review, Vol. 65, 031602, 2002, p. 6503162-1.

[57] D. L. Woodraska and J. A. Jaszczak, "A Monte Carlo Simulation Method for {111} Surfaces of Silicon and Other Diamond-cubic Material", Surface Sciences Vol. 374, 1997, pp. 319-332.

[58] K. Palanikumar, "Cutting Parameters Optimization for Surface Roughness in Machining of GFRP Composites Using Taguchi's Methods", Journal of Reinforced Plastics and Composites, Vol. 25, No. 16, 2006, p. 1739.

[59] K. Palanikumar, L. Karunamoorthy, N. Manoharan, "Mathematical Model to Predict the Surface Roughness on Machining of Glass Fiber Reinforced Polymer Composite", Journal of Reinforced Plastics and Composites, Vol. 25, No. 4, 2006, p. 407.

[60] P. Ferabili and A. Masini, "Development of Carbon/Epoxy Structural Components for High Performance Vehicle" Composite: Part B 35, 2004, p. 323.

[61] R. Saito, W. Ming, J. Kan, L. J. Lee, "Thickening Behavior and Shrinkage Control of Low Profile Unsaturated Polyester Resins", Polymer, Vol. 37, No. 16, 1996, pp.3567-3576.

[62] M. Kinkelaar, B. Wang and L. J. Lees "Shrinkage Behavior of Low-profile Unsaturated Polyester Resins", Polymer, Vol. 35, No. 14, 1994, p. 3011.

[63] G. A. Landsettle and J. C. Jensen, " Factors that affect Class A Surface Quality", 41st Annual Conference, Reinforced Plastics/ Composites Institute, The Society of the Plastics, Inc., Jan. 27-31, 1986, Section 1/18-B.

[64] D. G. Jeffs, "New Filler for Low Profile Polyester DMC/BMC", 46th Annual Conference, Composite Institute, The Society of the Plastics Industry, Inc., Feb. 18-21, 1991, Section 7-F/1.

[65] M. Kinkelaar, S. Muzumdar, and L. J. Lees, "Dilatometric Study of Low Profile Unsaturated Polyester Resins", Polymer Engineering and Science, Vol. 35, No. 10, May 1995, p. 823.

[66] W. Li and L. J. Lees, "Shrinkage Control of Low Profile Unsaturated Polyester Resins Cured at Low Temperature", Polymer, Vol. 39, No. 23, 1998, pp.5677-5687.

[67] T. Mitani and H. Shiraishi, K. Honda and G. E. Owen, "Mechanism of Low Profile Behavior by Quantitative Morphology Observation and Dilatometer", 44th Annual Conference, Composites Institute, The Society of the plastics Industry, Inc., Feb., 1989, 1/Section 12-F.

[68] S. Bickerton, H. C. Stadtfeld, K. V. Steiner, and S. G. Advani, " Design and Application of Actively Controlled Injection Schemes for Resin Transfer Molding", Composite Science and Technology, Vol. 61, 2001, pp. 1625-1637.

[69] J. Luo, Z. Liang, C. Zhang, and B. Wang, " Optimization Tooling Design for Resin Transfer Molding with Virtual Manufacturing and Artificial Intelligence", Composite Part A, No. 32, 2001, pp. 877-888.

[70] K. Arakawa, E. Iwami, K. Kimura and K. Nomaguchi, "Factors Affecting Surface Smoothness and Role of Unsaturated Polyester Resin and Class fiber", Journal of Reinforced Plastics and Composites, Vol. 13, Dec., 1994, p.1100.

[71] J. W. Raye, and D. W. Cassil, "Advancements in Injection in-mold Coating Technology", Metal Finishing, Vol. 93, No. 9, 1995, pp. 41-46.

[72] M. A. Debolt, "Surface Finish Evaluation Method for Class A Composite Substrates", Proceeding of 36th International SAMPE Technical Conference, San Diego, USA, 2004.

[73] "SURFPAK-SV/PRO/SJ Surface Texture Parameter User's Manual", Mitutoyo Corporation, Japan.

[74] ASTM Standards, F1811-97.

[75] G. He, S. Ma, "Measurement of Surface Roughness", China Measurement Publisher, 1998.

[76] A. Papoulis and S. U. Pillai, "Probability, Random Variables, and Stochastic Processes", The McGraw-Hill Companies, Inc., 2002.

[77] A.V. Oppenheim, R.W. Schafer, "Digital Signal Processing", Prenti-Hall, Inc, 1975

[78] F. Zhang, S. Guo, L. Xiao, and L. Fu, "Probability, statistics and Stochastic Processes", Beijing University of Aeronautics & Astronautics, 2000.

[79] T. Chen and Z. Xu, "Mathematic Methods in Geo-exploration Data processing," Geology Press Beijing China, 1989.

[80] G. B. Lockhart and B.M.G. Cheetham, "Basic digital signal processing", Butterworths & Co. Ltd., 1989.

[81] S. W. Smith, "The Scientist and Engineer's Guide to Digital Signal Processing,"

California Technical Publishing, 1998.

[82] L. Jing and G. Wei, "Modern Digital Signals Processing", Tsinghua University, China, 2004.

[83] E. Lai, "Practical Digital Signal Processing," IDC Technologies, 2004.

[84] A.R.H. Swan and Sandilands, "Introduction to Geological Data Analysis", Blackwell Science Ltd., 1995.

[85] M. Friedman and A. Kandel, "Introduction to Pattern Recognition", Imperial College Press., 1999.

[86] L. A. Finelli, P. Achermann and A. A. Borbély, "Individual 'Fingerprints' in Human Sleep EEG Topography", Neuropsychopharmacology, Volume 25, Issue 5, Supplement 1, November 2001, pp. S57-S62.

[87] P. Lagacherie, J. M. Robbez-Masson, N. Nguyen and J. P. Barthès, "Mapping of Reference Area Representativity Using a Mathematical Soilscape Distance", Geoderma, Volume 101, Issues 3-4, April 2001, pp. 105-118.

[88] M. E. Siddall, "Stratigraphic Fit to Phylogenies: A Proposed Solution", Cladistics, Volume 14, Issue 2, June 1998, pp. 201-208.

[89] G. J. Tielen, T. Lulek, M. R. M. J. Traa, M. Kuzma and W. J. Caspers, "The Role of the Manhattan Distance in Antiferromagnetic Ordering", Physica A: Statistical and Theoretical Physics, Volume 246, Issues 1-2, 15 November 1997, pp. 199-220.

[90] Abe and Shigeo, "Pattern Classification: Neuron-fuzzy Methods and their Comparison", Springer, 2001.

[91] "PostStack Family Reference Manual", Landmark Graphics Corporation, May 2002, pp. 105-106.

[92] www.micro-epsilon.com/en/Sensors/Optical---Laser/

[93] www.surfacesensor.com

[94] www.predev.com/smg/instrument.htm

[95] "SURFPAK-SV/PRO/SJ Operation Guide User's Manual", Mitutoyo Corporation, Japan.

[96] J. N. Siddall, "Probabilistic Engineering Design (Principles and Applications)", Marcel Dekker Inc., 1983.

[97] S. M Kay, "Modern Spectral Estimation: Theory and Application", Englewood Cliiffs, N.J. Prentice Hall, 1987.

[98] S. J. Orfnidis, "Introduction to Signal Processing", New York: Prentice Hall International, Inc., 1986.

[99] www.lgc.com

[100] www.lgc.com/landmark/contact+us/index.htm

[101] www.gravmag.com/**oil**2.html

[102] R. Walker, C. Wong, H. Malcotti, E. Pèrez, and J. Sierra, "Seismic Multi-attribute Analysis for Lithology Discrimination in Ganso Field, Oficina Formation, Venezuela", The Leading Edge, Nov., 2005; 24: pp. 1160 - 1166.

[103] M. V. DeAngelo, M. Backus, B. A. Hardage, P. Murray, and S. Knapp, "Depth Registration of P-wave and C-wave Seismic Data for Shallow Marine Sediment Characterization, Gulf of Mexico", The Leading Edge, Feb., 2003; 22: pp. 96 - 105.

[104] B. Hart and M. A Chen, "Understanding Seismic Attributes through Forward Modeling" The Leading Edge, Sep., 2004; 23: pp. 834 - 841.

[105] "PostStack Family Reference Manual", Landmark Graphics Corporation, May 2002.

[106] "SpecDecomp Used Guide", Landmark Graphics Corporation, 2003, pp. 5-120.

[107] PostStack Family Reference Manual, Landmark Graphics Corporation, May 2002, pp. 33-36.

[108] Sheriff, R. E., "Encyclopedic Dictionary of Exploration Geophysics", 3rd ed., Tulsa, SEG., 1991, p. 376.

[109] C. W. Therrien, "Decision Estimation and Classification: An Introduction to Pattern Recognition and Related Topics", John Wiley & Sons, New York, 1989.

[110] E. A. Patrick, "Fundamental of Pattern Recognition", Prentica-Hall, Englewood Cliff, N. J., 1972.

[111] K. S. Fu and T.Y. Young, "Handbook of Pattern Recognition and Image Processing", Academic Press., New York, 1985.

[112] S. Hu, S.V. Hoa and R. Ganesan., "Evaluation of Surface Finish of Composite Automobile Panel", The 21st Annual Technical Conference of the American Society for Composites, The University of Michigan, Dearborn Michigan, September17-20, 2006.

[113] Y. Zhou, "Introduction to Stochastic Processes", Beijing University of Aeronautics & Astronautics, 2000.

[114] "Open books" Landmark Graphics Corporation, August, 2003.

[115] "PostStack Family Reference Manual", Landmark Graphics Corporation, 2003, pp. 362-436.

[116] M. H. Raja, "Experimental Optimization of Process Parameters to Obtain Class A Surface Finish in Resin Transfer Molding Process", Ph. D. thesis, McGill University, 2005.

[117] http://people.ccmr.cornell.edu/~emmanuel/research/afm.html

[118] L. Xu, L. J. Lee, "Effect of Nanoclay on Shrinkage Control of Low Profile Unsaturated Polymer(UP) Resin Cured at Room Temperature", Polymer, 45, 2004, pp. 7325-7334.

Appendix A

Frequency and spectrum analysis

- **Periodic signals and Fourier series**

Many signals are encountered which are periodic but not sinusoidal. For example, a periodic signal *x(t)*, with period *P* seconds, satisfies:

$$x(t+P) = x(t) \qquad \text{for all values of t from } -\infty \text{ to } +\infty \tag{A1}$$

Under certain conditions normally satisfied by signals of practical interest, the periodic waveform *x(t)* may be expressed as the sum of a series of sinusoids, i.e.:

$$x(t) = A_0 + \sum_{n=1}^{\infty} A_n \cos(n\Omega_0 t + \Phi_n) \tag{A2}$$

This is known as a Fourier series with a fundamental frequency of Ω_0 radians/second. When *x(t)* has a period of *P* seconds, $\Omega_0 = 2\pi/P$. The amplitude coefficients of Fourier series, Ao, A_1, A_2, etc and phase coefficients Φ_1, Φ_2, etc, are constants which characterize *x(t)*. Therefore *x(t)* has been expressed as the sum of a constant *Ao* and angular frequency Ω_0, $2\Omega_0$, $3\Omega_0$, and so on.

The complex Fourier series can be expressed as:

$$x(t) = A_0 + \frac{1}{2}\sum_{n=1}^{\infty} A_n[e^{j(n\Omega_0 t+\Phi_n)} + e^{-j(n\Omega_0 t+\Phi_n)}] = \sum_{n=-\infty}^{\infty} C_n e^{jn\Omega_0 t} \tag{A3}$$

where $C_0 = A_0$, $C_n = 1/2\ A_n\ e^{jn\Omega_0 t}$ and $C_{-n} = 1/2\ A_n\ e^{-jn\Omega_0 t}$, for n=1,2,3.... (A4)

- **Aperiodic signal and Fourier transforms**

Aperiodic (non-periodic) signals do not have Fourier series and it is therefore necessary to relate them to sinusoids in a different way. It is convenient to restrict attention initially

to signal waveforms $x(t)$ which satisfy the condition:

$$\int_{-\infty}^{+\infty} |x(t)| dt < \infty \qquad \text{(A5)}$$

The Fourier transform $X(\Omega)$ of a signal $x(t)$ which satisfies (2.31) is defined as:

$$X(\Omega) = \int_{-\infty}^{+\infty} x(t) e^{-j\Omega t} dt \text{ (Fourier transform)} \qquad \text{(A6)}$$

Inverse Fourier transform may be shown to be:

$$x(t) = \frac{1}{2\pi} \int_{-\infty}^{+\infty} X(j\Omega) e^{j\Omega t} d\Omega \qquad \text{(Inverse Fourier transform)} \qquad \text{(A7)}$$

This equation gives some insight into the physical meaning of $X(\Omega)$ as a "spectral density" function whose magnitude and phase determine how the characteristics of $x(t)$ are distributed across a continuous spectrum of sinusoidal frequency components with frequency Ω ranging from 0 to ∞.

- **Discrete Fourier Transform (DFT)**

The DFT may be defined as the transformation:

$$X[k] = \sum_{n=0}^{N-1} x[n] e^{-j\omega_k n} \qquad \omega_k = 2\pi k/N \;\; k, n=0, 1, 2, 3, 4 \ldots\ldots N-1 \qquad \text{(A8)}$$

Following inverse DFT formula is obtained:

$$x[n] = \frac{1}{N} \sum_{n=0}^{N-1} X[k] e^{j\omega_k n} \qquad \text{(Inverse DFT)} \qquad \text{(A9)}$$

- **Signal energy and power**

Familiar concepts such as intensity, volume and loudness are given mathematical expression by defining energy and power for signals. The energy of an analogue signal $x_a(t)$ is defined as the energy in joules that would be dissipated in a one ohm resistor

when a voltage $x_a(t)$ is applied across it. It may be calculated by integrating $|x_a|^2$ over t = - ∞ to + ∞ or by integrating the energy spectral density (1/2π) $|X_a(\Omega)|^2$ over Ω = - ∞ to + ∞:

$$\int_{-\infty}^{\infty} |x_a(t)|^2 dt = \frac{1}{2\pi} \int_{-\infty}^{\infty} |X_a(\Omega)|^2 d\Omega \qquad \text{(A10)}$$

Parseval's theorem shows that these two formulae give the same result. For a signal with finite energy, the average power will always be zero, and signals with finite power, such as sinusoids for example, will have infinite energy. Average power can be calculated as:

$$\lim_{T\to\infty} \frac{1}{T} \int_{-T}^{T} |x_a(t)|^2 dt \qquad \text{(A11)}$$

Analogue concepts of energy and power may be extended to discrete time signals. The energy of a sequence is the sum of its samples squared, and its power is the average value of its samples squared, i.e. its 'mean square value'. A discrete time version of Parseval' s theorem shows that energy may be calculated from the energy spectral density function *(1/2π)* $|X_a(j\Omega)|^2$:

$$\sum_{n=\infty}^{\infty} |x[n]|^2 = \frac{1}{2\pi} \int_{-\pi}^{\pi} |X_a(e^{j\omega})|^2 d\omega \qquad \text{(A12)}$$

Average power is

$$\lim_{M\to\infty} \frac{1}{2M+1} \sum_{n-M}^{M} |x\,[n]|^2 \qquad \text{(A13)}$$